DEVELOPMENT OF ELECTROCHEMICAL BIOSENSORS AND SOLID-PHASE AMPLIFICATION METHODS FOR THE DETECTION OF HUMAN PAPILLOMAVIRUS GENES

Laia Civit Pitarch

Dipòsit Legal: T. 1050-2012

Laia Civit Pitarch

Development of electrochemical biosensors and solid-phase amplification methods for the detection of human papillomavirus genes

DOCTORAL THESIS

Department of Chemical Engineering

UNIVERSITAT ROVIRA I VIRGILI

Laia Civit Pitarch

Development of electrochemical biosensors and solid-phase amplification methods for the detection of human papillomavirus genes

DOCTORAL THESIS

Supervised by Dr. Alex Fragoso and Dr. Ciara K. O'Sullivan

Department of Chemical Engineering

UNIVERSITAT ROVIRA I VIRGILI

Tarragona

2012

UNIVERSITAT ROVIRA I VIRGILI

Departament d'Enginyeria Quimica
Universitat Rovira i Virgili
Campus Sescelades,
Avda. Països Catalans, 26
43007 Tarragona
Tel: 977 55 96 58
Fax: 977 55 96 67

Dr. Alex Fragoso and Dr. Ciara K. O'Sullivan,

CERTIFY:

That the present study, entitled "Development of electrochemical biosensors and solid-phase amplification methods for the detection of human papillomavirus genes" presented by Laia Civit Pitarch for the award of the degree of Doctor, has been carried out under our supervision at the Chemical Engineering Department of the University Rovira i Virgili, and that it fulfils the requirements to obtain the Doctor European Mention.

Tarragona, 24th January 2012,

Dr. Alex Fragoso

Dr. Ciara K. O'Sullivan

Acknowledgements

First of all I would like to thank my supervisors, Alex Fragoso and Ciara O'Sullivan, for trusting me when I joined the group and for their guidance and encouragement through my Master and PhD studies. I also want to thank Hossam that had the patience of helping me in my introduction to the electrochemical biosensors world.

I would also thank Prof. Graham Leggett, for giving me the opportunity to work and learn from his laboratory during my stage at the University of Sheffield. I also appreciate the efforts of Osama for helping me.

I would like to thank the doctoral scholarship of Chemical Engineering Department, for the economical support.

I also would like to express gratitude to all the people from NBG group, the present members and the former members. I would specially thank Valerio for his help and chats during this years, I really miss him this last months. Big thank goes to Sira, which help me a lot these last weeks. Also, to Rukan, Hamdi, Alessandro, Pedro, Viji... that we share this PhD experience. I don't miss Jos, Carmen, Mary Luz and Marketa. I really enjoyed this experience, and it was in big part thanks to you and your friendship!

Also I would like to thank to my childhood friends, especially to Laia and Vicky, which ones I spend really good times during all this years.

I cannot finish this, without giving big thanks to my family, Nunu, Clàudia i Helena, Jaume, Matt, Beni and Julián (father). Special mention goes to my mum, for her encouragement and support during all my life. Also, I would like to dedicate this thesis and be grateful to my grandmother, Josi, that I know that she is very proud that I finally finished!

And finally, but not the least important, I want to thank Julián for being with me during all this years, for his wise advises, and for all the love that I receive from him. Thank you!

To my family

A la meva mare, al Julián i a tu, Josi

Table of contents

Summary

A rapid, accurate and reliable diagnosis is crucial for the identification of a disease, in particular in cancer patients, where an early detection can improve patient survival outcomes. Cancer continues to be one of the primary causes of death worldwide, with cervical cancer being the third most commonly diagnosed and the fourth leading cause of cancer death in women. It is well known that persistent infections with high-risk human papillomaviruses (HPV) are the primary cause of cervical cancer, as well as other types such as anal cancer.

Electrochemical DNA biosensors have received important attention owing to their simplicity, low cost, portability, multiplexing capability and high sensitivity. Moreover, their compatibility with microfabrication technologies makes them attractive for DNA diagnostics.

The first objective of the work described in this thesis is the development of an electrochemical DNA sensor array for the multiplex detection of high-risk HPV sequences (HPV16, 18 and 45) and its application to human clinical samples. A second objective is the demonstration of a proof-of-concept of the development of isothermal (helicase-dependent amplification) solid-phase amplification methods with electrochemical real-time monitoring.

This thesis is divided in seven chapters. A general introduction covering the different topics of the thesis is presented in Chapter 1. Chapters 2 to 4 are related with the development of electrochemical DNA sensors for the multiplex detection of HPV related exons, while Chapters 5, 6 and 7 comprise the studies carried out for the development of methods for the electrochemical monitoring of solid-phase amplification.

In Chapter 2, the proof-of-concept of the electrochemical genosensor array for the individual and simultaneous detection of two high-risk human papillomavirus DNA sequences, HPV16E7p and HPV45E6 is presented. In this case, optimum conditions

for surface chemistry preparation and detection of hybridised target were evaluated using synthetic DNA targets.

Chapter 3 is focused on a comparative study involving different methods for the preparation of single-stranded DNA (ssDNA). In DNA biosensors, thermal denaturation (*heat and cool*) of the dsDNA target is the most widespread technique, despite the significant disadvantages it presents. Thus, a comparison in terms of ssDNA recovery and reproducibility of the technique with alternative techniques including magnetic bead separation and exonuclease digestion was performed. These alternative methodologies showed far superior ssDNA recoveries (between 50 - 70% of the theoretical maximum ssDNA) as compared to the thermal denaturation methodology. In particular, for the preparation of ssDNA from clinical samples of HPV previously amplified by PCR, streptavidin-coated magnetic beads was selected to be optimal.

Then, in Chapter 4, an extended work based on Chapter 2 and 3, where a new high-risk HPV target (HPV 45) was included and the analysis of real patient samples was performed using real PCR products. An exhaustive study of the cross-reactivity between the three target sequences and reporter probes, multiplexed detection of the three targets and the reusability and stability of the genosensor array was carried out. To evaluate the genosensor performance in a real clinical scenario, samples obtained from cervical scrapes were amplified and detected and an excellent correlation was obtained with HPV genotyping of the same clinical samples carried out in a hospital laboratory.

Even though electrochemical biosensors provide quantitative detection, the need for DNA amplification of clinical samples, and the subsequent generation of ssDNA, not only increases the total assay time, but different yields of ssDNA are obtained dependent on, for example, GC content, amplicon length, which can extensively complicate true quantitation for medium-high multiplexing. Electrochemical monitoring of solid-phase immobilised real time amplification would obviate the need for the generation of ssDNA, and asides from facilitating a more reliable and accurate

quantitation. Multiplex detection could be easily achieved using an electrochemical array.

For the development of electrode immobilised real-time amplification, the choice of a stable surface chemistry is essential as repeated thermal cycles will be implemented. Chapter 5 details an evaluation of the thermal stability of gold surfaces modified with mono- and dithiol molecules, and diazonium salts with one and two diazo- groups. Electrochemical techniques were explored to assess the influence of temperature on the formed layers, indicating that diazonium salt derived layers are thermally more stable at significantly higher temperatures than alkanethiol SAMs, which start to desorb from the surface at temperatures above 65ºC. Furthermore, in order to test the applicability of these thermally exposed surfaces, a complete sandwich assay was built for the detection of human papillomavirus DNA sequences on electrodes modified with the dithiol and diazonium salt with two diazo-groups.

Based on the superior thermal stability of the diazonium with two diazo-groups grafted on gold surfaces, Chapter 6 focuses on the synthesis and characterisation of the electrografting of 3,5-(4-diazophenoxy)benzoic acid. Characterisation of the diazonium salt was performed using nuclear magnetic resonance (NMR) and infrared spectroscopy (IR), whereas atomic force microscopy (AFM) and X-ray photoelectron spectroscopy (XPS) were employed for the characterisation of its deposition on gold surfaces.

Finally, in Chapter 7 the proof-of-concept of an electrochemical monitoring of solid-phase helicase-dependent amplification (HDA) is described. Using HPV45 (79 bp) as a model sequence to perform this work, forward primer was immobilised on the surface of gold electrodes. For electrochemical detection, the electrostatic interaction of a ruthenium salt with DNA was used to monitor the progress of HDA. A preliminary implementation of this specific DNA amplification and detection methodology in a microfluidic system was explored.

Overall, this work constitutes a complete overview of the development of quantitative electrochemical detection of DNA with potential applications in real clinical scenarios, from the very fundamental aspects such as the choice of a robust

and reliable surface chemistry, ssDNA generation or DNA amplification methodology to the implementation of these key parameters into a microfluidic platform and the development of electrochemical real-time solid-phase amplification of DNA.

List of publications

Publications derived from Master

1. Nassef, H.M.; Civit, L.; Fragoso, A.; O'Sullivan, C.K., Amperometric sensing of ascorbic acid using a disposable screen-printed electrode modified with electrografted *o*-aminophenol film, *Analyst*, 2008, **133**, 1736-1741.

2. Civit, L.; Nassef, H.M.; Fragoso, A.; O'Sullivan, C.K., Amperometric determination of ascorbic acid in real samples using a disposable screen-printed electrode modified with electrografted *o*-aminiphenol film, *Journal of agricultural and food chemistry*, 2008, **56**, 10452-10455.

3. Nassef, H.M.; Civit, L.; Fragoso, A.; O'Sullivan, C.K., Amperometric immunosensor for detection of celiac disease toxic gliadin based on Fab fragments, *Analytical Chemistry*, 2009, **81**, 5299-5307.

Publications derived from PhD thesis

4. Civit, L.; Fragoso, A.; O'Sullivan, C.K., Thermal stability of diazonium derived and thiol-derived layers on gold for application in genosensors, *Electrochemistry communications,* 2010, **12**, 1045-1048.

5. Civit, L.; Fragoso, A.; O'Sullivan, C.K., Electrochemical biosensor for the multiplexed detection of human papillomavirus genes, *Biosensors & Bioelectronics,* 2010, **26**, 1684-1687.

6. Civit, L.; Fragoso, A.; Hölters, S.; Dürst, M.; O'Sullivan, C.K., Electrochemical genosensor array for the simultaneous detection of multiple high-risk HPV sequences in clinical samples, *Analytica Chimica Acta*, 2012, **715**, 93-98.

7. Civit, L.; El-Zubir, O.; Fragoso, A.; O'Sullivan, C.K., Spectroscopic and atomic force microscopy characterization of the electrografting of 3,5-bis(4-diazophenoxy)benzoic acid on gold surfaces, *Manuscript submitted.*

8. Civit, L.; Fragoso, A.; O'Sullivan, C.K., Evaluation of techniques for generation of single-stranded DNA for quantitative detection, *Manuscript submitted.*

List of Abbreviations

3,5-BDBA	3,5-(4-diazophenoxy)benzoic acid
ACN	Acetonitrile
AFM	Atomic Force Microscopy
AP	Alkaline phosphatase
bp	Base pair
C	Carbon
cDNA	Complementary deoxyribonucleic acid
CFU	Colony forming units
CV	Cyclic voltammetry
DNA	Deoxyribonucleic acid, single-stranded DNA (ssDNA) or double-stranded DNA (dsDNA)
dNTP	Deoxyribonucleotide triphosphate
DPV	Differential pulse voltammetry
DT1	10-(3,5-bis((6-mercaptohexyl)oxy)phenyl)-3,6,9-trioxadecanol
DT2	22-(3,5-bis((6-mercaptohexyl)oxy)phenyl)-3,6,9,12,15,18,21-heptaoxadocosanoic acid
EC	Electrochemical
EDC	1-Ethyl-3-[3-dimethylaminopropyl]carbodiimide hydrochloride
EDTA	Ethylenediaminetetraacetic acid
EIA	Enzyme immunoassay
EIS	Electrochemical impedance spectroscopy
ELISA	Enzyme-linked immunosorbent assay
ELONA	Enzyme-linked oligonucleotide assay
Fw	Forward (primer)
GOD	Glucose oxidase
HDA	Helicase-dependent amplification
HEPES	(4-(2-hydroxyethyl)-1-piperazineethanesulfonic acid

HIV	Human immunodeficiency virus
HPV	Human papillomavirus
HRP	Horse-radish peroxidase
IR	Infra-red
IUPAC	International Union and Applied Chemistry
LAMP	Loop-mediated isothermal amplification
LNA	Locked nucleic acid
LOD	Limit of detection
M	Metal
MAPH	Multiplex amplification and probe hybridisation
MB	Methylene blue
MCH	Mercaptohexanol
MHA	6-mercaptohexanoic acid
MLPA	Multiplex ligation-dependent probe amplification
mRNA	Messenger ribonucleic acid
NHS	*N*-Hydroxysuccinimide
PCR	Polymerase Chain Reaction
PDMS	Polydimethylsiloxane
PEG	Polyethylene glycol
PID	Proportional–integral–derivative
PNA	Peptide nucleic acids
POC	Point of care
polyA	Polyadenine
pRb	Retinoblastoma protein
RCA	Rolling circle amplification
R_{ct}	Charge transfer resistance
RNA	Ribonucleic acid
RSD	Relative standard deviation
RT	Room temperature
RT-PCR	Real time polymerase chain reaction

Rv	Reverse (primer)
SAM	Self-assembled monolayer
SAS	Step and sweep voltammetry
SCE	Silver chloride electrode
SDA	Strand displacement amplification
SELEX	Systematic evolution of ligands by exponentional enrichment
SERS	Surface-enhanced Raman scattering spectroscopy
SNP	Single nucleotide polymorphism
SPR	Surface Plasmon Resonance
tHDA	Thermal Helicase-dependent amplification
TMB	3,3',5,5'-tetramethylbenzidine
ToF-SIMS	Time-of-Flight Secondary Ion Mass Spectrometry
U	Enzyme units
Urea-PAGE	Urea-polyacrylamide gel electrophoresis
UV	Ultraviolet
XPS	X-ray photoelectron spectroscopy

List of Figures and Schemes

Chapter 3

Chapter 4

Chapter 5

Chapter 6

Chapter 7

List of Tables

Chapter 1

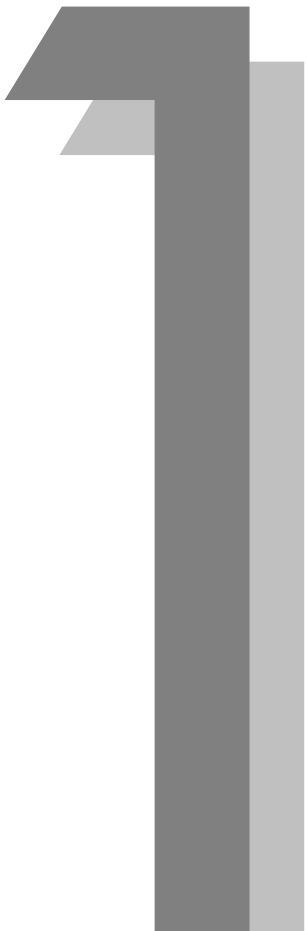

Chapter 1

Introduction

1.1 Biosensors

According to the International Union of Pure and Applied Chemistry (IUPAC), a biosensor "is an integrated receptor-transducer device, which is capable of providing selective quantitative or semi-quantitative analytical information using a biological recognition element" (Figure 1.1).[1]

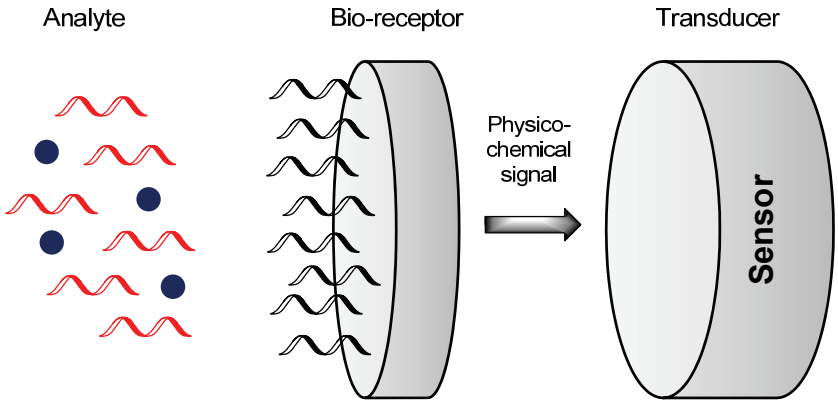

Figure 1.1. Schematic representation of a biosensor.

The biological sensing material may be a protein such as an enzyme or antibody, a nucleic acid, antibody fragment, a whole microbial cell, or even a plant or animal tissue,

and biosensors can be divided into catalytic (enzyme) and affinity (antibodies, lectine, DNA) sensors.

1.2 DNA biosensors

Nucleic acid analysis has played an important role in the detection of pathogens and genetic diseases. In recent years, its usefulness has been seen in many decentralised applications such as point-of-care diagnostics, environmental and food monitoring, and the detection of biological warfare agents.

Conventional DNA hybridisation detecting methods, such as gel electrophoresis or Southern blotting, are usually time-consuming and laborious.[2] The majority of DNA biosensors take advantage of the preferential binding of complementary single-stranded nucleic-acid sequences, commonly relying on the immobilisation of a single-stranded nucleic acid probe on a surface to recognise its complementary nucleic acid target sequence by hybridisation (Figure 1.2).[3]

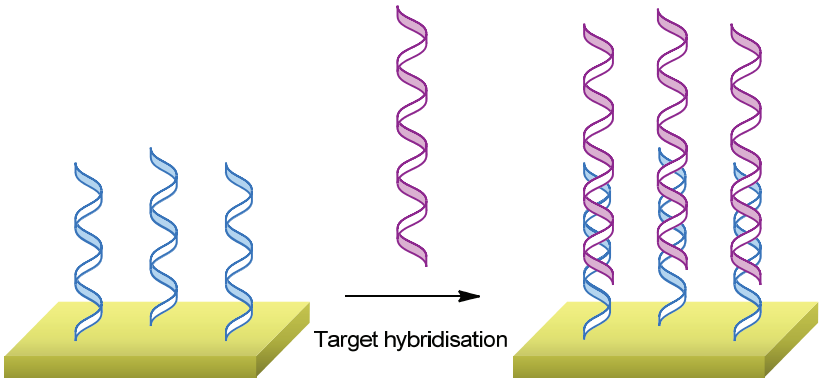

Figure 1.2. Schematic representation of the detection of a DNA sequence.

Sensitivity and selectivity are the two crucial aspects in the development of hybridisation biosensors. The first one is important to detect concentrations of DNA as low as possible and the latter one is necessary for the detection of mutations.[4] For

the development of a DNA biosensor, there are two key components; the recognition layer and transduction of the recognition event.

Integration of numerous DNA biosensors on the same detection platform results in DNA microarrays, commonly referred as DNA chips, gene chips or biochips.[5] The advantage of DNA microarrays is their capability to simultaneously detect different sequences providing an advanced level of information in a shorter time.[6] High-density arrays consisting of hundreds of thousands of sensors are well established as genetic screening tools and typically require long hybridisation times (from 16 – 18 h).[7] Although this technique is extremely valuable in areas such as the identification of disease associated genes and whole genome expression analysis, the huge amount of time and effort required to carry out the test makes it prohibitively expensive for point-of-care diagnostics (POC). Low-density microarrays are focused on the detection of narrower sets of genetic sequences, and offer rapid and low-cost tests. Herein, this technology can find applications such as the fast screening of a particular disease pharmacogenomics, or the control of cancer progression looking at multiplexed mRNA patterns.[8-9]

1.2.1 Hybridisation detection

The hybridisation of the immobilised probe and its complementary target strand is translated into a signal which is proportional to the level of hybridisation, and thus, to the amount of target present in the sample. Transduction of the surface hybridisation event can be optically measured for example using fluorescence,[10-11] Surface Plasmon Resonance (SPR),[12] colorimetry,[13-14] chemiluminescence[15] or surface-enhanced Raman Scattering spectroscopy (SERS).[16] Using mass-sensitive detection quartz crystal microbalance sensors[17-18] and microcantilever sensors have been reported.[19-20] Electrochemical transducers have received important attention owing to their simplicity, compatibility with microfabrication technologies, low cost, portability, independence from sample turbidity, multiplexing and high sensitivity.[2, 21-23] In particular, their features make them attractive for DNA diagnostics.[22, 24-27] Electrochemical transduction of DNA hybridisation can be broadly divided into label-

free (direct)[28-31] and label-based (indirect)[32-41] systems. Labelled systems use redox indicators to transduce the hybridisation event. This redox compounds can be attached to the electrode, to a reporter probe or in the solution. On the other hand, label-free systems detect changes in the physical properties of the recognition layer that results in a change in the obtained signal.[21, 23]

1.2.1.1 Labelled methods

Electroactive hybridisation indicators have been widely exploited for the detection of hybridisation. These species bind to ssDNA and to dsDNA with different affinities, resulting in a change in electrochemical signal. These indicators can be based on cationic metal complexes, such as $Co(phen)_3^{3+}$,[42-43] $Co(bpy)_3^{3+}$ [44] and $Ru(bpy)_3^{3+}$,[45] and non-metal containing compounds, such as Hoechst33258,[46] methylene blue (MB),[32, 47] ethidium bromide[48] and daunomycine,[49] among others. These indicators have specific characteristics to assure high sensitivity and selectivity, such as a well-defined, low potential voltammetric response.[2]

The advantages of this approach include (i) no requirement for modification of target DNA; (ii) no additional hybridisation with further labelled DNA reporter probes and (iii) relatively rapid detection. However, these electrochemical hybridisation indicators are not very sensitive and for the detection of ultralow concentrations of nucleic acids, signal amplification is required.[50] The use of a labelled reporter probe leads to a sandwich type assay, where two hybridisation events took place. The first step involves the hybridisation of the ssDNA target with the immobilised probe, followed by the hybridisation of a reporter probe, which is a short ssDNA sequence bound to the enzyme or nanoparticle.

One solution is the use of a gold nanoparticle linked seconday reporter probe, which effectively "sandwiches" the target DNA. Subsequently, the hybridisation event is detected by measuring the electrochemical signal of the gold nanoparticles following acidic dissolution,[51] direct detection of the gold nanoparticles on the electrode surface (based on stripping voltammetry),[52-53] using silver deposition on the gold nanoparticle in order to enhance the electrochemical signal[54-55] or the use of gold nanoparticles as

carriers for other electroactive labels.[56-57] An alternative approach uses ferrocene as the label.[58]

Another common method is the use of redox-active enzyme labels, which enhances the hybridisation signal. Horse-radish peroxidase (HRP), alkaline phosphatase (AP) and glucose oxidase (GOD) are typical enzyme labels. These enzymes are relatively stable, cheap and they possess high turnover rates.[5] Enzymes are also commercialised as avidin or streptavidin conjugates, and can be attached via biotin/streptavidin link to the target or reporter probe,[59] or enzymes can be directly conjugated to the reporter probe.[8]

1.2.1.2 Label-free methods

Label-free method detects the hybridisation event through changes in the physical properties of the recognition layer that results in a change in the electrical signal.[23] One approach is based on the natural electroactivity of the nucleotide residues present in DNA, first reported by the Palecek group,[60] who monitored the electroactivity of DNA and RNA by studying the signals of adenine, cytosine and guanine by oscillopolarograms of ssDNA, while signals were absent for dsDNA. Among the three bases studied, guanine was described as the most redox-active base in DNA. Other reports detail the guanine oxidation signal for the detection of hybridisation.[61-62]

A second approach is based on changes in properties of the double helix such as conductivity, capacitance or impedance, which can be used to monitor hybridisation. Impedance has been used for the direct *in situ* detection of hybridisation between immobilised oligomer probes with its complementary target DNA, observing a significant shift of the impedance curves along the potential axis.[63] Since then, impedance has been extensively used for label-free electrochemical detection, including femtomolar detection of viral DNA,[64] and reagentless picomolar detection of human immunodeficiency virus (HIV) associated sequences.[65]

1.2.2 Surface chemistry of electrochemical DNA biosensors

Probe immobilisation plays an important role in the performance of electrochemical (EC) DNA biosensors. The most common probes are single-stranded DNA sequences or linear oligonucleotides (18 - 25-mer) although there are other literature examples based on alternative probes such as hairpin oligonucleotide probes,[66] peptide nucleic acids (PNAs)[67] or locked nucleic acids (LNAs)[68]. Short probes show high levels of specificity to the hybridisation step, although longer probes exhibit poor hybridisation specificity and yields.[5]

The electrode surface functionalisation needs an accurate control of the immobilisation process to have optimal and reproducible DNA probe density, spacing and orientation at the electrode surface. Moreover, it should provide an efficient hybridisation of the target DNA sequence, achieving high sensitivity, minimum non-specific adsorption, and consequently high selectivity of the electrode performance. Another important requirement is that the attached layer should not behave as a total insulator, thus allowing electron transfer at the electrode surface.[5]

Typical DNA probe surface coverage is in the order of 10^{11}-10^{13} molecules/cm^2. It is crucial to avoid highly dense surfaces, which can cause charge repulsion between the probes and hence repulsion of target DNA.[21] It has been demonstrated that the probe density can influence the thermodynamics of hybridisation, which, in turn affects the selectivity of the biosensor.[69]

The most commonly used methods for probe immobilisation include adsorption of the oligonucleotides on the surface,[70] retention in a polymeric matrix,[71] covalent attachment on derivatised surfaces[72] and self-assembling of thiolated oligonucleotides.[73] This latter method is currently the most widely used and reported.

The formation of self-assembled monolayers (SAMs) of thiol, sulphide or disulphide containing molecules is one of the most widely used methods for the modification of metal surfaces.[74-75] The attractiveness of SAMs relies on the facility to form a well-defined monolayer.[76] In this case, there is no ambiguity in the nature of the layer formed (i.e. mono- or multilayer) as the driving force is the interaction of the thiol with the gold surface.[77]

Clear advantages can be found for the use of SAMs in DNA sensor formats. SAMs are relatively ordered, with a reasonably strong bond and a simple and cost-effective method for anchoring DNA probes.[27]

The gold-thiol (Au-S) bond energy is 170 kJ/mol, and is thus considered a pseudo-covalent bond and stabilisation of the monolayer is due to van der Waals forces between the neighbouring molecules.[78] However, SAM systems have limitations, particularly with regards to their stability. The potential window is narrow, typically between +1.0 to -1.0 V versus silver/silver chloride, although, this depends on the chain length, the functional group and the quality of the gold surface.[79] The gold-thiolate bond is also prone to oxidisation in air media to sulfinates or sulfonates, limiting its stability to one to two weeks in air.[80] Furthermore, a low thermal stability of SAMs on gold, below 100ºC,[81-82] have limited their usefulness for certain applications. Attempts to increase the stability of SAMs on gold have been made by using multi-thiol anchored molecules[83-84] or *via* the incorporation of cross-linking groups within the alkyl chains.[85-88]

The first reports of the use of SAMs for the development of DNA biosensors were focused on the formation of a reactive thiol SAM followed by the attachment of phosphate, amino or carboxyl-terminated oligonucleotides *via* carbodiimide coupling.[49, 89-90] In order to decrease the number of steps for probe immobilisation, the majority of recent publications have focused on direct immobilisation via the use of thiol modified probes.[73, 91] The first report describing a two-step approach for DNA immobilisation was published in 1997 by Herne and Tarlov,[92] where a second thiolated molecule known as "diluent" or backfiller (e.g. mercaptohexanol (MCH)) was immobilised on the surface following exposure to the thiolated probe (Figure 1.3). As a result, they observed that non-specifically adsorbed DNA was largely removed from the surface, with the probes adopting an optimal orientation, thus improving the overall organisation of the DNA monolayer. This two-step approach is currently still the most reported method for the preparation of DNA biosensors.

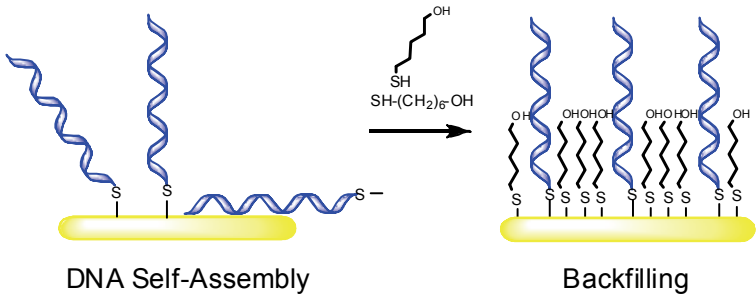

Figure 1.3. DNA immobilisation by two-step approach. First immobilisation of thiol-derivatised probe on the surface of the gold electrode and second exposure to backfiller

A more recently reported approach consists of the simultaneous co-immobilisation of the thiolated probe with the backfiller. This is an attractive methodology which reduces the surface modification to one single step, with a higher control over the final probe density.[93-95] In a recent report, the performance of surfaces prepared by co-immobilisation of thiolated ssDNA probe in the presence of mercaptohexanol at different ratios was studied *via* electrochemical impedance spectroscopy.[93] It was found that the best hybridisation efficiency was achieved at a DNA/MCH ratio of 1:100. Higher ratios of thiolated DNA gave lower hybridisation efficiencies, probably due to steric hindrance at the electrode surface, whilst lower amounts of probe DNA did not improve sensitivity. Furthermore, better results were also obtained by using co-immobilisation in comparison with the two-step "backfilling" approach.

An alternative to the classical immobilisation techniques mentioned above is the electrochemical reduction of aryl diazonium salts.[96] Aromatic diazonium salts, $ArN_2^+X^-$, are well known organic compounds that have been extensively used for years, as for example as a basis for the production of dyes, with the preparation of such compounds normally involving the treatment of aromatic amines with a source of nitrite.

The first report describing the electrochemistry of diazonium salts in mercury electrodes was published in 1958 by Elofson.[97] Later, in 1980, Parker and co-workers reported the formation of a blocking layer on the surface of metallic electrodes such as platinum, gold and mercury, although the nature of this layer was not studied.[98] In

1992, Pinson and co-workers demonstrated that the electrochemical reduction of diazonium salts on carbon surfaces leads to strong chemisorption rather than mere physisorption.[99] Since then, the grafting of diazonium salts has attracted huge interest and grafting and electrografting of diazonium salts have been performed in a large number of materials. Although modification of different forms of carbon surfaces were initially the most studied,[100-107] there are a plethora of reports focused on other substrates such as metals,[108-116] semi-conductors,[117-119] oxides[120-121] and polymers.[122] The high degree of functionalisation of these diazonium based systems allow their application to a wide variety of areas such as biosensors,[77, 123-124] catalysis,[125] and molecular materials (e.g. nanotubes,[126-127] and anti-corrosive agents[115, 128]) among other applications. Their easy preparation, fast reduction and the strong aryl-surface covalent bonding observed has garnered much interest in diazonium based systems.[116, 129]

The classical synthesis of diazonium salts involves the reaction between an aromatic amine and a source of nitrite in an ice-cold aqueous acidic solution, and subsequent filtration and washing of the corresponding precipitate. It can also be performed in aprotic medium (e.g. acetonitrile (ACN)) in the presence of *tert*-butyl nitrile.[96] An easier way is to directly prepare and graft the diazonium salts *in situ*,[104, 109, 130] but this has the drawback that the diazonium compound cannot be characterised. However, studies demonstrate that the electrografting of either isolated or *in-situ* prepared diazonium salt afford similar results.[131]

The modification of substrates with diazonium salts has been carried out in aqueous[128] or organic[130] media and by electrochemical[104, 109, 132] or spontaneous grafting.[128, 133-134]

Reduction of the diazonium cation close to the electrode surface causes elimination of N_2, yielding an aryl radical which attacks the substrate to form a covalent bond (Figure 1.4).[116] However, radicals can either attack already grafted aryl groups resulting in a multilayer film structure.[107, 110] The existence of azo groups within the layers has also been observed[96] and sonication is required to remove organic compounds physisorbed on the surface.

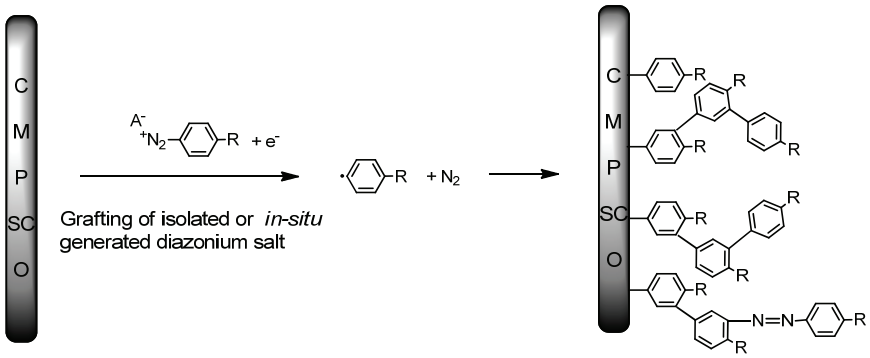

Figure 1.4. Schematic representation of the different reactive possibilities during the surface modifications by reduction of diazonium salts. (C, carbon; M, metal; P, polymer; SC, semi-conductor and O, oxide).

As mentioned above, the resulting organic layers deposited on the surface can have variable thicknesses formed, from monolayers to multilayers.[96] The thickness/number of layers prepared by electrografting not only depends on the exposure time and the potential applied but also on the nature of the starting material.[110,135] Control of the charge consumed during the electrografting step is a convenient way to control the thickness of the layer.[96] Anariba *et al.* reported on the layer thickness of four different diazonium salts deposited under the same electrografting conditions, obtaining different film thicknesses from 1.11 to 2.6 nm and, in all cases, multilayers were formed for more extensive electrolysis or at higher diazonium ion concentrations.[102]

Addressing the difficulty in the control of deposition parameters, efforts have been made to prevent multilayer formation by hindering different positions, *meta* or *para*, of the diazonium ion, resulting in a markedly slower growth of multilayers when substituted in the *para* position in comparison with a non-hindered analogous molecule.[136] More thoroughly, a second report studies the position of the different bulky substituents and its influence on the reaction of aryl radicals with surfaces, demonstrating that grafting efficiency depends on the nature of the amine, the chain length of the alkyl substituent and the substitution position on the aromatic ring showing that the blockage of the grafting and the formation of either mono- and multilayers can be controlled by tuning the diazonium position in the aryl moiety.[137]

Many techniques have been used for the characterisation of the nature of the electrografted layers on different surfaces, for example, X-ray photoelectron spectroscopy (XPS) is used to study the covalent bond formed between the substrate and the organic layer[116, 138-139] and Infrared spectroscopy and ToF-SIMS are also used for its characterisation.[110, 140] On the other hand, film thickness is principally investigated by atomic force microscopy (AFM), ellipsometry, infrared spectroscopic ellipsometry, X-ray reflectivity and X-ray standing waves.[101-102, 141-142]

Aryl diazonium salt derived layers on gold surfaces offer more stable layers than the alkanethiol self-assembly method, although there is less control over the molecular organisation of the layers.[143] Recent computational work indicates comparable aryl-Au and thiol-Au bond energies, of a maximum of 133 and 119 kJ/mol respectively,[144] and experimental work evidences an enhanced stability of diazonium-derived films compared with thiol SAMs analogues.[113]

In recent years, electrodes functionalised with aryl diazonium salts have been reported for a wide range of biosensing applications such as the detection of co-factors, proteins, enzymes and DNA among other relevant biomolecules.[145-151]

1.3 Electrochemical biosensors for DNA diagnostics

Early detection and accurate diagnosis are crucial for patient survival and successful prognosis of disease, particularly for cancer, with electrochemical biosensors offering several advantages over other detection methods,[152-153] such as high sensitivity and specificity. Detection of DNA requires sample manipulation, DNA hybridisation and signal readout, and using EC biosensors, DNA recognition step can take place in minutes, decreasing the total assay time in comparison to other methodologies. In addition, all the steps could be integrated onto portable platforms. An ever increasing important aspect in diagnostics is the capability for multiplexed detection. In the post-genome era, the measurement of a single biomarker particularly for cancer diagnostics and theranostics, is no longer sufficient. Due to the fact that most cancers have many associated markers, multiplex assays are essential for the monitoring of cancer post-

therapy and surgery. Thus, EC arrays, that contain multiple electrodes that are individually targeted to different specific probes, are of great interest for this purpose.[24]

In recent years, many research articles and patents based on biosensors for clinical diagnosis have been published, but the commercialisation of biosensors is still far behind research.[25] Ensafi *et al.* reported a highly sensitive impedimetric DNA sensor based on porphobilinogen deaminase (PBGD) probe to detect specific sequence of porphobilinogen deaminase gene, which is highly associated with Chronic lymphocytic leukemia (CLL) cancer obtaining a detection limit in the range of picomolar.[154]

Bouchet *et al.* presented a multidetection biosensor developed using the electrochemical properties of cylinder-shaped conducting polypyrrole grown on miniaturized graphite electrodes for the discrimination between Human Immunodeficiency Virus (HIV) and Hepatitis B Virus (HBV),[155] reaching a DNA detection limit of 100 pM.

In recent years my research group has been working on the development of sensor arrays for the detection of several diseases, such as several types of cancer, cystic fibrosis and coeliac disease, and its final application at the POC.[8-9, 32, 47, 156-157]

1.4 Single-stranded DNA generation

For analytical applications, including DNA chips, microarrays[158-159] and genosensors, amongst other applications of molecular biology and biotechnology applications, the efficient generation of single-stranded DNA is fundamental.

In the field of genosensors, the most used methodology for ssDNA generation is thermal denaturation commonly termed as *heat and cool*. This consists in heating the dsDNA sample (normally PCR products) to high temperatures (90-95ºC) followed by instantaneous cooling on ice prior to hybridisation.[160-161] The advantages of this methodology are its low cost and simplicity, but the method suffers from very low efficiency and is highly irreproducible. Several alternative methods have been reported for the generation of single stranded DNA, including asymmetric polymerase chain

reaction (PCR), urea-polyacrylamide gel electrophoresis (Urea-PAGE), exonuclease digestion and the use of magnetic beads.

An alternative approach is selective strand digestion using exonuclease digestion. Lambda and T7 Gene 6 exonucleases are the two most commonly used. Lambda exonuclease selectively digests a 5'-phosphorylated strand of dsDNA with a high processivity. In this case, one of the primer pairs used in PCR is 5'-phosphorylated resulting in a dsDNA duplex, where one of the strands has a phosphate group introduced in the 5' position. Following incubation with the lambda exonuclease this strand is selectively digested and the exonuclease activity is then stopped by heating at 85ºC.[162] On the other hand, T7 Gene 6 exonuclease acts non-processively in the 5´- 3´ direction from both 5´-phosphoryl or 5´-hydroxyl nucleotides.[163] To protect from T7 Gene 6 exonuclease, one of the primers is capped with phosphorothioates, so the strand containing this modification will not be digested.[164] After incubation, the enzyme is inactivated by heating. Both these approaches have been effectively used for the generation of ssDNA, but do involve extra costs in terms of the modified primers and the enzymes themselves.

Apart from the *heat and cool* method, one of the most widely used techniques for the generation of ssDNA is the use of a biotinylated dsDNA.[165] The biotinylated dsDNA PCR product is immobilised on streptavidin coated magnetic beads and the non-biotinylated ssDNA is isolated by alkaline/heat denaturation.

1.5 DNA amplification

DNA amplification is a key concept in molecular genetics, clinical analysis, environmental microbiology, forensics, etc.

In the development of DNA biosensors, a limiting factor is the required sensitivity when working with real samples, e.g. in a viral infection the amount of DNA that has to be detected can be in the attomolar range.[6]

The polymerase chain reaction (PCR) is the most popular method used for DNA amplification, although alternative methods based on isothermal methods are also of interest.

1.5.1 Non-isothermal methods

The polymerase chain reaction (PCR) is the most well known and widely used technique for the amplification of DNA. It was developed in the mid-80s by Kary Mullis and co-workers,[166] for which Mullis won the Nobel prize in Chemistry in 1993.

Thermal PCR is based on thermal cycling and polymerase activity for primer-directed target amplification (Figure 1.5). This is made possible by using *Taq* DNA Polymerase, a highly thermostable DNA polymerase of the thermophilic bacterium *Thermus aquaticus,* which maintains its activity at elevated temperatures.

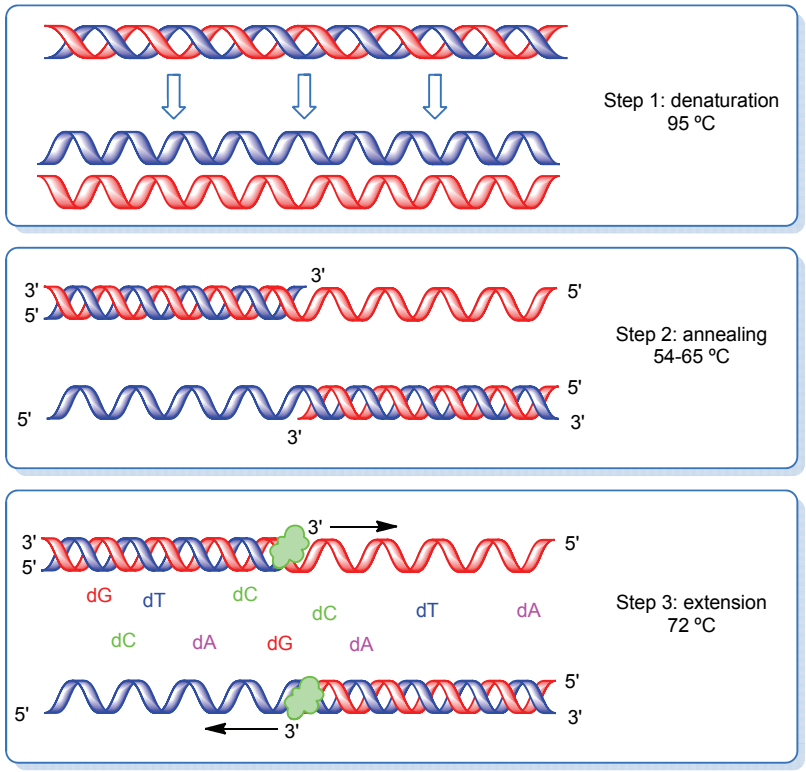

Figure 1.5. Schematic representation of the polymerase chain reaction.

During PCR, the amount of DNA template (either ssDNA or dsDNA) is exponentially amplified by repetitive cycles. Its principle is based on the mechanism of DNA replication *in vivo*, denaturation of the dsDNA template to ssDNA and duplication. High temperature, normally around 95ºC, is used in order to separate the two strands and then, the temperature is decreased to allow the primers to anneal to the template. The annealing temperature depends on the primers. Normally it should be around 5ºC below the melting temperature of the primers in order to anneal with the targeted sequences. Finally the temperature is increased to 72ºC, which is the normal optimal temperature for the polymerase that extends the primers by incorporating the corresponding dNTPs.

Traditional PCR as an analytical technique has some limitations. The most important is that the exponential amplification of the target, independent of the initial concentration, reaches saturation after a certain number of cycles, and thus the initial concentration of DNA target cannot be quantified, but real-time PCR addresses this limitation.[167] In this case, the amplification is monitored during the course of the reaction due to the monitoring of the change in the fluorescence of a reporter probe. This change is proportional to the amount of product amplified. Reporter probes include DNA binding dyes, e.g. SYBR Green, which gave non-specific detection, or for better specificity, detection can be carried out with target specific probes (e.g. molecular beacons). Multiplexing with target binding dyes is facilitated by melting curve analysis but is not straightforward, whilst the grade of multiplexing for target specific probes is currently limited by the overlapping spectra of fluorophore labels available and the resolution of the optical detectors.

1.5.2 Isothermal methods

Whilst the use of PCR-based amplification is extensive, the need for temperature cycling to separate the two strands is a drawback, limiting its use in point-of-care applications, particularly in low resource settings. To overcome this, different isothermal amplification methods that do not require extreme heating or thermal cycling of the dsDNA for the separation of the two strands have been developed.

The most common isothermal methods include nucleic acid sequence-based amplification (NASBA),[168-169] loop-mediated isothermal amplification (LAMP),[170] rolling circle amplification (RCA),[171] strand displacement amplification (SDA)[172-173] and helicase-dependent amplification (HDA).[174]

1.5.2.1 Helicase-dependent amplification (HDA)

Isothermal helicase-dependent amplification methodology was introduced by Vincent *et al.* in 2004 and is based on the natural mechanism of the DNA replication fork.[174] The advantage of HDA is its PCR like reaction scheme (denaturation, primer annealing and primer extension steps).[175] The key difference relies on the use of helicase to unwind the dsDNA and allow annealing of the two specific primers. DNA polymerase extends the primers to produce two dsDNA target copies which can be copied again, thus allowing exponential amplification (Figure 1.6).

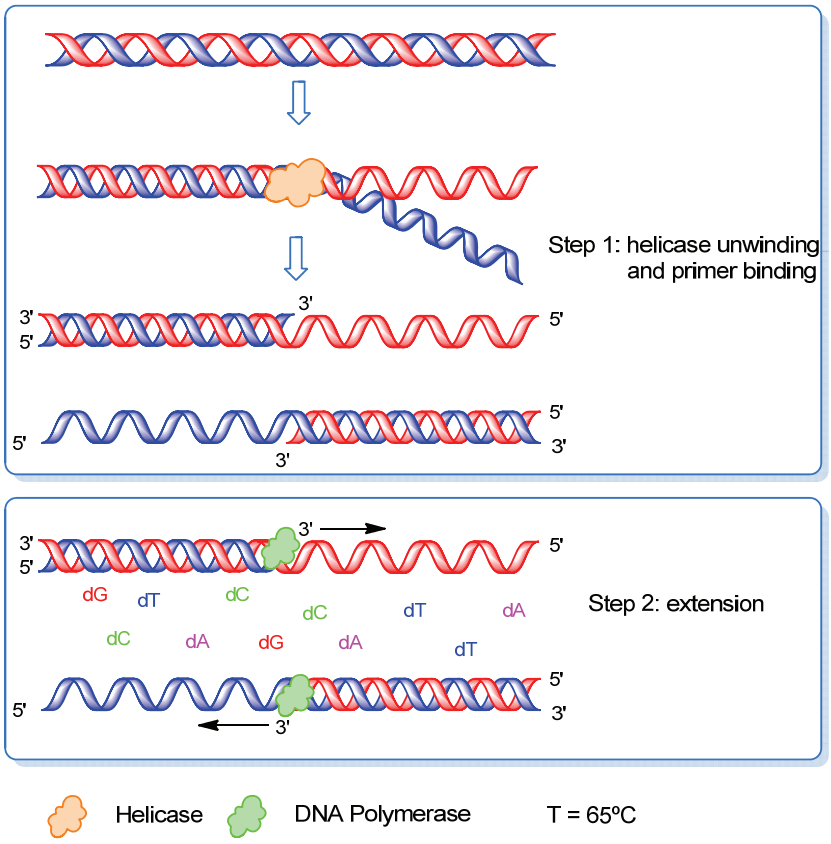

Figure 1.6. Schematic representation of the helicase-dependent DNA amplification.

Vincent *et al.* reported a mesophilic form of HDA (mHDA), using the *Escherichia coli* UvrD helicase (active at 37ºC), with DNA polymerase and two accessory proteins (methyl-directed mismatch repair protein MutL and single-stranded binding protein SSB). With this amplification system they were able to detect 500 copies of *Brugia malayi* genomic DNA directly from blood samples. Nevertheless, this mHDA system cannot amplify long target sequences efficiently, due to its longer reaction times and processivity.[176] An *et al.* reported an improved HDA (tHDA) using a thermostable UvrD helicase (taken from *Thermoanaerobacter tengcongensis*), that allows the reaction to occur at higher temperature (60-65ºC). Sensitivity and specificity were improved due to more stringent primer annealing conditions, reporting a sensitivity of as few as 10 copies of bacterial genomic DNA.[177]

The major drawback of HDA methodology is the lack of processivity and the fact that only short DNA sequences of between 70-120 bp can be amplified with the current HDA systems[175] (IsoAmpIII Universal tHDA Kit from BioHelix), due to the deficient coordination between the helicase and the polymerase during the process. To overcome these restrictions, Motre *et al.* reported the 'helimerase', a hybrid protein halfway between the helicase and the DNA polymerase which permits DNA amplification up to 2.3 kb.[178]

HDA has the potential to be integrated in miniaturised, automated point-of-care devices and in microarray technology due to its simplicity, multiplexing capability and isothermal characteristic, thus avoiding thermocycling and Peltier integration.[175] Andersen *et al.* reported the adaptation of HDA on a microarray for the detection of two pathogens. One primer was immobilised on the microarray surface (glass slide) and the second labelled primer was added to the reaction solution. Amplified products remained attached and were detected by laser scanning or total internal reflection fluorescence (TIRF) technologies.[179]

The development of HDA microfluidic chips has garnered an enormous interest in the recent years. Ramalingam *et al.* developed a real-time HDA PDMS microfluidic device consisting of four parallel microchambers with pre-loaded pairs of primers.[180] On the other hand, a fully integrated microfluidic device combining sample preparation and real-time HDA starting from whole cells was developed by Mahalanabis *et al.* The device was proved to detect as few as ten colony forming units (CFU) of *E. coli* in growth medium.[181]

More recently, Kivlehan *et al.* reported the first electrochemical detection method for real-time monitoring of isothermal HDA, using a DNA intercalating redox probe that becomes less electrochemically detectable upon binding with the amplified dsDNA, in comparison with the signal obtained when it is free in solution.[182]

1.5.3 Miniaturised nucleic acid amplification

In recent years, there has been an increased interest in the generation of POC molecular diagnostic devices. Miniaturisation of nucleic acid amplification methods

offers several advantages such as the possibility to decrease required time, the use of lower sample volumes, reduction of instrumentation costs and the ability to perform the complete analysis on a single chip. On the other hand, as previously commented, electrochemical DNA methods are extensively used in POC applications due to their features, and in the last decade, several examples of detection of real-time nucleic acid amplification have been reported.

For PCR, different electrochemical detection techniques have been described. Marchal *et al.*[183] indirectly monitored the amplified DNA product generated in the PCR reaction solution after each PCR cycle, by electrochemically monitoring the catalytic oxidation of free dGTP or 7-deaza-dGTP in the presence of $Ru(bpy)_3^{3+}$ or $Os(bpy)_3^{3+}$ respectively and Limoges *et al.*[184] used a redox intercalating probe which became electrochemically less active upon dsDNA intercalation.

Another electrochemical RT-PCR system based on the intercalative binding of methylene blue with dsDNA was reported by Park *et al,*[185] whilst Hsing and co-workers described for the first time a solid-phase electrochemical real-time PCR.[186] In this case, a ferrocene-tagged dUTP was used to monitor the change in current signal associated to the base extension of the immobilised primers on a silicon-glass microchip surface. The first report describing the electrochemical real-time monitoring of isothermal HDA was published by Marchal *et al,*[187] with a similar detection strategy.

1.6 Human Papillomavirus and cervical cancer

Papillomaviruses, including human papillomavirus (HPV), are nonenveloped, double-stranded DNA viruses. The HPV genome (Figure 1.7) is relatively small (6.9 to 8 kb) and encodes 8 genes, 6 of them coding for nonstructural early proteins (E1, E2, E4, E5, E6 and E7) and 2 for structural or late proteins (L1 and L2).[188]

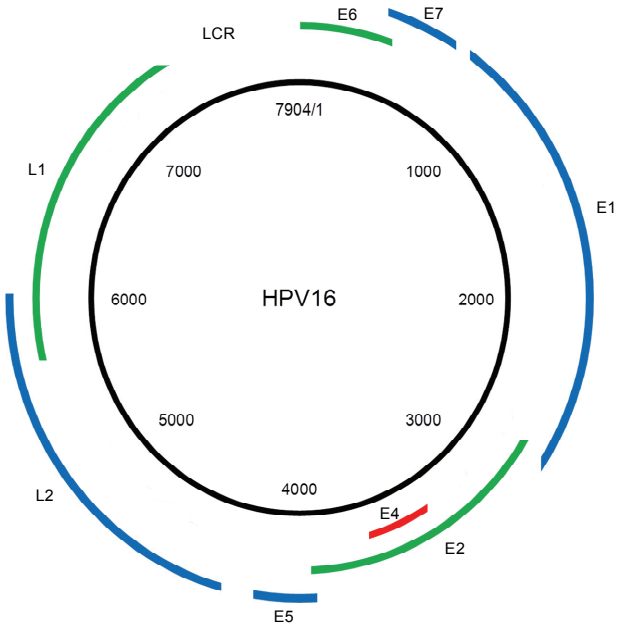

Figure 1.7. Schematic representation of the HPV16 genome, where E1-E7 are the early genes, L1 and L2 the late genes and the long control region (LCR).

HPV is one of the most common sexually transmitted infections, affecting the skin and mucous membranes.[189] More than 200 HPV types have been identified with greater than 40 HPV types infecting the genital areas of men and women that can induce a wide range of clinical manifestations, including cervical, vaginal, and vulvar intraepithelial neoplasias, genital warts and cancer of cervix, vagina, and vulva.[188, 190] It is predicted that around 30-50% of the women will be infected during their lifetime.

Genital HPV types have been subdivided into low-risk, forming genital warts (HPV6, 11, 40, 42, 43, 44, 53, 54, 61, 72, 73 and 81) and the high-risk types (HPV16, 18, 31, 33, 35, 39, 45, 51, 52, 56, 58, 59 and 68), which are detected in virtually all invasive cervical cancers and have been confirmed as the major cause of this cancer.[190] The classic high-risk HPV types are 16 and 18[191] although types 31 and 45 are also found in approximately 80% of cervical cancer cases together with types 16 and 18.[192] A key step in the development of cervical cancers is the dysregulated expression of the viral oncogenes E6 and E7. Expression of the corresponding oncoproteins interferes

with the protective function of the cellular proteins p53 and retinoblastoma protein (pRb) respectively, and thereby induce uncontrolled cell growth and genetic instability.[193-194]

Cervical cancer ranks as the 11th most frequent cancer in Spain and the 2nd among women between 15-44 years old. In Spain, there are 18.83 million women older than 15 years that have a risk of developing cervical cancer. Every year, 1948 women are diagnosed with cervical cancer and 712 die from the disease.[195]

1.6.1 Human papillomavirus diagnostics

The recognition that persistent infection of the high-risk HPV types is essential for the development of cervical cancer has been extremely important[196] and highlights the importance of the early and cost-effective detection of these DNA strains.[197]

HPV diagnostics are commonly based on molecular recognition for the detection of HPV DNA related sequences in cervical scrape samples. These molecular tools can be divided into two major groups: those based on nucleic acid assays, where hybrid capture technology (developed by Digene Corporation) is the most widely used technique, and the other major group based on amplification techniques such as the polymerase chain reaction (PCR).[198]

Another, less explored possibility for the detection of HPV is the use of DNA biosensors. Different types of genosensors with piezoelectric,[160] leaky surface acoustic wave[199] or giant magnetoresistive detection[200] have been reported for the detection of HPV. The electrochemical detection of HPV related sequences has been also reported in the past few years, using for instance, methylene-blue as a hybridisation indicator [201] or exploiting reporter probes labelled with ferrocene.[202] In the first case, a 20-mer probe related to the HPV major capsid protein L1 was immobilised on a graphite electrode and the methylene-blue response was recorded before and after target recognition and hybridisation, achieving a limit of detection of 1.2 ng/μL (200 nM). The second example involved the use of a hybridisation-based bioelectronic DNA detection platform (eSensor™), for the detection of HPV sequences based on 14

thiolated probes immobilised on the chip surface and hybridisation with a ferrocene-labelled reporter sequence. Hybridisation required up to 8 h at 40ºC, detecting 86 % of the HPV targets in clinical samples giving a positive/negative type response.

1.7 Thesis objectives

Current efforts in the development of biosensors focus on new platforms for accurate and sensitive analysis for disease diagnostics. With the increasing number of cancer cases being diagnosed worldwide and the high number of deaths due to a late diagnosis, biosensors can play an important role in the early diagnosis of cancer.

In this work, we focused our attention on the development of an electrochemical DNA biosensor and solid-phase amplification method for the detection of human papillomavirus genes.

Human papillomavirus is one of the most common sexually transmitted infections, and it has been proved that persistent infection of the high-risk HPV types probably leads to the development of cervical cancer. At this moment, many of the commercial tests available are slow, expensive, require large amounts of sample materials, and can lead to false positive or negative results.

For this reason, an electrochemical biosensor array has been postulated as a promising alternative to analyse multiple high-risk HPV sequences (HPV16, HPV18 and HPV45), capable of overcoming most of the issues of traditional healthcare sensors. To accomplish this, specific objectives have been set:

- Determine the optimal surface functionalisation approach in order to achieve high sensitivity, stability and occurrence of non-specific interactions.
- Determine optimum hybridisation conditions and detection strategy.
- Study cross-reactivity between selected HPV sequences and multiplex measurements.
- Study other parameters such as reusability and stability of the platform.
- Evaluate the use of the electrochemical biosensor for the detection of clinical samples.
- Determine the best strategy to generate ssDNA in order to detect the clinical samples.

Even though electrochemical biosensors provide quantitative detection, additional DNA amplification step of clinical samples, and the subsequent generation of ssDNA is commonly required. This, not only increases the total assay time, but different yields of ssDNA could be obtained dependent on, for example, GC content or amplicon length, which can extensively complicate true quantitation for medium-high multiplexing. A solution would consist of the real-time monitoring of solid-phase amplification, which would permit the rapid and facile measurement of specific nucleic acid sequences, providing a more reliable and accurate quantitation.

In order to develop and further investigate this approach, an electrochemical monitoring of the helicase-dependent amplification in solid phase assay has been proposed. For this, several sub-objectives have been established:

- Choice of a suitable surface chemistry able to satisfy important requirements such as robustness, thermal stability and reproducibility.
- Design of a robust electrochemical real-time solid-phase amplification setup capable of allowing in-time monitorisation of the reaction fulfilling temperature requisites for an optimal amplification.
- Optimisation of the assay conditions which is based on the selection of a primer immobilisation strategy, the amplification method protocol and the electrochemical technique to monitor the reaction.
- Study the biocompatibility with the microfluidic device. Overcome possible solvent evaporation issues, non-specific adsorption on the walls of the channels and surface side-effects.

Overall, this work will contribute in different areas involved in the development of electrochemical quantitative sensing platforms and solid-phase amplification methods, from fundamental aspects such as the choice of a robust and reliable surface chemistry to ssDNA generation.

1.8 References

1. D. R. Thévenot, K. Toth, R. A. Durst and G. S. Wilson, *Biosensors and Bioelectronics*, 2001, **16**, 121-131.
2. W. Joseph, *Analytica Chimica Acta*, 2002, **469**, 63-71.
3. A. Sassolas, B. D. Leca-Bouvier and L. J. Blum, *Chemical Reviews*, 2007, **108**, 109-139.
4. G. A. Rivas, M. L. Pedano and N. F. Ferreyra, *Analytical Letters*, 2005, **38**, 2653-2703.
5. F. Lucarelli, S. Tombelli, M. Minunni, G. Marrazza and M. Mascini, *Analytica Chimica Acta*, 2008, **609**, 139-159.
6. M. Campàs and I. Katakis, *TrAC Trends in Analytical Chemistry*, 2004, **23**, 49-62.
7. L. De Lellis, M. C. Curia, S. Veschi, G. M. Aceto, A. Morgano and A. Cama, *Expert Review of Molecular Diagnostics*, 2008, **8**, 41-52.
8. O. Y. F. Henry, J. L. A. Sanchez and C. K. O'Sullivan, *Biosensors and Bioelectronics*, 2010, **26**, 1500-1506.
9. O. Y. Henry, A. Fragoso, V. Beni, N. Laboria, J. L. A. Sánchez, D. Latta, F. Von Germar, K. Drese, I. Katakis and C. K. O'Sullivan, *Electrophoresis*, 2009, **30**, 3398-3405.
10. X. Fang, X. Liu, S. Schuster and W. Tan, *Journal of the American Chemical Society*, 1999, **121**, 2921-2922.
11. L. Song, S. Ahn and D. R. Walt, *Analytical Chemistry*, 2006, **78**, 1023-1033.
12. A. Rachkov, S. Patskovsky, A. Soldatkin and M. Meunier, *Talanta*, 2011, **85**, 2094-2099.
13. Y. L. Jung, C. Jung, H. Parab, T. Li and H. G. Park, *Biosensors and Bioelectronics*, 2010, **25**, 1941-1946.
14. R. Kanjanawarut and X. Su, *Analytical Chemistry*, 2009, **81**, 6122-6129.
15. P. Liu, X. Hun and H. Qing, *Microchimica Acta*, 2011, **175**, 201-207.
16. E. Papadopoulou and S. E. J. Bell, *Chemical Communications*, 2011, **47**, 10966-10968.
17. A. B. Mattos, T. A. Freitas, V. L. Silva and R. F. Dutra, *Sensors and Actuators B: Chemical*, 2012, **161**, 439-446.
18. G. García-Martinez, E. A. Bustabad, H. Perrot, C. Gabrielli, B. Bucur, M. Lazerges, D. Rose, L. Rodriguez-Pardo, J. Fariña, C. Compère and A. A. Vives, *Sensors*, 2011, **11**, 7656-7664.
19. B. H. Cha, S.-M. Lee, J. C. Park, K. S. Hwang, S. K. Kim, Y.-S. Lee, B.-K. Ju and T. S. Kim, *Biosensors and Bioelectronics*, 2009, **25**, 130-135.

20. S. M. Yang, C. Chang, T. I. Yin and P. L. Kuo, *Sensors and Actuators B: Chemical*, 2008, **130**, 674-681.
21. J. J. Gooding, *Electroanalysis*, 2002, **14**, 1149-1156.
22. J. P. Tosar, G. Brañas and J. Laíz, *Biosensors and Bioelectronics*, 2010, **26**, 1205-1217.
23. C. Batchelor-McAuley, G. G. Wildgoose and R. G. Compton, *Biosensors and Bioelectronics*, 2009, **24**, 3183-3190.
24. F. Wei, P. B. Lillehoj and C. M. Ho, *Pediatric Research*, 2010, **67**, 458-468.
25. P. D'Orazio, *Clinica Chimica Acta*, 2011, **412**, 1749-1761.
26. M. Mir, A. Homs and J. Samitier, *Electrophoresis*, 2009, **30**, 3386-3397.
27. F. R. R. Teles and L. P. Fonseca, *Talanta*, 2008, **77**, 606-623.
28. K. Jayakumar, R. Rajesh, V. Dharuman, R. Venkatasan, J. H. Hahn and S. Karutha Pandian, *Biosensors and Bioelectronics*, 2012, **31**, 406-412.
29. C. A. Marquette, M. F. Lawrence and L. J. Blum, *Analytical Chemistry*, 2006, **78**, 959-964.
30. C. Tlili, H. Korri-Youssoufi, L. Ponsonnet, C. Martelet and N. J. Jaffrezic-Renault, *Talanta*, 2005, **68**, 131-137.
31. Q. D. Zhang, G. March, V. Noel, B. Piro, S. Reisberg, L. D. Tran, L. V. Hai, E. Abadia, P. E. Nielsen, C. Sola and M. C. Pham, *Biosensors and Bioelectronics,* 2012, **32**, 163-168.
32. O. Y. F. Henry, J. L. Acero Sanchez, D. Latta and C. K. O'Sullivan, *Biosensors and Bioelectronics*, 2009, **24**, 2064-2070.
33. M. Tichoniuk, D. Gwiazdowska, M. Ligaj and M. Filipiak, *Biosensors and Bioelectronics*, 2010, **26**, 1618-1623.
34. M. Steichen, Y. Decrem, E. Godfroid and C. Buess-Herman, *Biosensors and Bioelectronics*, 2007, **22**, 2237-2243.
35. K. Hashimoto, K. Ito and Y. Ishimori, *Sensors and Actuators B: Chemical*, 1998, **46**, 220-225.
36. J. Wang, J. Li, A. J. Baca, J. Hu, F. Zhou, W. Yan and D.-W. Pang, *Analytical Chemistry*, 2003, **75**, 3941-3945.
37. Z.-S. Wu, J.-H. Jiang, G.-L. Shen and R.-Q. Yu, *Human Mutation*, 2007, **28**, 630-637.
38. X. Jiang, K. Chen and H. Han, *Biosensors and Bioelectronics*, 2011, **28**, 464-468.
39. X.-M. Li, P.-Y. Fu, J.-M. Liu and S.-S. Zhang, *Analytica Chimica Acta*, 2010, **673**, 133-138.

40. Z. P. Aguilar and I. Fritsch, *Analytical Chemistry*, 2003, **75**, 3890-3897.
41. S. Suye, T. Matsuura, T. Kimura, H. Zheng, T. Hori, Y. Amano and H. Katayama, *Microelectronic Engineering*, 2005, **81**, 441-447.
42. K. M. Millan, A. Saraullo and S. R. Mikkelsen, *Analytical Chemistry*, 1994, **66**, 2943-2948.
43. J. Wang, G. Rivas, X. Cai, M. Chicharro, C. Parrado, N. Dontha, A. Begleiter, M. Mowat, E. Palecek and P. E. Nielsen, *Analytica Chimica Acta*, 1997, **344**, 111-118.
44. K. M. Millan and S. R. Mikkelsen, *Analytical Chemistry*, 1993, **65**, 2317-2323.
45. M. E. Napier, C. R. Loomis, M. F. Sistare, J. Kim, A. E. Eckhardt and H. H. Thorp, *Bioconjugate Chemistry*, 1997, **8**, 906-913.
46. Y.-S. Choi, K.-S. Lee and D.-H. Park, *Current Applied Physics*, 2006, **6**, 777-780.
47. H. Nasef, V. Beni and C. O'Sullivan, *Analytical and Bioanalytical Chemistry*, 2010, **396**, 1423-1432.
48. S. Liu, J. Ye, P. He and Y. Fang, *Analytica Chimica Acta*, 1996, **335**, 239-243.
49. X. Sun, P. He, S. Liu, J. Ye and Y. Fang, *Talanta*, 1998, **47**, 487-495.
50. P. Scrimin and L. J. Prins, *Chemical Society Reviews*, 2011, **40**, 4488-4505.
51. L. Authier, C. Grossiord, P. Brossier and B. Limoges, *Analytical Chemistry*, 2001, **73**, 4450-4456.
52. M. Ozsoz, A. Erdem, K. Kerman, D. Ozkan, B. Tugrul, N. Topcuoglu, H. Ekren and M. Taylan, *Analytical Chemistry*, 2003, **75**, 2181-2187.
53. C. S. Ah, Y. J. Yun, H. J. Park, S. K. Jung, W.-J. Kim, D. H. Ha and W. S. Yun, *Current Applied Physics*, 2006, **6**, e157-e160.
54. R. Möller, R. D. Powell, J. F. Hainfeld and W. Fritzsche, *Nano Letters*, 2005, **5**, 1475-1482.
55. T. A. Taton, C. A. Mirkin and R. L. Letsinger, *Science*, 2000, **289**, 1757-1760.
56. A. J. Baca, F. Zhou, J. Wang, J. Hu, J. Li, J. Wang and Z. S. Chikneyan, *Electroanalysis*, 2004, **16**, 73-80.
57. A.-N. Kawde and J. Wang, *Electroanalysis*, 2004, **16**, 101-107.
58. R. M. Umek, S. W. Lin, J. Vielmetter, R. H. Terbrueggen, B. Irvine, C. J. Yu, J. F. Kayyem, H. Yowanto, G. F. Blackburn, D. H. Farkas and Y.-P. Chen, *The Journal of Molecular Diagnostics*, 2001, **3**, 74-84.
59. G. Carpini, F. Lucarelli, G. Marrazza and M. Mascini, *Biosensors and Bioelectronics*, 2004, **20**, 167-175.

60. E. Palecek, *Nature*, 1960, **188**, 656-657.
61. K. Kerman, Y. Morita, Y. Takamura and E. Tamiya, *Electrochemistry Communications*, 2003, **5**, 887-891.
62. B. Meric, K. Kerman, D. Ozkan, P. Kara and M. Ozsoz, *Electroanalysis*, 2002, **14**, 1245-1250.
63. E. Souteyrand, J. P. Cloarec, J. R. Martin, C. Wilson, I. Lawrence, S. Mikkelsen and M. F. Lawrence, *The Journal of Physical Chemistry B*, 1997, **101**, 2980-2985.
64. F. Patolsky, A. Lichtenstein, M. Kotler and I. Willner, *Angewandte Chemie International Edition*, 2001, **40**, 2261-2265.
65. Y. Fu, R. Yuan, Y. Chai, L. Zhou and Y. Zhang, *Analytical Letters*, 2006, **39**, 467-482.
66. P. V. Riccelli, F. Merante, K. T. Leung, S. Bortolin, R. L. Zastawny, R. Janeczko and A. S. Benight, *Nucleic Acids Research*, 2001, **29**, 996-1004.
67. D. P. Chandler, J. R. Stults, K. K. Anderson, S. Cebula, B. L. Schuck and F. J. Brockman, *Analytical Biochemistry*, 2000, **283**, 241-249.
68. K. Wang, Z. Sun, M. Feng, A. Liu, S. Yang, Y. Chen and X. Lin, *Biosensors and Bioelectronics*, 2011, **26**, 2870-2876.
69. J. H. Watterson, P. A. E. Piunno, C. C. Wust and U. J. Krull, *Langmuir*, 2000, **16**, 4984-4992.
70. F. Azek, C. Grossiord, M. Joannes, B. Limoges and P. Brossier, *Analytical Biochemistry*, 2000, **284**, 107-113.
71. Y. Hasebe, K. Hamada, T. Hirano and S. Uchiyama, *Analytical Communications*, 1997, **34**, 153-154.
72. D. J. Caruana and A. Heller, *Journal of the American Chemical Society*, 1999, **121**, 769-774.
73. D. M. Jenkins, B. Chami, M. Kreuzer, G. Presting, A. M. Alvarez and B. Y. Liaw, *Analytical Chemistry*, 2006, **78**, 2314-2318.
74. J. C. Love, L. A. Estroff, J. K. Kriebel, R. G. Nuzzo and G. M. Whitesides, *Chemical Reviews*, 2005, **105**, 1103-1169.
75. C. D. Bain, E. B. Troughton, Y. T. Tao, J. Evall, G. M. Whitesides and R. G. Nuzzo, *Journal of the American Chemical Society*, 1989, **111**, 321-335.
76. J. C. Love, L. A. Estroff, J. K. Kriebel, R. G. Nuzzo and G. M. Whitesides, *Chemical Reviews*, 2005, **105**, 1103-1170.
77. J. J. Gooding, *Electroanalysis*, 2008, **20**, 573-582.

78. C. Vericat, M. E. Vela and R. C. Salvarezza, *Physical Chemistry Chemical Physics*, 2005, **7**, 3258-3268.
79. H. O. Finklea, S. Avery, M. Lynch and T. Furtsch, *Langmuir*, 1987, **3**, 409-413.
80. T. M. Willey, A. L. Vance, T. van Buuren, C. Bostedt, L. J. Terminello and C. S. Fadley, *Surface Science*, 2005, **576**, 188-196.
81. F. Bensebaa, T. H. Ellis, A. Badia and R. B. Lennox, *Langmuir*, 1998, **14**, 2361-2367.
82. E. Delamarche, B. Michel, H. Kang and C. Gerber, *Langmuir*, 1994, **10**, 4103-4108.
83. Z. Li, R. C. Jin, C. A. Mirkin and R. L. Letsinger, *Nucleic Acids Research*, 2002, **30**, 1558-1562.
84. T. T. Wooster, P. R. Gamm, W. E. Geiger, A. M. Oliver, A. J. Black, D. C. Craig and M. N. PaddonRow, *Langmuir*, 1996, **12**, 6616-6626.
85. N. Garg, E. Carrasquillo-Molina and T. R. Lee, *Langmuir*, 2002, **18**, 2717-2726.
86. R. Valiokas, M. Ostblom, S. Svedhem, S. C. T. Svensson and B. Liedberg, *Journal of Physical Chemistry B*, 2002, **106**, 10401-10409.
87. R. S. Clegg, S. M. Reed and J. E. Hutchison, *Journal of the American Chemical Society*, 1998, **120**, 2486-2487.
88. T. Kim, K. C. Chan and R. M. Crooks, *Journal of the American Chemical Society*, 1997, **119**, 189-193.
89. Y.-D. Zhao, D.-W. Pang, S. Hu, Z.-L. Wang, J.-K. Cheng and H.-P. Dai, *Talanta*, 1999, **49**, 751-756.
90. M. E. Napier and H. H. Thorp, *Langmuir*, 1997, **13**, 6342-6344.
91. A. B. Steel, T. M. Herne and M. J. Tarlov, *Analytical Chemistry*, 1998, **70**, 4670-4677.
92. T. M. Herne and M. J. Tarlov, *Journal of the American Chemical Society*, 1997, **119**, 8916-8920.
93. O. Y. F. Henry, J. G. Perez, J. L. A. Sanchez and C. K. O'Sullivan, *Biosensors and Bioelectronics*, 2010, **25**, 978-983.
94. S. D. Keighley, P. Li, P. Estrela and P. Migliorato, *Biosensors and Bioelectronics*, 2008, **23**, 1291-1297.
95. C. Boozer, S. Chen and S. Jiang, *Langmuir*, 2006, **22**, 4694-4698.
96. D. Belanger and J. Pinson, *Chemical Society Reviews*, 2011, **40**, 3995-4048.
97. R. M. Elofson, *Canadian Journal of Chemistry*, 1958, **36**, 1207-1210.
98. E. Ahlberg, B. Helgée and V. D. Parker, *Acta Chemica Scandinavica B*, 1980, **34**, 181-186.

99. M. Delamar, R. Hitmi, J. Pinson and J. M. Saveant, *Journal of the American Chemical Society*, 1992, **114**, 5883-5884.
100. C. Saby, B. Ortiz, G. Y. Champagne and D. Belanger, *Langmuir*, 1997, **13**, 6805-6813.
101. P. A. Brooksby and A. J. Downard, *Langmuir*, 2004, **20**, 5038-5045.
102. F. Anariba, S. H. DuVall and R. L. McCreery, *Analytical Chemistry*, 2003, **75**, 3837-3844.
103. G. Liu, J. Liu, T. Böcking, P. K. Eggers and J. J. Gooding, *Chemical Physics*, 2005, **319**, 136-146.
104. S. Baranton and D. Belanger, *Journal of Physical Chemistry B*, 2005, **109**, 24401-24410.
105. P. Allongue, M. Delamar, B. Desbat, O. Fagebaume, R. Hitmi, J. Pinson and J. M. Saveant, *Journal of the American Chemical Society*, 1997, **119**, 201-207.
106. T. Breton and D. Belanger, *Langmuir*, 2008, **24**, 8711-8718.
107. J. K. Kariuki and M. T. McDermott, *Langmuir*, 2001, **17**, 5947-5951.
108. A. Laforgue, T. Addou and D. Belanger, *Langmuir*, 2005, **21**, 6855-6865.
109. J. Lyskawa and D. Belanger, *Chemistry of Materials*, 2006, **18**, 4755-4763.
110. A. Ricci, C. Bonazzola and E. J. Calvo, *Physical Chemistry Chemical Physics*, 2006, **8**, 4297-4299.
111. M. G. Paulik, P. A. Brooksby, A. D. Abell and A. J. Downard, *Journal of Physical Chemistry C*, 2007, **111**, 7808-7815.
112. J. Haccoun, C. Vautrin-Ul, A. Chaussé and A. Adenier, *Progress in Organic Coatings*, 2008, **63**, 18-24.
113. D. M. Shewchuk and M. T. McDermott, *Langmuir*, 2009, **25**, 4556-4563.
114. A. Adenier, C. Combellas, F. Kanoufi, J. Pinson and F. I. Podvorica, *Chemistry of Materials*, 2006, **18**, 2021-2029.
115. A. Chausse, M. M. Chehimi, N. Karsi, J. Pinson, F. Podvorica and C. Vautrin-Ul, *Chemistry of Materials*, 2002, **14**, 392-400.
116. K. Boukerma, M. M. Chehimi, J. Pinson and C. Blomfield, *Langmuir*, 2003, **19**, 6333-6335.
117. J. Pinson and F. Podvorica, *Chemical Society Reviews*, 2005, **34**, 429-439.
118. C. H. de Villeneuve, J. Pinson, M. C. Bernard and P. Allongue, *The Journal of Physical Chemistry B*, 1997, **101**, 2415-2420.
119. P. Allongue, C. H. de Villeneuve, J. Pinson, F. Ozanam, J. N. Chazalviel and X. Wallart, *Electrochimica Acta*, 1998, **43**, 2791-2798.
120. F. Mirkhalaf, T. J. Mason, D. J. Morgan and V. Saez, *Langmuir*, 2011, **27**, 1853-1858.

121. A. Merson, T. Dittrich, Y. Zidon, J. Rappich and Y. Shapira, *Applied Physics Letters*, 2004, **85**, 1075-1076.
122. C. Combellas, F. Kanoufi, D. Mazouzi, A. Thiébault, P. Bertrand and N. Médard, *Polymer*, 2003, **44**, 19-24.
123. F. Li, W. Chen, P. Dong and S. Zhang, *Biosensors and Bioelectronics*, 2009, **24**, 2160-2164.
124. A. E. Radi, V. Lates and J. L. Marty, *Electroanalysis*, 2008, **20**, 2557-2562.
125. S. Liu, Z. Tang, Z. Shi, L. Niu, E. Wang and S. Dong, *Langmuir*, 1999, **15**, 7268-7275.
126. C. S. Lee, S. E. Baker, M. S. Marcus, W. S. Yang, M. A. Eriksson and R. J. Hamers, *Nano Letters*, 2004, **4**, 1713-1716.
127. M. Majumder, K. Keis, X. Zhan, C. Meadows, J. Cole and B. J. Hinds, *Journal of Membrane Science*, 2008, **316**, 89-96.
128. C. Combellas, M. Delamar, F. Kanoufi, J. Pinson and F. I. Podvorica, *Chemistry of Materials*, 2005, **17**, 3968-3975.
129. S. Mahouche-Chergui, S. Gam-Derouich, C. Mangeney and M. M. Chehimi, *Chemical Society Reviews*, 2011, **40**, 4143-4166.
130. S. Baranton and D. Bélanger, *Electrochimica Acta*, 2008, **53**, 6961-6967.
131. G. Liu, M. Chockalingham, S. M. Khor, A. L. Gui and J. J. Gooding, *Electroanalysis*, 2010, **22**, 918-926.
132. M. Khoshroo and A. A. Rostami, *Journal of Electroanalytical Chemistry*, 2010, **647**, 117-122.
133. M. Toupin and D. Belanger, *Langmuir*, 2008, **24**, 1910-1917.
134. A. Adenier, N. Barré, E. Cabet-Deliry, A. Chaussé, S. Griveau, F. Mercier, J. Pinson and C. Vautrin-Ul, *Surface Science*, 2006, **600**, 4801-4812.
135. P. Allongue, C. Henry de Villeneuve, G. Cherouvrier, R. Cortès and M. C. Bernard, *Journal of Electroanalytical Chemistry*, 2003, **550-551**, 161-174.
136. C. Combellas, F. Kanoufi, J. Pinson and F. I. Podvorica, *Journal of the American Chemical Society*, 2008, **130**, 8576-8577.
137. C. Combellas, D.-e. Jiang, F. d. r. Kanoufi, J. Pinson and F. I. Podvorica, *Langmuir*, 2008, **25**, 286-293.
138. B. L. Hurley and R. L. McCreery, *Journal of The Electrochemical Society*, 2004, **151**, B252-B259.

139. A. Adenier, M. C. Bernard, M. M. Chehimi, E. Cabet-Deliry, B. Desbat, O. Fagebaume, J. Pinson and F. Podvorica, *Journal of the American Chemical Society*, 2001, **123**, 4541-4549.

140. P. Doppelt, G. Hallais, J. Pinson, F. Podvorica and S. Verneyre, *Chemistry of Materials*, 2007, **19**, 4570-4575.

141. R. W. Carpick and M. Salmeron, *Chemical Reviews*, 1997, **97**, 1163-1194.

142. M. Krämer, K. Roodenko, B. Pollakowski, K. Hinrichs, J. Rappich, N. Esser, A. von Bohlen and R. Hergenröder, *Thin Solid Films*, 2010, **518**, 5509-5514.

143. J. J. Gooding and S. Ciampi, *Chemical Society Reviews*, 2011, **40**, 2704-2718.

144. E. de la Llave, A. Ricci, E. J. Calvo and D. A. Scherlis, *The Journal of Physical Chemistry C*, 2008, **112**, 17611-17617.

145. H. M. Nassef, L. Civit, A. Fragoso and C. K. O'Sullivan, *Analyst*, 2008, **133**, 1736-1741.

146. S. Griveau, D. Mercier, C. Vautrin-Ul and A. Chaussé, *Electrochemistry Communications*, 2007, **9**, 2768-2773.

147. B. P. Corgier, A. Laurent, P. Perriat, L. J. Blum and C. A. Marquette, *Angewandte Chemie-International Edition*, 2007, **46**, 4108-4110.

148. R. Polsky, J. C. Harper, D. R. Wheeler and S. M. Brozik, *Electroanalysis*, 2008, **20**, 671-679.

149. J. C. Harper, R. Polsky, D. R. Wheeler, S. M. Dirk and S. M. Brozik, *Langmuir*, 2007, **23**, 8285-8287.

150. A. Ruffien, M. Dequaire and P. Brossier, *Chemical Communications*, 2003, 912-913.

151. M. N. Hansen, E. Farjami, M. Kristiansen, L. Clima, S. U. Pedersen, K. Daasbjerg, E. E. Ferapontova and K. V. Gothelf, *The Journal of Organic Chemistry*, 2010, **75**, 2474-2481.

152. A. Rasooly and J. Jacobson, *Biosensors and Bioelectronics*, 2006, **21**, 1851-1858.

153. D. O. Paul, *Clinica Chimica Acta*, 2003, **334**, 41-69.

154. A. A. Ensafi, M. Taei, H. R. Rahmani and T. Khayamian, *Electrochimica Acta*, 2011, **56**, 8176-8183.

155. A. Bouchet, C. Chaix, C. A. Marquette, L. J. Blum and B. Mandrand, *Biosensors and Bioelectronics*, 2007, **23**, 735-740.

156. M. Ortiz, M. Torrens, N. Canela, A. Fragoso and C. K. O'Sullivan, *Soft Matter*, 2011, **7**, 10925-10930.

157. H. Nasef, V. Beni, V. C. Ozalp and C. K. O'Sullivan, *Analytical and Bioanalytical Chemistry*, 2010, **396**, 2565-2574.

158. K. Tang, D. J. Fu, D. Julien, A. Braun, C. R. Cantor and H. Koster, *Proceedings of the National Academy of Sciences of the United States of America*, 1999, **96**, 10016-10020.

159. D. Wang, H. Gao, R. Zhang, X. Ma, Y. Zhou and J. Cheng, *Biotechniques*, 2003, **35**, 300-308.

160. D. Dell'Atti, M. Zavaglia, S. Tombelli, G. Bertacca, A. O. Cavazzana, G. Bevilacqua, M. Minunni and M. Mascini, *Clinica Chimica Acta*, 2007, **383**, 140-146.

161. F. Lucarelli, G. Marrazza and M. Mascini, *Biosensors and Bioelectronics*, 2005, **20**, 2001-2009.

162. R. G. Higuchi and H. Ochman, *Nucleic Acids Research*, 1989, **17**, 5865-5865.

163. C. Kerr and P. D. Sadowski, *Journal of Biological Chemistry*, 1972, **247**, 311-318.

164. T. T. Nikiforov, R. B. Rendle, M. L. Kotewicz and Y. H. Rogers, *Genome Research*, 1994, **3**, 285-291.

165. M. Espelund, R. A. P. Stacy and K. S. Jakobsen, *Nucleic Acids Research*, 1990, **18**, 6157-6158.

166. R. Saiki, S. Scharf, F. Faloona, K. Mullis, G. Horn, H. Erlich and N. Arnheim, *Science*, 1985, **230**, 1350-1354.

167. R. Higuchi, G. Dollinger, P. S. Walsh and R. Griffith, *Nature Biotechnology*, 1992, **10**, 413-417.

168. J. Compton, *Nature*, 1991, **350**, 91-92.

169. P. J. Asiello and A. J. Baeumner, *Lab on a Chip*, 2011, **11**, 1420-1430.

170. T. Notomi, H. Okayama, H. Masubuchi, T. Yonekawa, K. Watanabe, N. Amino and T. Hase, *Nucleic Acids Research*, 2000, **28**, e63.

171. D. Liu, S. L. Daubendiek, M. A. Zillman, K. Ryan and E. T. Kool, *Journal of the American Chemical Society*, 1996, **118**, 1587-1594.

172. G. T. Walker, M. S. Fraiser, J. L. Schram, M. C. Little, J. G. Nadeau and D. P. Malinowski, *Nucleic Acids Research*, 1992, **20**, 1691-1696.

173. G. T. Walker, M. C. Little, J. G. Nadeau and D. D. Shank, *Proceedings of the National Academy of Sciences*, 1992, **89**, 392-396.

174. M. Vincent, Y. Xu and H. Kong, *EMBO Reports*, 2004, **5**, 795-800.

175. D. Andresen, M. Von Nickisch-Rosenegk and F. F. Bier, *Expert Review of Molecular Diagnostics*, 2009, **9**, 645-650.

176. Y. J. Jeong, K. Park and D. E. Kim, *Cellular and molecular life sciences : CMLS*, 2009, **66**, 3325-3336.
177. L. An, W. Tang, T. A. Ranalli, H. J. Kim, J. Wytiaz and H. Kong, *Journal of Biological Chemistry*, 2005, **280**, 28952-28958.
178. A. Motré, Y. Li and H. Kong, *Gene*, 2008, **420**, 17-22.
179. D. Andresen, M. von Nickisch-Rosenegk and F. F. Bier, *Clinica Chimica Acta*, 2009, **403**, 244-248.
180. N. Ramalingam, T. San, T. Kai, M. Mak and H.-Q. Gong, *Microfluidics and Nanofluidics*, 2009, **7**, 325-336.
181. M. Mahalanabis, J. Do, H. Almuayad, J. Zhang and C. Klapperich, *Biomedical Microdevices*, 2010, **12**, 353-359.
182. F. Kivlehan, F. Mavré, L. Talini, B. Limoges and D. Marchal, *Analyst*, 2011, **136**, 3635-3642.
183. T. Deféver, M. Druet, M. Rochelet-Dequaire, M. Joannes, C. l. Grossiord, B. Limoges and D. Marchal, *Journal of the American Chemical Society*, 2009, **131**, 11433-11441.
184. T. Deféver, M. Druet, D. Evrard, D. Marchal and B. Limoges, *Analytical Chemistry*, 2011, **83**, 1815-1821.
185. B. Y. Won, S. Shin, S. Baek, Y. L. Jung, T. Li, S. C. Shin, D.-Y. Cho, S. B. Lee and H. G. Park, *Analyst*, 2011, **136**, 1573-1579.
186. S. S. W. Yeung, T. M. H. Lee and I. M. Hsing, *Analytical Chemistry*, 2007, **80**, 363-368.
187. F. Kivlehan, F. Mavre, L. Talini, B. Limoges and D. Marchal, *Analyst*, 2011, **136**, 3635-3642.
188. J. Paavonen, *International Journal of Infectious Diseases*, 2007, **11**, S3-S9.
189. H. z. Hausen, *Biochimica et Biophysica Acta - Reviews on Cancer*, 1996, **1288**, F55-F78.
190. N. Munoz, F. X. Bosch, S. de Sanjose, R. Herrero, X. Castellsague, K. V. Shah, P. J. F. Snijders, C. Meijer and C. Int Agcy Res Canc Multicenter, *New England Journal of Medicine*, 2003, **348**, 518-527.
191. J. Thomison Iii, L. K. Thomas and K. R. Shroyer, *Human Pathology*, 2008, **39**, 154-166.
192. M. H. Stoler, *International Journal of Gynecological Pathology*, 2000, **19**, 16-28.
193. Y. Nomine, M. Masson, S. Charbonnier, K. Zanier, T. Ristriani, F. Deryckere, A. P. Sibler, D. Desplancq, R. A. Atkinson, E. Weiss, G. Orfanoudakis, B. Kieffer and G. Trave, *Molecular Cell*, 2006, **21**, 665-678.

194. X. Liu, A. Clements, K. H. Zhao and R. Marmorstein, *Journal of Biological Chemistry*, 2006, **281**, 578-586.

195. *Human Papillomavirus and Related Cancers in Spain. Summary Report 2010*, WHO/ICO Information Centre on HPV and Cervical Cancer, 2010.

196. K. S. Cuschieri and H. A. Cubie, *Journal of Clinical Virology*, 2005, **32**, 34-42.

197. M. Arbyn, P. Sasieni, C. J. L. M. Meijer, C. Clavel, G. Koliopoulos and J. Dillner, *Vaccine*, 2006, **24**, S78-S89.

198. J. Cuzick, M. Arbyn, R. Sankaranarayanan, V. Tsu, G. Ronco, M.-H. Mayrand, J. Dillner and C. J. L. M. Meijer, *Vaccine*, 2008, **26**, K29-K41.

199. Y. Wang, M. Chen, L. Zhang, Y. Ding, Y. Luo, Q. Xu, J. Shi, L. Cao and W. Fu, *Biosensors and Bioelectronics*, 2009, **24**, 3455-3460.

200. L. Xu, H. Yu, M. S. Akhras, S.-J. Han, S. Osterfeld, R. L. White, N. Pourmand and S. X. Wang, *Biosensors and Bioelectronics*, 2008, **24**, 99-103.

201. R. E. Sabzi, B. Sehatnia, M. H. Pournaghi-Azar and M. S. Hejazi, *Journal of the Iranian Chemical Society*, 2008, **5**, 476-483.

202. S. D. Vernon, D. H. Farkas, E. R. Unger, V. Chan, D. L. Miller, Y. P. Chen, G. F. Blackburn and W. C. Reeves, *Bmc Infectious Diseases*, 2003, **3**, 12.

Chapter 2

Electrochemical biosensor for the multiplexed detection of human papillomavirus genes

Biosensors and Bioelectronics 26 (2010) 1684-1687.

L. Civit[a], A. Fragoso[a*], C.K. O' Sullivan[a,b *]

[a] Nanobiotechnology and Bioanalysis Group, Departament d'Enginyeria Química, Universitat Rovira i Virgili, Tarragona, Spain.
[b] Institució Catalana de Recerca i Estudis Avançats, Passeig Lluís Companys 23, 08010 Barcelona, Spain

Keywords: Multiplexing, Human papillomavirus, DNA detection, Amperometric detection, clinical diagnostics

2.1 Abstract

A proof-of-concept of an electrochemical genosensor array for the individual and simultaneous detection of two high-risk human papillomavirus DNA sequences, HPV16E7p and HPV45E6 that exhibits high sensitivity and selectivity is reported. The optimum conditions for surface chemistry preparation and detection of hybridised target were investigated. The LOD obtained are in the pM range, which are sufficient for most real RNA/DNA samples obtained from PCR amplification, usually in the nanomolar range. In a multiplexed detection format, high selectivity was observed over the non-specific sequence, opening the way for the development of an electrochemical high throughput screening assay for multiple high risk DNA sequences.

2.2 Introduction

The human papillomavirus (HPV) is one of the most common sexually transmitted infections, affecting the skin and mucous membranes. There are more than 40 HPV types that can infect the genital areas of men and women.[1] HPV has been detected in virtually all invasive cervical cancers and has been confirmed as the major cause of this cancer. It is believed that most cervical cancers develop when various aggressive genetic HPV strains activate certain oncogenes. Oncogenes E6 and E7 are particularly important because they interfere with protective proteins p53 and pRb, respectively. These proteins limit cell growth under normal conditions, but once they are blocked, cell growth is not controlled, resulting in tumor development and cancer.[2-3]

Owing to the difficulties to perform serological assays and HPV cultures efficiently, some tools based on molecular recognition have been developed for the diagnosis of HPV infections. At the basis of molecular recognition, the detection of HPV DNA are in use, based on the extraction of genomic DNA from clinical samples with posterior PCR amplification and detection.[4-5] However due to the high mutation rates of viruses, detection by PCR is complicated.

Another, less explored, possibility for HPV detection is the use of electrochemical biosensors with amperometric (labeled) and/or impedimetric (label-free) detection.

Electrochemical biosensors have received considerable attention regarding the detection of DNA hybridisation due to the advantages of low cost, simplicity, high sensitivity, compatibility with mass manufacturing, possibility of microfabrication technologies and portability, making them excellent candidates for point-of-care DNA diagnostics. Electrochemical detection of HPV related sequences has been reported in the past by using methylene-blue as hybridisation indicator[6] or secondary probes labelled with ferrocene.[7] In the first case, a 20-mer probe sequence was adsorbed on the surface of a graphite electrode and used for the detection of a 20-mer target related to L1 gene of identical length by recording the variations in methylene-blue response before and after target recognition, achieving a limit of detection of 1.2 ng/μL (0.5 nM). The other example involved the use of a bioelectronic DNA detection platform formerly commercialised as eSensor™, for the detection of HPV sequences based on thiolated probes immobilised on the chip surface. After target immobilisation, a ferrocene-labelled probe was hybridised and the current response was measured. These chips were able to detect 86% of the HPV targets contained in clinical samples using a positive/negative type response. In a more recent report, detection of HPV was carried out by treating a captured dsDNA duplex with acid and directly measuring the released purine bases by square wave voltammetry.[8] In the present work, we report an electrochemical sensor microarray based on DNA detection for the individual and simultaneous detection of specific high-risk HPV sequences, more specifically HPV16 and 45 and analytical parameters such as sensitivity, specificity and reproducibility have been studied.

2.3 Experimental

2.3.1 Electrochemical instrumentation

All electrochemical measurements were performed with a PGSTAT 12 potentiostat (Autolab, The Netherlands) controlled with the General Purpose Electrochemical

System (GPES) software and equipped with a MUX module (Eco Chemie B.V., The Netherlands).

The electrode array consisted of a 16 gold working electrodes arranged in a four by four distribution on a borosilicate glass chip measuring 21 mm × 23 mm. Each working electrode (1 mm × 1 mm) was placed between a silver pseudo reference (0.2 mm × 1 mm) and a gold counter electrode of the same size in order to create 16 planar electrochemical cells. The electrode array was integrated within a microfluidic cell. The microfluidic channels were realised by mounting an electrode array onto a polycarbonate fluidic chip using double-sided medical grade adhesive foil of 50 μm thickness, which was previously laser machined to generate microchannel structures of 1 mm width. Connection of the assembled chip was realised *via* pogo-pin connectors to each of the 18 electrodes (16 working electrodes and 1 plus 1 reference and counter electrodes).

2.3.2 Materials

Dithiol 1 (DT1, 16-(3,5-bis((6-mercaptohexyl)oxy)phenyl)-3,6,9,12,15-pentaoxahexadecane) was purchased from SensoPath Technologies (Bozeman, NT). Phosphate buffered saline with Tween 20 (pH 7.4) and 3,3',5,5'-Tetramethylbenzidine (TMB) liquid substrate system were from Sigma-Aldrich (Barcelona, Spain). Potassium dihydrogen phosphate and sodium hydroxide were purchased by Scharlau (Barcelona, Spain). All solutions were prepared with MilliQ water (18 MΩ) produced with a Milli-Q RG system (Millipore Ibérica, Madrid, Spain).

Synthetic oligonucleotides were purchased from Biomers.net (Ulm, Germany). Sequences for HPV16E7p are listed below.

HPV16E7p thiolated capture probe (24-mer sequence): 5'-Thiol C_6-GAG GAG GAG GAT GAA ATA GAT GGT-3'.

HPV16E7p HRP-labelled reporter probe (21-mer sequence): 5'-TTG GAA GAC CTG TTA ATG GGC-HRP-3'.

HPV16E7p target (159-mer sequence): 5'-GCC CAT TAA CAG GTC TTC CAA AGT ACG AAT GTC TAC GTG TGT GCT TTG TAC GCA CAA CCG AAG CGT AGA GTC ACA CTT GCA ACA AAA GGT TAC AAT ATT GTA ATG GGC TCT GTC CGG TTC TGC TTG TCC AGC TGG ACC ATC TAT TTC ATC CTC CTC CTC-3'.

2.3.3 Probe immobilisation on electrode array

Prior to modification, electrode arrays were cleaned following a two steps protocol. First, in order to remove the protective resist used during storage, the arrays were sequentially sonicated for 5 min in acetone and isopropanol and rinsed with water. In a second step, each electrode array was electrochemically cleaned in 0.5 M H_2SO_4 by application of a constant potential of 1.6 V for 10 sec followed by 40 voltammetric cycles in the potential range -0.2 to 1.6 V at a scan rate of 0.5 $V \cdot s^{-1}$. Finally, electrodes were rinsed with milliQ water and dried with nitrogen. The cleaned electrode arrays were modified via co-immobilisation of the thiolated probe (1 μM) and the backfiller DT1 (100 μM) in 1 M KH_2PO_4 aqueous solution (pH 3.5) for 3 h at room temperature under humid environment (minimum 90%). The electrode arrays were then washed in a stirring solution of PBS-Tween for 15 min, rinsed with water and dried with nitrogen.

2.3.4 DNA detection

DNA detection of both synthetic oligonucleotides (HPV16E7p and HPV45E6) was performed using a so-called sandwich type format (Figure 2.1). First, 0.5 μL of HPV target of various concentrations ranged of 0.1-50 nM in PBS-Tween were cast on each of the oligonucleotide modified gold electrodes and were incubated for 1 h at room temperature. The sensors were then washed for 15 min in a stirring solution of PBS-Tween and dried with nitrogen. The second hybridisation was subsequently performed by spotting 0.5 μL of 10 nM reporter probe in PBS-Tween and incubating for 1 h at room temperature. The hybridised microarray was washed with PBS-Tween

for 15 min and dried in nitrogen. The hybridisations of the target and detection probe were performed under a humid environment (minimum 90%).

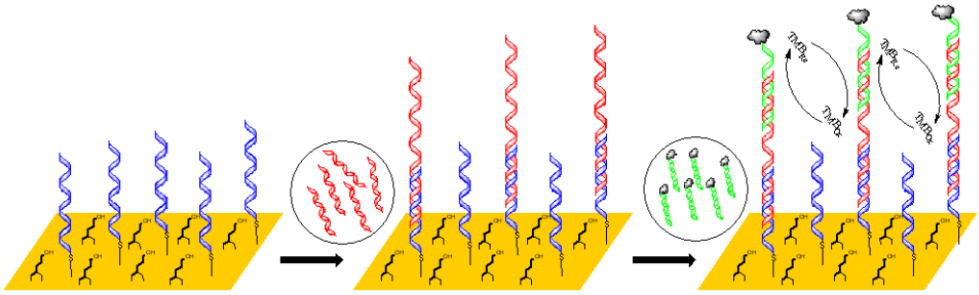

Figure 2.1. Schematic description of the developed assay based on co-immobilisation of thiolated probe with backfiller, hybridisation process and electrochemical detection

2.3.5 Electrochemical detection

Modified electrode arrays were assembled on the microfluidic cell to perform the electrochemical detection. The detection process was carried out in the created microfluidic channels in the presence of TMB substrate. The reduction of TMB was detected using a steps and sweeps technique by applying two consecutive steps at 0 V for 1 msec and -0.2 V for 0.5 sec.

2.4 Results and discussion

The hybridisation behaviour was detected by incorporating a HRP-labelled reporter probe that pairs with the target to form a "sandwich" structure at the electrode surface (Figure 2.1). In this work, TMB was used as a chromogenic substrate for HRP. TMB is commonly used in ELISA assays and is oxidised to form a blue coloured product, which is known to be a single oxidised TMB complexed with a neutral TMB molecule.[9] The oxidised TMB can be detected through its reduction at the electrode surface.[10]

2.4.1 Proof-of-concept of electrochemical detection of individual HPV sequences

The classic high-risk HPV types are 16 and 18[11] although types 31 and 45 have also been found to be present in approximately the 80% of cases of cervical cancer together with types 16 and 18[12]. For this reason HPV types 16 and 45 were chosen for this work.

To evaluate the analytical performance of the genosensor, two calibration curves were obtained using synthetic oligonucleotides of both specific high-risk HPV sequences. Figure 2.2 shows the amperometric response of the reduction of oxidised TMB for a series of target concentrations ranging from 0.1 to 50 nM. First, a blank steps and sweep (SAS) measurement was carried out with PBS-tween, followed by TMB measurement. The final amperometric response used for construction of the calibration curve resulted from the subtraction of the blank value from the TMB response. As can be seen, the signal tends to saturation for concentration above 50 nM of target, as expected for the interaction of a solution analyte with an immobilised catching probe. Analysis of the data in terms of the Langmuir isotherm[13] afforded association constants of 2.3 and 0.17 nM^{-1} for HPV16E7p and HPV45E6,respectively. Assuming a linear behavior at low target concentrations the electrochemical assays showed a sensitivity of (0.15 ± 0.02) μA nM^{-1} (r^2 = 0.997) in the range of 0.1 – 10 nM for HPV16E7p and (1.02 ± 0.09) μA nM^{-1} (r^2 = 0.999) in the range of 0.1 – 1 nM in the case of HPV45E6, with LOD of 490 and 110 pM, respectively. These differences in sensor parameters may be due to the fact that HPV16e7p amplicon is considerably longer (159-mer) than the HPV45E6 (78-mer) amplicon.

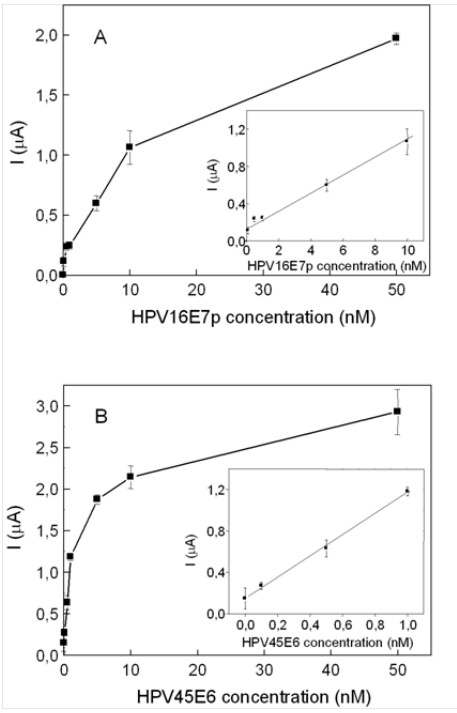

Figure 2.2. Calibration curves obtained with: A) HPV16E7p and B) HPV45E6. Target concentration range: 0.1-50 nM.

2.4.2 Multiplexed detection of HPV sequences

Quantitative identification of biomarkers in a mixture without separation and at clinically relevant concentrations is a crucial requirement for the development of more effective and simpler diagnostic devices particularly when monitoring expression levels of disease associated RNA. Arrayed tests enable the use of pattern recognition approaches to assess disease changes, which is important in both diagnostics and monitoring. In the new and evolving paradigm of clinical diagnostics, the measurement of a single tumour marker does not give sufficient information for a complete clinical picture, and there is a growing requirement for low-density multiplex assays. The 16 gold working electrodes sensor array used in this work permits parallel detection of multiple targets.

For the simultaneous detection of several high-risk HPV sequences, a chip was modified with thiolated HPV16E7p and HPV45E6 probes in alternating electrode spots as depicted in Figure 2.3.

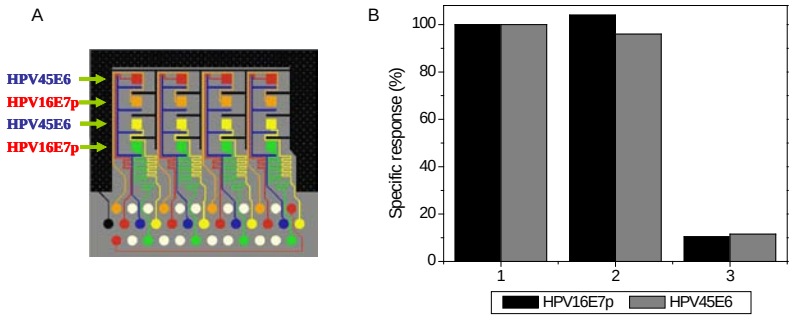

Figure 2.3. A. Modification map used for multiplexed electrochemical detection of HPV16E7p and HPV45E6. B. Relative responses to the specific signal obtained for the simultaneous detection of HPV16E7p and HPV45E6: 1) with addition of 10 nM specific target; 2) with addition of a mixture of 10 nM specific + 100 nM non-specific targets, respectively; 3) with addition of 10 nM non-specific target.

Specific and non-specific targets (i.e. for a spot modified with thiolated HPV16E7p, specific target refers to HPV16E7p sequence and HPV45E6 refers to non-specific target) were then applied at a 10 nM concentration as well as a mixture of 10 nM specific and 100 nM non-specific target, respectively. The responses obtained (n = 4) are presented in Figure 2.3 corresponding to different chips in order to test inter-array reproducibility. From the data obtained a high specificity of the sensor array was observed with negligible hybridisation signal with the non-specific target. The signal recovery upon addition of a high concentration of non-specific target (10 times) was 104 ± 8% for HPV45E6 and 96 ± 5% for HPV16E7p. These results demonstrate the applicability of the electrochemical genosensor array described here for multiplexed detection of DNA sequences. The application of this strategy for the detection of a panel of 18 HPV associated sequences is currently under evaluation.

2.5 Conclusions

This report demonstrates the proof-of-concept of an electrochemical genosensor array for the individual and simultaneous detection of two high-risk HPV types, HPV16E7p and HPV45E6 sequences that exhibits high sensitivity and selectivity. The optimum conditions for surface chemistry preparation and detection of hybridised target were investigated. The LOD obtained in the pM range are sufficient for most real RNA/DNA samples obtained from PCR amplification, usually in the nanomolar range. In a multiplexed detection format, high selectivity was observed over the non-specific sequence. Following this initial work, our attention is now focused on the introduction of additional high-risk HPV sequences in the multiplexed assay for the development of an electrochemical high throughput screening assay for multiple HPV markers.

2.6 Acknowledgements

HPV16E7p and HPV45E6 sequences were identified by TATAA Biocenter (Gothenburg, Sweden). This research has been carried out with financial support from the Commission of the European Communities, RTD programme "Smart Integrated Biodiagnostic Systems for Healthcare, SmartHEALTH, FP6-2004-IST-NMP-2-016817". A. F. thanks Ministerio de Ciencia y Tecnología, Spain, for a "Ramón y Cajal" Research Professorship. L. C. acknowledges Universitat Rovira i Virgili for a predoctoral scholarship.

2.7 References

1. N. Munoz, F. X. Bosch, S. de Sanjose, R. Herrero, X. Castellsague, K. V. Shah, P. J. F. Snijders, C. Meijer and C. Int Agcy Res Canc Multicenter, *New England Journal of Medicine*, 2003, **348**, 518-527.
2. Y. Nomine, M. Masson, S. Charbonnier, K. Zanier, T. Ristriani, F. Deryckere, A. P. Sibler, D. Desplancq, R. A. Atkinson, E. Weiss, G. Orfanoudakis, B. Kieffer and G. Trave, *Molecular Cell*, 2006, **21**, 665-678.

3. X. Liu, A. Clements, K. H. Zhao and R. Marmorstein, *Journal of Biological Chemistry*, 2006, **281**, 578-586.
4. R. Klaes, S. M. Woerner, R. Ridder, N. Wentzensen, M. Duerst, A. Schneider, B. Lotz, P. Melsheimer and M. V. Doeberitz, *Cancer Research*, 1999, **59**, 6132-6136.
5. S. Nagao, M. Yoshinouchi, Y. Miyagi, A. Hongo, J. Kodama, S. Itoh and T. Kudo, *Journal of Clinical Microbiology*, 2002, **40**, 863-867.
6. R. E. Sabzi, B. Sehatnia, M. H. Pournaghi-Azar and M. S. Hejazi, *Journal of the Iranian Chemical Society*, 2008, **5**, 476-483.
7. S. D. Vernon, D. H. Farkas, E. R. Unger, V. Chan, D. L. Miller, Y. P. Chen, G. F. Blackburn and W. C. Reeves, *Bmc Infectious Diseases*, 2003, **3**, 12.
8. N. Zari, A. Amine and M. M. Ennaji, *Analytical Letters*, 2009, **42**, 519-535.
9. J.-I. Kim, A. Bordeanu and J.-C. Pyun, *Biosensors and Bioelectronics*, 2009, **24**, 1394-1398.
10. P. Fanjul-Bolado, M. B. Gonzalez-Garia and A. Costa-Garcia, *Analytical and Bioanalytical Chemistry*, 2005, **382**, 297-302.
11. J. Thomison Iii, L. K. Thomas and K. R. Shroyer, *Human Pathology*, 2008, **39**, 154-166.
12. M. H. Stoler, *International Journal of Gynecological Pathology*, 2000, **19**, 16-28.
13. A. Fragoso, N. Laboria, D. Latta and C. K. O'Sullivan, *Analytical Chemistry*, 2008, **80**, 2556-2563.

Chapter 3

Evaluation of techniques for generation of single-stranded DNA for quantitative detection

Manuscript submitted

L. Civit[a], A. Fragoso[a*], C.K. O' Sullivan[a,b *]

[a] Nanobiotechnology and Bioanalysis Group, Departament d'Enginyeria Química, Universitat Rovira i Virgili, Tarragona, Spain.
[b] Institució Catalana de Recerca i Estudis Avançats, Passeig Lluís Companys 23, 08010 Barcelona, Spain

Keywords: Single-stranded DNA, streptavidin-coated magnetic beads, exonuclease digestion, thermal denaturation, alkaline denaturation, sensing applications.

3.1 Abstract

A simple and efficient method for the generation of clean single-stranded DNA with a high recovery and purity from a double-stranded PCR product is required for nucleic acid sensing and microarray applications. Currently, the most widely used technique is thermal denaturation (*heat and cool*) due to its simplicity and low cost, but this technique has drawbacks in terms of recovery and reproducibility. The work presented here compares this technique with alternative approaches for single-stranded DNA generation exploiting affinity magnetic separation and exonuclease digestion. The quality and quantity of the single-stranded DNA recovered was evaluated using gel electrophoresis and enzyme linked-oligonucleotide assay. Recoveries of between 50-70% of the theoretical maximum of generatable single-stranded DNA were obtained for the studied techniques with an excellent reproducibility, demonstrating a marked improvement in performance as compared to the *heat and cool* method.

3.2 Introduction

The efficient generation of single-stranded DNA is required for many molecular biology and biotechnology applications, including pyrosequencing technology,[1] single-stranded conformation polymorphism analysis,[2] solid phase DNA sequencing,[3] single nucleotide polymorphism analysis[4] as well as analytical applications, including DNA chips, microarrays[5-6] and genosensors, amongst other applications.

The quantitative identification of biomarkers in a mixture without separation and at clinically relevant concentrations is a crucial requirement for the development of more effective and simpler diagnostic/monitoring devices, e.g. monitoring of expression levels of disease associated RNA. The most commonly used method for analysis and quantitation of mRNA levels is real time RT-PCR, which is currently limited by the number of fluorophore labels available and the resolution of the optical detectors. Alternatively RNA can be reverse transcribed and amplified using conventional PCR exploiting multiplex amplification (e.g. MLPA, MAPH), resulting in 50-100 double-stranded amplicons, which can subsequently be quantitatively detected using

genosensors/microarrays. These arrays are based on immobilised probes of 20-25 bases in length that specifically bind to single-stranded DNA (ssDNA), which is generated from the double-stranded PCR amplicons. These oligonucleotide and cDNA arrayed tests enable the use of pattern recognition approaches to assess disease changes, which is of increasing importance in both diagnostics, monitoring and the future paradigm of individualised theranostics. In order to be able to truly quantify the levels of RNA, it is thus of crucial importance to be able to generate high quality ssDNA.

The most exploited methodology for ssDNA generation is thermal denaturation, named *heat and cool,* which consists of heating the dsDNA sample (normally PCR products) to high temperatures (90-95ºC) and immediate cooling on ice prior to hybridisation.[7-8] This is used mainly due to its low cost and simplicity, but has very low efficiency and is highly irreproducible. Several alternative methods have been reported for the generation of single-stranded DNA, including asymmetric polymerase chain reaction (PCR), urea-polyacrylamide gel electrophoresis (Urea-PAGE), exonuclease digestion and the use of magnetic beads. Asymmetric PCR, first reported in 1988 by Gyllensten and Ehrlich,[9] exploits the use of an unequal molar ratio of forward and reverse primer, where the primer of lower concentration is consumed in the generation of double-stranded DNA (dsDNA) whilst the primer of higher concentration then produces single-stranded DNA (ssDNA). Initial reports gave rise to inconsistent results and the technique was evolved to first produce dsDNA, which then acts as a template for the generation of ssDNA.[10-13] The drawbacks associated with the method include difficulties associated with multiplex asymmetric PCR,[4] as well as the requirement to separate ssDNA from dsDNA using PAGE, from which the ssDNA is eluted for subsequent analysis. In an another approach, Urea-PAGE involves the use of a primer pair, one of which contains a polyadenine (polyA) spacer and/or a terminator or stopper molecule, such as hexaethylene glycol.[14] As with asymmetric PCR, the technique requires a post-PCR PAGE separation of the unequal strands and subsequent elution of the ssDNA. Whilst resulting in a pure sample of ssDNA, the

methods requiring electrophoretic separation lose a large and irreproducible amount of DNA in the process.

Selective strand digestion using exonuclease digestion presents an approach that obviates the requirement for post-PCR electrophoretic separation and the associated loss of DNA. The two most commonly used exonucleases are the lambda exonuclease and the T7 Gene 6 exonuclease. Lambda exonuclease selectively digests a 5'-phosphorylated strand of dsDNA with a high processivity. In this case, one of the primer pairs used in PCR is 5'-phosphorylated resulting in a dsDNA duplex, where one of the strands has a phosphate group introduced in the 5' position. Following incubation with the lambda exonuclease this strand is selectively digested and the exonuclease activity is then disrupted by heating at 85ºC, with release of ssDNA.[15] T7 Gene 6 exonuclease, on the other hand, acts non-processively in the 5´- 3´ direction from both 5´-phosphoryl or 5´-hydroxyl nucleotides by releasing mononucleotides until about 50% of the DNA is acid soluble.[16] To protect from the T7 Gene 6 exonuclease, one of the primers is capped with phosphorothioates, so the strand containing this modification is not digested[17] whilst the other strand is efficiently hydrolysed and again, the enzyme is then inactivated by heating. Both these approaches are very elegant and have been effectively used for the generation of ssDNA, particularly for use in SELEX, but do involve extra costs in terms of the modified primers and the enzymes themselves, and, furthermore, the presence of the inactivated enzyme could interfere with the further analysis of the generated ssDNA, e.g. in pyrosequencing. Apart from the *heat and cool* method, one of the most widely used techniques for the generation of ssDNA uses a primer pair where one of the primers is biotinylated.[18] Post-PCR, the biotinylated dsDNA PCR product is captured on streptavidin-coated magnetic beads and the non-biotinylated ssDNA is liberated by alkaline/heat denaturation of the surface immobilised duplex. There are reports that alkaline denaturation also results in the dissociation of streptavidin from the beads, resulting in a liberation of the streptavidin/streptavidin-biotin-ssDNA/ streptavidin-biotin-dsDNA from the bead surface.[19] This has been observed to interfere in SELEX

studies, where aptamers have undesirably been generated against streptavidin rather than the target.[20]

In this work, the human papillomavirus (HPV) associated high-risk types 16 and 45 exons were used as targets, as a model system for the comparison of different techniques for the generation of ssDNA. HPV is one of the most common sexually transmitted infections, affecting the skin and mucous membranes, and is a double-stranded DNA virus[21] of which more than 200 HPV types have been identified with greater than 40 HPV types infecting the genital areas of men and women.[22] Genital HPV types have been subdivided into low-risk, forming genital warts and the high-risk types which are detected in virtually all invasive cervical cancers and have been confirmed as the major cause of this cancer. The classic high-risk HPV types are 16 and 18[23] although types 31 and 45 have also been found to be present in approximately 80% of cervical cancer cases together with types 16 and 18.[24]

Amplified products from HPV16 and HPV45, representing two different length amplicons, of 79 bp and 159 bp, respectively, were used as a model for the generation of ssDNA using different methodologies including *heat and cool,* streptavidin-coated magnetic beads, T7 Gene 6 Exonuclease digestion and Lambda Exonuclease digestion (Figure 3.1). The single-stranded DNA amplicons generated were characterised using gel electrophoresis and Enzyme Linked OligoNucleotide assay (ELONA).

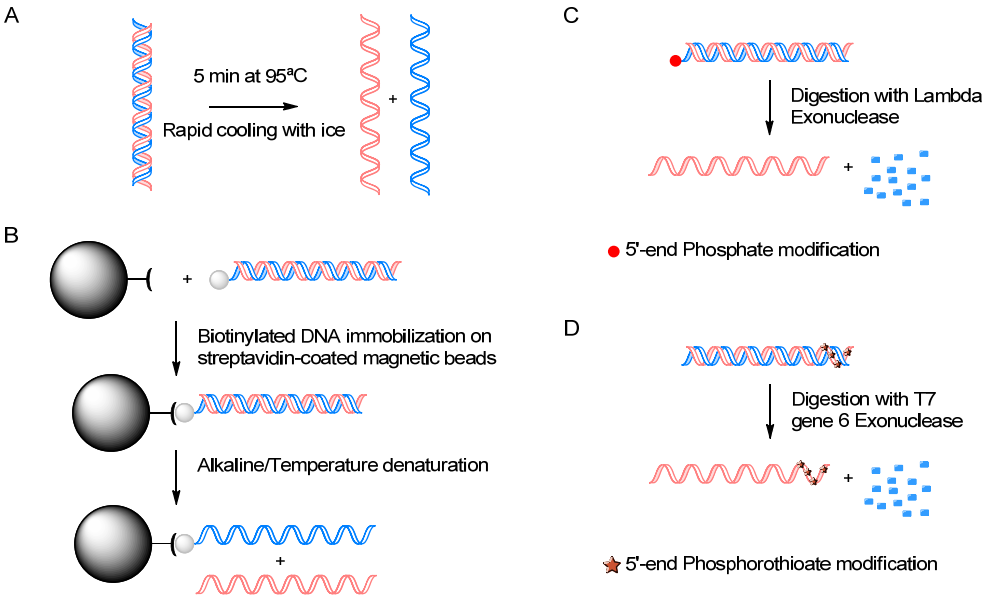

Figure 3.1. Scheme of the different methodologies studied for the ssDNA generation A) heat and cool, B) streptavidin-coated magnetic beads, C) Lambda exonuclease digestion and D) T7Gene 6 exonuclease digestion.

3.3 Experimental

3.3.1 Chemicals

Phosphate buffered saline (pH 7.4) and 3,3',5,5'-Tetramethylbenzidine (TMB) liquid substrate system were purchased from Sigma-Aldrich (Barcelona, Spain). Potassium dihydrogen phosphate and sodium hydroxide were provided by Scharlau (Barcelona, Spain). All solutions were prepared with MilliQ water (18 MΩ) produced with a Milli-Q RG system (Millipore Ibérica, Madrid, Spain). Streptavidin-coated magnetic beads (Dynabeads MyOne Streptavidin C1) were obtained from Invitrogen (Barcelona, Spain). T7 Gene 6 Exonuclease and Lambda Exonuclease were purchased from Affymetrix (Wycombe Lane, UK).

Synthetic target sequences (HPV16E7p of 159-mer and HPV45E6 of 78-mer), modified and non-modified forward (HPV16E7p of 24-mer and HPV45E6 of 23-mer), and reverse primers (HPV16E7p of 21-mer and HPV45E6 of 18-mer) were

purchased from Biomers.net (Ulm, Germany). TATAA Biocentre (www.tataa.com) can be contacted for further details on the specific sequences of the probes, primers and target amplicons.

3.3.2 Instrumentation

3.3.2.1 Enzyme linked oligonucleotide assay (ELONA) measurements

Absorbance was read with a Spectra max 340PC, 348, Microplate Spectrophotometer (Molecular Devices, Bionova Cientifica, s.l, Madrid). All the immobilisation and hybridisation steps were performed at 37ºC in a Titramax 1000 incubator (Heidolph, Barcelona).

3.3.3 PCR protocol

The 159-bp region of HPV16E7p was amplified using modified and non-modified primers depending on the ssDNA generation technique utilised. The 100 µL reaction mixture contained 1 U of Taq polymerase (Invitrogen), 1X PCR reaction buffer, 3 mM $MgCl_2$, 200 µM dNTP and 400 nM of each primer. Thermal conditions were optimised to be 2 min at 95°C followed by 30 cycles of 20 s at 95°C, 20 s at 60°C, and 20 s at 72°C.

The 79-bp region of HPV45E6 synthetic DNA was amplified using the following protocol. The 100 µL reaction mixture contained 1U of Taq polymerase, 1X PCR reaction buffer, 2 mM $MgCl_2$, 200 µM dNTP and 200 nM of each primer. Thermal protocol was optimised to be 2 min at 95°C followed by 25 cycles of 20 s at 95°C, 20 s at 60°C, and 20 s at 72°C.

A final extension step of 72°C for 7 min was included in all protocols. Thermal cycling was performed in an ICycler Thermal Cycler (Bio-Rad Laboratories, S.A, Barcelona).

Sample analysis was performed by electrophoresis on a 4% agarose gel (Certified Low Range Ultra Agarose, Bio-rad, Barcelona). For a direct comparison of the

different techniques, in the first instance dsDNA was purified from the PCR product and the concentration was determined via UV spectroscopy. One hundred microlitres of the PCR product was purified with PureLink™ Quick Gel Extraction and PCR Purification Combo Kit (Invitrogen, Barcelona) in order to obtain dsDNA purified from primers, dNTPs, enzymes and salts by the selective binding of dsDNA to a silica membrane-based spin column in the presence of chaotropic salts. Extraction was performed following the manufacturer's manual procedure. Finally, the purified PCR product was eluted with elution buffer (10 mM Tris-HCl buffer, pH 8.5) and measured by UV spectroscopy at 260 nm, determining the concentration to be 49.5 ± 6.0 nM and 55.4 ± 8.8 nM for HPV16 and 45, respectively.

3.3.4 Methodologies for single-stranded DNA preparation

3.3.4.1 Heat and cool

Non-modified primers were used for amplification. From purified PCR product, aliquots were diluted by a factor of 4 in PBS (pH 7.4). Some of these aliquots were heated at 95ºC for 5 min and then rapidly cooled down on ice. These samples were used directly for ELONA analysis to quantify the ssDNA recovered.

3.3.4.2 Streptavidin-coated magnetic beads

Capture of the biotinylated PCR product (biotinylated forward primer) using the streptavidin-coated beads was carried out according to the manufacturer's instructions. Firstly, the optimised concentration of beads required for the dsDNA used in the present study (Results and discussion section), was washed to remove any preservatives by 3 consecutive washings with 1X B&W buffer (5 mM Tris-HCl pH 7.5, 0.5 mM EDTA and 2 M NaCl). Between each washing step, Eppendorf tubes containing the solution with the magnetic beads were placed in contact with a magnet for 2 min and the supernatant was removed by aspiration with a micro-pipette. The isolated magnetic beads were subsequently re-suspended with 100 µl of PCR product (purified and non-

purified) and the same volume of 2X B&W buffer and incubated for an optimised time at room temperature with gentle rotation. Following immobilisation of the biotinylated PCR product on the streptavidin magnetic beads, the Eppendorf tubes were again placed in contact with a magnet for 3 mins in order to discard the supernatant and the isolated beads were washed three times with 1X B&W buffer. Separation of ssDNA was performed either by temperature or alkaline denaturation.

3.3.4.3 T7 Gene E6 and Lambda Exonucleases digestion

A reverse primer containing 5 consecutive phosphorothioate groups at its 5' end was used, as the enzyme activity of the T7 Gene E6 Exonuclease is completely inhibited by the presence of more than one phosphorothioate residue. A forward primer with no modification was used and this generated strand will be hydrolysed, whilst the other will be protected. Purified dsDNA from PCR product and direct PCR product were then diluted to 100 μL with 5X T7 reaction buffer to a final concentration of 1X. Two microliters of T7 enzyme (40 U) were added to the solution and incubated at 37ºC for 10, 30 (as recommended by the manufacturer) and 60 min.

In the case of the Lambda exonuclease, PCR amplification was performed with a phosphorylated forward primer and a non-modified reverse primer. Again, the purified and non-purified PCR product was diluted to 100 μL with 10X Lambda exonuclease reaction buffer to a final concentration of 1X. Two microliters of enzyme (10 U) were then added and samples were incubated at 37ºC for 10, 30 and 60 min.

Reaction tubes were placed at 85ºC for 10 min in order to inactivate the enzymes and stop the reaction.

3.3.5 ELISA for streptavidin detection

Anti-streptavidin polyclonal antibody (1/1000 dilution in carbonate buffer, pH 9.5) was added to each well of a Nunc Immunosorp microtiter plate and incubated for 1 h at 37ºC. A washing step with PBS-Tween (pH 7.4 10 mM 0.05% v/v Tween) was then performed. Blocking of the plate was carried out by the addition of PBS-Tween and

incubation for another hour at 37ºC and a second washing step was performed. For the immunorecognition step, a calibration curve was constructed using streptavidin from 0 to 0.1 μg/mL in 1 in 2 dilution factors in PBS (pH 7.4). Samples from treatment of streptavidin-coated magnetic beads by heating at 95ºC for 5 min and samples from treatment with 150 mM of NaOH for 3 min (previously neutralised with 300 mM of HCl and PBS buffer), were added to each well. This step was incubated for 1 h at 37ºC and a washing step was carried out. Finally, a 1/640 dilution of a commercial biotinylated-HRP in PBS-Tween was added to each well and left to incubate for 1 h at 37ºC. A final washing step was performed and 50 μL of HRP substrate (TMB) was added to each well and product formation was allowed to proceed for 15 min at RT. Reaction was then stopped with 1 M H_2SO_4, and absorbance was read at 450 nm.

3.3.6 ssDNA quantification techniques

3.3.6.1 Gel electrophoresis analysis

Ten microliters of each ssDNA sample was loaded with 4 μL of 6X loading buffer (40% sucrose and bromophenol blue) and 2 μL of 150 mM NaOH in a 4% agarose gel, stained with GelRed nucleic acid stain (Bioutium). Synthetic ssDNA of known concentrations were prepared in the same manner as the samples, and loaded together. Gels were analysed with ImageJ software.

3.3.6.2 Enzyme-linked oligonucleotide assay (ELONA)

Fifty microliters of biotinylated HPV forward primer (20 nM in 0.1 M PBS, pH 7.4) was added to each well of a Microtiter* Streptavidin-Coated Strip Plate and incubated for 1 h. Three consecutive washing steps with 200 μL 0.1 M PBS-Tween, pH 7.4 were performed. To construct calibration curves, synthetic HPV ssDNA, from 40 – 0 nM for HPV16 and 60 – 0 nM in the case of HPV45, using in both cases a 1 in 2 dilution factor in 0.1M PBS, was added to the Fw primer coated wells and incubated for

another 1 h. Any non-hybridised DNA was removed in 3 washing steps as described before. In the same manner, 50 μL of the prepared samples were added to the wells, using 3 different dilutions of each sample. The ssDNA samples prepared with streptavidin-coated magnetic beads and exonuclease digestion, were previously purified with the Qiaex II Gel Extraction Kit (Qiagen, Barcelona) in order to avoid the presence of streptavidin or exonucleases that could interfere in the hybridisation step. Horseradish peroxidase labeled secondary reporter probe (HPV reverse complementary primer) was added to each well (50 μl of 0.4 nM in 0.1 M PBS, pH 7.4) and left to incubate for 1 h before a final washing step was performed. All steps were carried out at a constant temperature of 37ºC. For the detection step, 50 μl of TMB substrate was added to each well and allowed to react for 15 min, prior to addition of 50 μl of 1 M H_2SO_4 to stop the reaction, turning the blue coloured solution to yellow, and the absorbance was read at 450 nm.

The ssDNA percentage recovery of each sample was calculated by dividing the ssDNA concentration obtained using ELONA by the initial dsDNA concentration determined.

3.4 Results and discussion

The purpose of the work reported here was to carry out a quantitative evaluation of the use of different well known ssDNA preparation methods, including *heat and cool,* streptavidin-coated magnetic beads and the use of exonucleases (T7 Gene 6 and Lambda exonuclease) for use in genosensing applications. As outlined previously, genosensors, similar to DNA chips and microarrays, exploit a short surface immobilised probe for hybridisation to its complementary target sequence. To this end, a technique exploiting surface immobilised probes, ELONA, was used to quantify the amount of ssDNA generated and compared to the theoretical maximum amount of ssDNA obtainable (Figure 3.2).

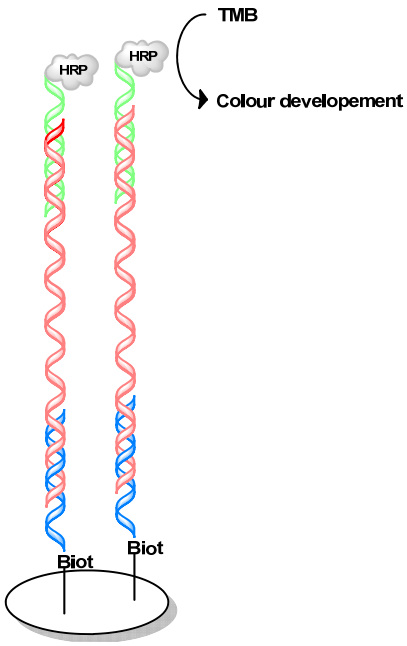

Figure 3.2. Schematic representation of Enzyme-Linked Oligonucleotide Assay (ELONA) methodology.

3.4.1 Evaluation of effect of immobilisation time and concentration of MB

In order to determine the optimum conditions for the generation of ssDNA with streptavidin-coated magnetic beads, the concentration of magnetic beads as well as the duration of incubation step was studied.

From 100 µL of PCR product, 50 nM dsDNA was mixed with different concentrations of pre-washed streptavidin-coated magnetic beads, ranging from 0.5 to 2.0 mg/mL (equivalent to approximately $4.3 \cdot 10^8$ – $2.1 \cdot 10^9$ Dynabeads per mL) and incubated at RT using gentle rotation. The effect of incubation time was evaluated by sampling the incubation mixture every 10 minutes over a period of 1 hour. For sample recovery, tubes were placed in contact with a magnet for 3 min. Ten µL of the supernatant was used for gel electrophoresis analysis in order to evaluate the level of immobilisation of the biotinylated PCR product on the magnetic beads. For the 159bp PCR product (HPV16) used in this study, a concentration of 1.5 mg/mL of magnetic beads with an incubation time of 20 minutes was observed to be optimal. Using lower

concentrations of beads, a high percentage of dsDNA remained in the recovered supernatant, even after 60 min of incubation. On the other hand, increasing the amount of magnetic beads (2 mg/ml) did not improve capture of dsDNA (Figure 3.3).

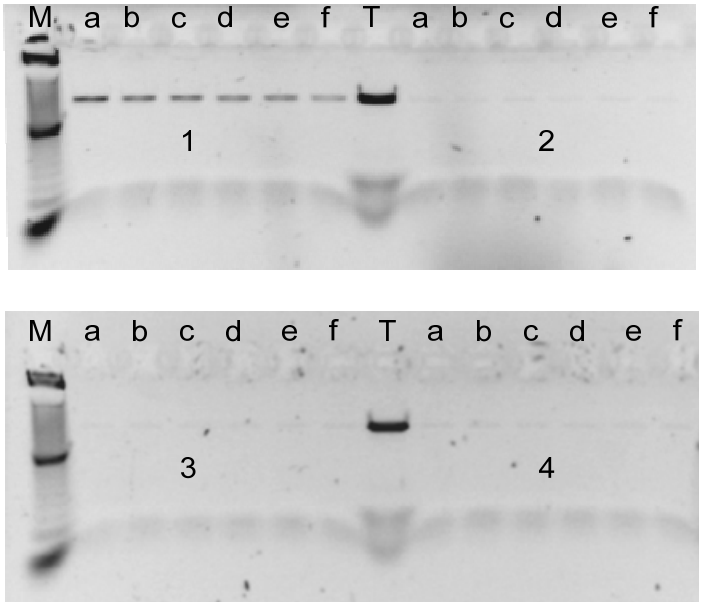

Figure 3.3. Agarose gel image for the optimisation of magnetic bead concentration. 1) 0.5 mg/mL, 2) 1 mg/mL, 3) 1.5 mg/mL and 4) 2 mg/mL. Wells: M) Marker 10bp, a-f) dsDNA in solution after incubation times from 10 to 60 min (in intervals of 10 min) and T) PCR product.

3.4.2 Single-stranded DNA separation and quantification of the streptavidin free in solution after alkaline or heat treatment.

Denaturation of the double-stranded DNA duplex captured on the magnetic beads was performed either by the addition of 20 µL of 150 mM NaOH solution for 3 min or heating at 95ºC for 5 min under shaking conditions in 10 mM PBS pH 7.4. The Eppendorf tubes were then placed in contact with a magnet for 3 minutes and the liberated ssDNA was recovered. For alkaline denaturation, neutralisation with 300 mM HCl and driven to the initial volume with 10 mM PBS was carried out.

An enzyme-linked immunosorbent assay was performed to quantify the possible loss of streptavidin from the magnetic beads due to the harsh thermal or alkaline treatment carried out in order to denature dsDNA to obtain the desired ssDNA. From the results observed in Figure 3.4, it can be determined that with heat treatment, 10 times more streptavidin/streptavidin-biotin-ssDNA/streptavidin-biotin-dsDNA had leached from the magnetic bead surface as compared with alkaline treatment, thus resulting in a loss of efficiency and thus alkaline treatment was used for further recovery experiments.

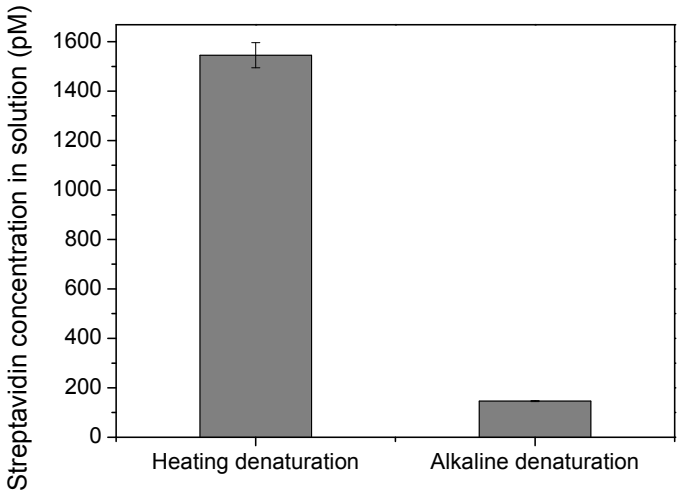

Figure 3.4. Concentration of free streptavidin in solution after alkaline and thermal denaturation.

3.4.3 Analysis of the generated single-stranded DNA

3.4.3.1 Gel electrophoresis

Qualitative determination of the single-stranded DNA generated by streptavidin-coated magnetic beads and exonuclease digestion was performed using gel electrophoresis. Samples prepared using *heat and cool* denaturation indicated a minor

degree of ssDNA generation, presumably attributable to the fact that in the cooling and electrophoretic process, annealing of the two complementary strands takes place, resulting in no differentiation between dsDNA and ssDNA bands on the gel. For the other three procedures studied, clear ssDNA bands appear in the agarose gel for both studied sequences (Figure 3.5). An advantage of ssDNA obtained using streptavidin-coated magnetic beads is the purity of the sample obtained, where no dsDNA band is observed in the gel, whereas with exonuclease digestion, dsDNA that was not digested remains.

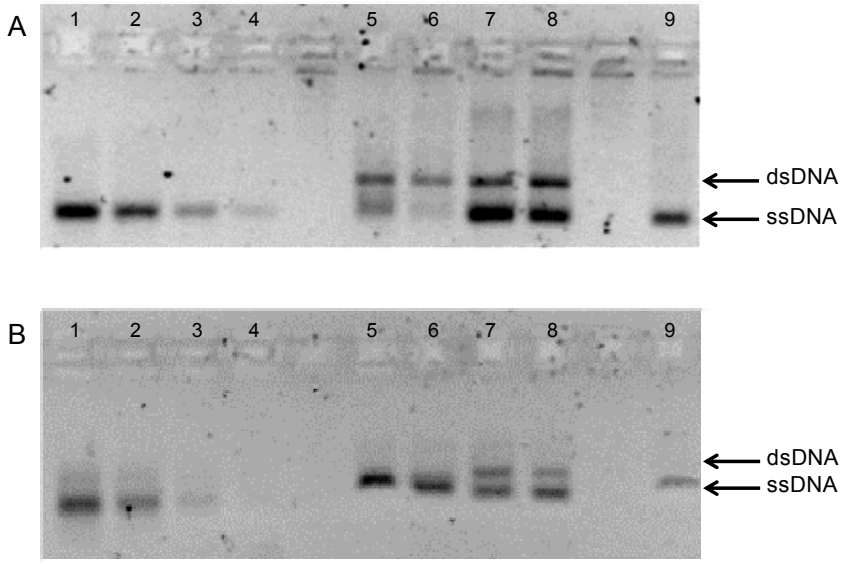

Figure 3.5. Agarose gel (4%) image of A) HPV16E7p and B) HPV45E6, where 1-4) Synthetic ssDNA at 60, 40, 20 and 10 nM; 5-6) T7 Gene 6 exonuclease; 7-8) Lambda exonuclease and 9) Streptavidin-coated magnetic beads.

In order to perform a semi-quantitative study of the ssDNA obtained, a range of concentrations (60, 40, 20 and 10 nM) of a synthetic ssDNA analogue of the studied sequences at different concentrations were run with the samples, based on the comparison of the intensity of the ssDNA bands using ImageJ software.

3.4.3.2 Enzyme-linked oligonucleotide assay (ELONA)

Single-stranded DNA from HPV16E7p and HPV45E6 prepared by the three different methodologies was characterised using ELONA and calibration plots for both sequences were constructed using synthetic ssDNA, obtaining sigmoidal relationships (LOD of 128 pM and R^2=0.9963 for HPV16 and a LOD of 142 pM and R^2= 0.9985 for HPV45), and the calibration plots are shown in Figure 3.6. Recoveries obtained for all methodologies are depicted in Table 3.1.

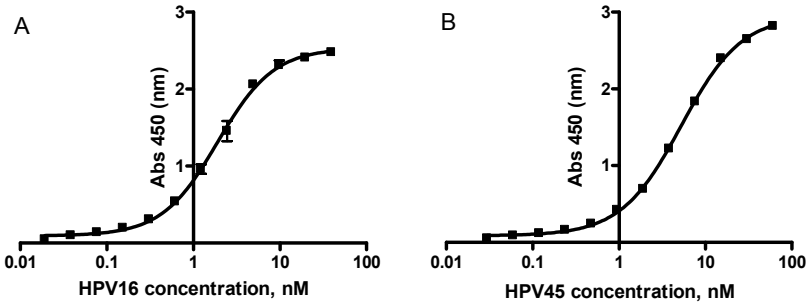

Figure 3.6. ELONA calibration plots for HPV16 and HPV45.

Table 3.1. Summary of the ssDNA recovery obtained for the three different techniques (n=5)

Methodology	**ssDNA recovery (%)**	
	HPV16 (159 bp)	HPV45 (78 bp)
Heat and cool	40 ± 37	22 ± 21
Streptavidin-coated magnetic beads	62 ± 7	62 ± 8
Lambda exonuclease	65 ± 8	70 ± 7
T7 Gene 6 exonuclease	54 ± 7	47 ± 8

3.4.3.2.1 Streptavidin-coated magnetic beads.

For ssDNA generated with streptavidin-coated magnetic beads from purified PCR product, biotinylated primer was used in the PCR reaction, for subsequent capture on

the streptavidin-coated magnetic beads. The beads were then incubated with an alkaline solution (150 mM NaOH) in order to denature the duplex to generate the desired ssDNA. The generated ssDNA was quantified using ELONA, revealing a 62 ± 7% recovery for HPV16 and 62 ± 8% of recovery for HPV45E6. The results obtained are considerably higher in terms of ssDNA yield than that presented by Wendel, H.P. *et al.*[25] where only 21% of the maximum possible amount of ssDNA was recovered by using M-280 Dynabeads from Invitrogen by using purified dsDNA from PCR product. The binding capacity of this magnetic beads is two times lower in comparison to the beads used in the present study (of approx. 10 μg of dsDNA versus 20 μg for Dynabeads MyOne Streptavidin C1), which may explain the lower efficiency.

3.4.3.2.2 Exonuclease digestion

For T7 Gene 6 and Lambda exonuclease digestion, a 5'-phosphorothioate modified reverse primer and 5'-phosphate modified forward primer, respectively, were used for PCR amplification. In both cases three different digestion times were studied, 10, 30 min and 1 h. After digestion, enzymes were inactivated by increasing the temperature to 85ºC and incubating for 10 min. Gel electrophoresis of the different samples was performed in order to follow the evolution of both dsDNA and ssDNA with digestion time. As can be observed in Figure 3.7, the band of dsDNA becomes lighter with increasing incubation time. After 30 min, no significant decrease in the dsDNA band was observed.

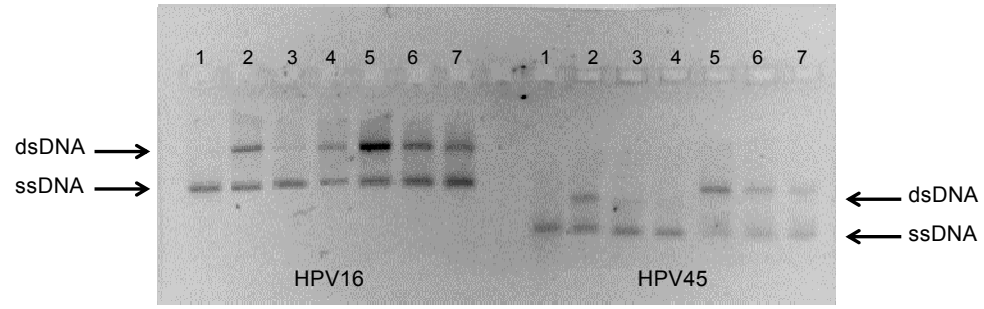

Figure 3.7. Evolution of the generation of ssDNA with digestion time for HPV16 and HPV45. Lane 1) Synthetic ssDNA; Lanes 2-4) Lambda exonuclease digestion for 10, 30 and 60 min respectively and Lanes 5-7) T7 Gene 6 exonuclease digestion for 10, 30 and 60 min respectively

In ELONA determination, Lambda exonuclease produces ssDNA in a 65 ± 7% (HPV16) and 70 ± 7% (FPV45) recovery from the initial amount of dsDNA. These results are higher than that reported by Gopinath *et al.*,[26] where an optimisation of the preparation of ssDNA from purified PCR product by lambda exonuclease digestion followed by phenol:chloroform extraction resulted in 39 ± 3% recovery. However, the results obtained are comparable with the data reported by Wendel *et al.*[25] where a 62 ± 8% of ssDNA was recovered after 2 h of digestion at 37ºC. Lower ssDNA recoveries were found with T7 Gene 6 exonuclease, being 54 ± 7% for HPV16 and 47 ± 8% for HPV45. This lower percentage recovery achieved with the T7 Gene 6 in comparison to the Lambda exonuclease can be attributed to the difference in the processivity of the two exonucleases, where one unit of the Lambda Exonuclease releases 10 nmol of acid-soluble deoxyribonucleotides from dsDNA template in 30 min, whilst one unit of T7 Gene 6 exonucleases produces 2 nmol in the same time period.

3.4.3.2.3 Heat and cool

Aliquots (in PBS, pH 7.4) of HPV16E7p and HPV45E6 purified PCR products were incubated at 95ºC for 5 minutes in order to separate the two strands. Rapid cooling down on ice was carried out in order to retard the re-annealing of the DNA strands. Samples were then analysed by ELONA. Results obtained show an evident

dependence of the single-stranded DNA recovery on the initial dsDNA concentration. Recoveries of 8 ± 7% (n=5) were found for more concentrated samples (around 10.0 nM), while for more diluted samples (around 0.5 - 1 nM), the recoveries achieved are higher, of 25 ± 16 % (n = 5) for HPV45 and 41 ± 38% (n = 5) in the case of HPV16, which can be explained by the higher probability of the two DNA strands colliding and re-hybridising when present at higher concentrations. Whilst the recoveries are improved for more diluted dsDNA, the deviation in obtainable ssDNA was huge using the same initial dsDNA sample.

3.4.3.2.4 Preparation of single-stranded DNA from purified or non-purified PCR product

Additional steps in the preparation of ssDNA such as the purification of the PCR product, can lead to losses in the initial concentration of dsDNA. Therefore, a comparison of the final ssDNA concentration obtained from purified and non-purified PCR product was performed with HPV45 sequence and for streptavidin-coated magnetic beads and exonuclease digestion techniques. In this case, concentration of purified PCR product was evaluated as explained above, via UV spectroscopy, while in the case of PCR product it is not possible due to the interfering of non-consumed primers, dNTPs and enzymes on the final absorbance. Then, concentration was determined by electrophoretic gel analysis based on the comparison of the intensity of known concentrations of dsDNA standards bands using ImageJ software. Calibration curve was built for five different samples of concentration ranging from 100 – 0 nM in ½ dilution factor (R^2 = 0.9985). Concentration of non-purified PCR products were 51 ± 3, 87 ± 4 and 68 ± 1 nM for phosphorothioated, phosphorylated and biotynilated PCR products respectively. Determination of the concentration after the purification of the three PCR products lead to looses of 11, 32 and 11% from the initial dsDNA concentration respectively. Samples were analysed by Bioanalyzer (Agilent) using a DNA 1000 chip, obtaining an excellent correlation.

Starting from the same PCR product, ssDNA was generated by using the different techniques from purified dsDNA or directly from the PCR product. Samples were

then quantified by ELONA (Table 3.2). It can be observed that slightly higher concentration of ssDNA was obtained from non-purified PCR product in the case of streptavidin-coated beads and T7 Gene 6 exonuclease, whilst in the case of Lambda exonuclease, the concentration is lower. However it is important to remark that in the purification step, between 10 and 30% of the initial dsDNA was lost. In terms of ssDNA recovery, it can be observed that comparable values were obtained for streptavidin-coated beads (62 ± 8% and 59 ± 4% for purified and non-purified PCR). Also, slightly improved recovery was obtained for ssDNA generation with T7 Gene 6 starting from non-purified product (50 ± 2%), against the one obtained for the purified sample (47 ± 8%). These comparable results could be explained by the similarity of the PCR buffer with the proper buffer of the techniques. Contrary, bigger differences in the composition of Lambda exonuclease buffer could explain the big decrease in recovery observed for Lambda exonuclease digestion from non-purified PCR product, obtaining 43 ± 9% while for purified sample, a recovery of 70 ± 7% was obtained.

Table 3.2. ssDNA concentration obtained from the same HPV45 PCR product (purified and non-purified).

Methodology	**ssDNA concentration (nM)**	
	Purified PCR	Non-purified PCR
Streptavidin-coated magnetic beads	37 ± 1	41 ± 2
Lambda exonuclease	42 ± 2	37 ± 6
T7 Gene 6 exonuclease	21 ± 1	25 ± 2

3.5 Conclusions

Different methods for the generation of single-stranded DNA from a double-stranded PCR product were evaluated using gel electrophoresies to qualitatvely evaluate the purity of the ssDNA generated, and enzyme-linked oligonucleotide assay for the quantitative determination of the amount of ssDNA produced. The widely

used *heat and cool* methodology was found to be the least reliable, showing very low efficiency and very high irreproducibility, and also showing a dependency on the concentration of the dsDNA template. The alternative methods studied, using streptavidin-coated magnetic beads or exonuclease digestion were demonstrated to be rapid methods for ssDNA generation with a high efficiency obtaining recoveries between 50-70% from the theoretical maximum with a good reproducibility, RSD% < 8 (n=5).

Using streptavidin-coated magnetic beads and biotinylated PCR products alkaline and heat denaturation of the dsDNA duplex were compared. Alkaline denaturation was found to perform better, which can be attributed to the less harsh environment on the denaturation process that gave rise to significantly less desorption of streptavidin (and obviously streptavidin-biotin-dsDNA), providing a percentage recovery of around 62%. For exonuclease digestion, T7 Gene 6 and Lambda exonuclease were studied. In both cases, a high recovery was obtained with the two HPV sequences studied, of around 50 and 70 % respectively.

Lambda exonuclease is the methodology which gives a higher recovery starting from purified PCR product with a lower cost in comparison to the other techniques reported in this study, to obtain the same final concentration of ssDNA. T7 Gene 6 exonuclease and streptavidin-coated magnetic beads used in this study are approximately 2 and 7 times more expensive. Another advantage is that the digestion approaches required 45 minutes, whilst the streptavidin magnetic isolation method required between 60-90 minutes. Additional time will be required if purification of the PCR product is performed.

In order to evaluate the need of the purification step of PCR product, a comparison of the final amount of ssDNA obtained and its recovery starting from the same PCR product (by purifying the sample or not) was carried out. We observed that around 10 – 30% of the initial amount of dsDNA was lost during the purification process. Slightly higher concentration of ssDNA was obtained from non-purified PCR product in the case of streptavidin-coated beads and T7 Gene 6 exonuclease, whilst in the case of Lambda exonuclease, the concentration was lower. In terms of ssDNA recovery,

comparable values were obtained for streptavidin-coated beads and T7 Gene 6 starting in both cases, but a big decrease in recovery was observed for Lambda exonuclease digestion from non-purified PCR product of 28%.

In conclusion, lambda exonuclease is the best methodology in terms of ssDNA recovery, cost and time consuming when starting from purified PCR product. Nevertheless, the purification step leads to losses of the initial dsDNA product and increases the time of the assay, being a disadvantage for its application in DNA biosensing quantification. Both streptavidin-coated magnetic beads with alkaline denaturation and the T7 Gene 6 Exonuclease resulted in good recoveries when starting from non-purified PCR product in comparison with Lambda exonuclease, that its recovery decreases.

Whilst none of the techniques provide 100% generation of ssDNA, they are very reproducible and thus a correlation factor can be used to provide an accurate quantitative determination of nucleic acid levels. Further work involves the application of the three techniques to genosensors and microarrays with a range of PCR products.

3.6 Acknowledgements

HPV sequences used in this work were identified by TATAA Biocenter, www.tataa.com (Gothenburg, Sweden). This research has been carried out with financial support from the Comission of the European Communities, RTD programme "Smart Integrated Biodiagnostic Systems for Healthcare, SmartHEALTH, FP6-2004-IST-NMP-2-016817". A. F. thanks Ministerio de Ciencia y Tecnología, Spain, for a "Ramón y Cajal" Research Professorship. L. C. acknowledges Universitat Rovira i Virgili for a predoctoral scholarship.

3.7 References

1. M. A. Diggle and S. C. Clarke, *Molecular Biotechnology*, 2003, **24**, 221-224.
2. M. Orita, H. Iwahana, H. Kanazawa, K. Hayashi and T. Sekiya, *Proceedings of the National Academy of Sciences of the United States of America*, 1989, **86**, 2766-2770.
3. S. Stahl, T. Hultman, A. Olsson, T. Moks and M. Uhlen, *Nucleic Acids Research*, 1988, **16**, 3025-3038.
4. F. Erdogan, R. Kirchner, W. Mann, H. H. Ropers and U. A. Nuber, *Nucleic Acids Research*, 2001, **29**, E36.
5. K. Tang, D. J. Fu, D. Julien, A. Braun, C. R. Cantor and H. Koster, *Proceedings of the National Academy of Sciences of the United States of America*, 1999, **96**, 10016-10020.
6. D. Wang, H. Gao, R. Zhang, X. Ma, Y. Zhou and J. Cheng, *Biotechniques*, 2003, **35**, 300-308.
7. D. Dell'Atti, M. Zavaglia, S. Tombelli, G. Bertacca, A. O. Cavazzana, G. Bevilacqua, M. Minunni and M. Mascini, *Clinica Chimica Acta*, 2007, **383**, 140-146.
8. F. Lucarelli, G. Marrazza and M. Mascini, *Biosensors and Bioelectronics*, 2005, **20**, 2001-2009.
9. U. B. Gyllensten and H. A. Erlich, *Proceedings of the National Academy of Sciences of the United States of America*, 1988, **85**, 7652-7656.
10. M. W. Allard, D. L. Ellsworth and R. L. Honeycutt, *Biotechniques*, 1991, **10**, 24-26.
11. B. Kaltenboeck, J. W. Spatafora, X. Zhang, K. G. Kousoulas, M. Blackwell and J. Storz, *Biotechniques*, 1992, **12**, 164-171.
12. L. F. Landweber and M. Kreitman, *Methods in Enzymology*, 1993, **218**, 17-26.
13. R. Medori, H. J. Tritschler and P. Gambetti, *Biotechniques*, 1992, **12**, 346-&350.
14. N. C. Pagratis, *Nucleic Acids Research*, 1996, **24**, 3645-3646.
15. R. G. Higuchi and H. Ochman, *Nucleic Acids Research*, 1989, **17**, 5865-5865.
16. C. Kerr and P. D. Sadowski, *Journal of Biological Chemistry*, 1972, **247**, 311-318.
17. T. T. Nikiforov, R. B. Rendle, M. L. Kotewicz and Y. H. Rogers, *Genome Research*, 1994, **3**, 285-291.
18. M. Espelund, R. A. P. Stacy and K. S. Jakobsen, *Nucleic Acids Research*, 1990, **18**, 6157-6158.
19. A. Paul, M. Avci-Adali, G. Ziemer and H. P. Wendel, *Oligonucleotides*, 2009, **19**, 243-254.

20. A. Tahiri-Alaoui, L. Frigotto, N. Manville, J. Ibrahim, P. Romby and W. James, *Nucleic Acids Research*, 2002, **30**, e45.
21. H. z. Hausen, *Biochimica et Biophysica Acta (BBA) - Reviews on Cancer*, 1996, **1288**, F55-F78.
22. N. Munoz, F. X. Bosch, S. de Sanjose, R. Herrero, X. Castellsague, K. V. Shah, P. J. F. Snijders, C. Meijer and C. Int Agcy Res Canc Multicenter, *New England Journal of Medicine*, 2003, **348**, 518-527.
23. J. Thomison Iii, L. K. Thomas and K. R. Shroyer, *Human Pathology*, 2008, **39**, 154-166.
24. M. H. Stoler, *International Journal of Gynecological Pathology*, 2000, **19**, 16-28.
25. M. Avci-Adali, A. Paul, N. Wilhelm, G. Ziemer and H. P. Wendel, *Molecules*, 2010, **15**, 1-11.
26. M. Citartan, T. H. Tang, S. C. Tan and S. C. B. Gopinath, *World Journal of Microbiology and Biotechnology*, 2011, **27**, 1167-1173.

Chapter 4

Electrochemical genosensor array for the simultaneous detection of multiple high-risk human papillomavirus sequences in clinical samples

Analytica Chimica Acta 715 (2012) 93-98

Laia Civit[a], Alex Fragoso[a,*], Sebastian Hölters[b], Matthias Dürst[b], Ciara K. O' Sullivan[a,c,*]

[a] Nanobiotechnology and Bioanalysis Group, Departament d'Enginyeria Química, Universitat Rovira i Virgili, 43007 Tarragona, Spain.
[b] Department for Gynecology, Jena University Hospital, Friedrich-Schiller-University Jena, D-07743 Jena, Germany
[c] Institució Catalana de Recerca i Estudis Avançats, Passeig Lluís Companys 23, 08010 Barcelona, Spain

Keywords: multiplexing, human papillomavirus, DNA detection, amperometric detection, clinical diagnostics

4.1 Abstract

An electrochemical genosensor array for the simultaneous detection of three high-risk human papillomavirus (HPV) DNA sequences, HPV16, 18 and 45, exhibiting high sensitivity and selectivity is presented. The electrodes of a 4 x 4 array were modified via co-immobilisation of a 1:100 (mol/mol) mixture of a thiolated probe and an oligoethyleneglycol-terminated bipodal thiol. Detection of synthetic and PCR products was carried out in a sandwich type format, with the target hybridised between a surface immobilised probe and a horseradish peroxidase-labelled secondary reporter probe. The detection limits obtained in the detection of each individual target were in the pM range, allowing the application of this sensor for the detection of samples obtained from PCR amplification of cervical scrape samples. The results obtained exhibited an excellent correlation with the HPV genotyping carried out within a hospital laboratory. Multiplexing and cross-reactivity studies demonstrated high selectivity over potential interfering sequences, facilitating application of the developed platform for the high-throughput screening of multiple high-risk DNA sequences.

4.2 Introduction

Human papillomavirus (HPV) is one of the most common sexually transmitted infections, affecting the skin and mucous membranes, and is a double-stranded DNA virus[1] of which more than 200 HPV types have been identified with greater than 40 HPV types infecting the genital areas of men and women.[2] Genital HPV types have been subdivided into low-risk, forming genital warts (HPV6, 11, 40, 42, 43, 44, 53, 54, 61, 72, 73 and 81) and the high-risk types (HPV16, 18, 31, 33, 35, 39, 45, 51, 52, 56, 58, 59 and 68), which are detected in virtually all invasive cervical cancers and have been confirmed as the major cause of this cancer. The classic high-risk HPV types are 16 and 18[3] although types 31 and 45 have also been found to be present in approximately 80% of cervical cancer cases together with types 16 and 18.[4] A key step in the development of cervical cancers is the dysregulated expression of the viral oncogenes E6 and E7. These oncoproteins interfere with the protective function of the cellular

proteins p53 and pRb, respectively and thereby induce uncontrolled cell growth and genetic instability.[5-6]

The existence of a strong relationship between persistent infection of the high-risk HPV types and development of cervical cancer highlights the importance of the early and cost-effective detection of these DNA strains.[7] HPV diagnostics are most commonly based on molecular recognition to detect HPV DNA related sequences in cervical scrape samples. These molecular tools can be divided into two major groups: those based on nucleic acid assays, where hybrid capture technology (developed by Digene Corporation) is the most widely used technique, and the other major group being based on amplification techniques such as the polymerase chain reaction (PCR).[8]

Another, less explored, possibility for the detection of HPV is the use of DNA biosensors, also known as genosensors. Different types of genosensors with piezoelectric,[9] leaky surface acoustic wave[10] or giant magnetoresistive detection[11] have been reported for the detection of HPV. The electrochemical detection of HPV related sequences has been reported in the past few years, using, for example, methylene-blue as a hybridisation indicator[12] or exploiting reporter probes labelled with ferrocene.[13] In the first case, a 20-mer probe related to the HPV major capsid protein L1 was immobilised on the surface of a graphite electrode and the methylene-blue response was recorded before and after target recognition and hybridisation, achieving a limit of detection of 1.2 ng μL^{-1} (200 nM). The second example involved the use of a hybridisation-based bioelectronic DNA detection platform (eSensor™), for the detection of HPV sequences based on 14 thiolated probes immobilised on the chip surface and hybridisation with a ferrocene-labelled reporter sequence. Hybridisation required up to 8 h at 40ºC, detecting 86 % of the HPV targets contained in clinical samples giving a positive/negative type response. In a more recent report, the detection of HPV was carried out by treating a captured double-stranded DNA duplex with acid and directly measuring the released purine bases using square wave voltammetry, obtaining a limit of detection of 2 pg mL^{-1} (330 fM).[14]

Multiplexed assays can screen multiple analytes in a single assay which is significantly simpler, more rapid and requires less sample and reagent consumption in

comparison to multiple single-target assays.[15] This is particularly important in the multiplexed detection of nucleic acids due to its key role in current and evolving clinical diagnostics and theranostics, where expression patterns of multiple RNA markers will be used to prescribe appropriate therapy.

In a recent preliminary study,[16] we demonstrated the ability of the proposed electrochemical sensor array for the individual and multiplex detection of HPV specific high-risk HPV sequences (HPV18 and 45) with high specificity and selectivity and in the work reported here, we extend and exploit the reported proof-of-concept by the introduction of a new high-risk HPV sequence, developing an electrochemical genosensor array for the simultaneous detection of three specific high-risk HPV sequences, HPV16, 18 and 45, typically found in invasive cervical cancer. Analytical parameters such as sensitivity and specificity were investigated and reusability was explored for developmental work. The 16 gold working electrodes sensor array used in this work permits parallel detection of multiple targets and multiplex studies were thus carried out by immobilising the three thiolated HPV probes on alternating electrodes. Detection was carried out via the hybridisation of a mixture of the three targets and specific HRP-labeled probe, demonstrating a high specificity of the sensor array and no significant cross-hybridisation was found between the three high-risk sequences studied. Finally, samples obtained from cervical scrapes were amplified and used in order to evaluate the genosensor performance in a real clinical scenario, comparing the response with HPV genotyping carried out in a hospital laboratory, and an excellent correlation was obtained.

4.3 Experimental

4.3.1 Instrumentation

All electrochemical measurements were performed with a PGSTAT 12 potentiostat (Autolab, The Netherlands) controlled with the General Purpose Electrochemical System (GPES) software and equipped with a MUX module (Eco Chemie B.V., The Netherlands).

The electrode array consists of 16 gold working electrodes arranged in a four by four distribution on a glass chip measuring 21 mm × 23 mm, fabricated at the Institut für Mikrotechnik Mainz (www.imm-mainz.de). Each working electrode (1mm × 1 mm) was placed between a silver pseudo reference (0.2 mm × 1 mm) and a gold counter electrode of the same size in order to create 16 planar electrochemical cells. The electrode array was integrated within a microfluidic cell, where the microfluidic channels were realised by mounting the array onto a polycarbonate fluidic chip using double-sided medical grade adhesive foil of 50 μm thickness, which had been previously laser machined to generate microchannel structures of 1 mm width. Connection of the assembled chip was realised via pogopin connectors to each of the 18 electrodes (16 working electrodes and 1 plus 1 reference and counter electrodes).[17]

4.3.2 Chemcials

Dithiol 16-(3,5-bis((6-mercaptohexyl)oxy)phenyl)-3,6,9,12,15-pentaoxahexa-decane) (DT1) was purchased from SensoPath Technologies (Bozeman, NT). Phosphate buffered saline with Tween 20 (pH 7.4) and 3,3',5,5'-Tetramethylbenzidine (TMB) Liquid Substrate System for ELISA were from Sigma-Aldrich (Barcelona, Spain). Potassium dihydrogen phosphate and sodium hydroxide were purchased by Scharlau (Barcelona, Spain). All solutions were prepared with MilliQ water (18 MΩ.cm) produced with a Milli-Q RG system (Millipore Ibérica, Madrid, Spain). Microtiter Streptavidin-Coated Strip Plates were from ThermoScientific (Barcelona, Spain).

Thiolated and biotinylated capture probes (HPV16E7p of 24-mer, HPV18E6 of 22-mer and HPV45E6 of 23-mer), target sequences (HPV16E7p of 159-mer, HPV18E6 of 139-mer and HPV45E6 of 78-mer) and HRP-labelled secondary reporter probe and reverse primers (HPV16E7p of 21-mer, HPV18E6 of 22-mer and HPV45E6 of 18-mer) were purchased from Biomers.net (Ulm, Germany). TATAA Biocentre (www.tataa.com) can be contacted for further details on the specific sequences of the probes, primers and target amplicons. High-risk HPV positive and

negative cervical scrapes of anonymous female patients were provided by the Jena University Hospital.

4.3.3 Probe immobilisation on electrode array

Prior to modification of the electrode arrays, a two-step cleaning protocol was applied. Initially in order to remove the protective resist used during storage, the arrays were sonicated for 5 min in acetone, 5 min in iso-propanol (3 times) and rinsed with water. In a second step, electrochemical cleaning was performed in 0.5 M H_2SO_4 by application of a constant potential of 1.6 V for 10 sec followed by 40 voltammetric cycles in the potential range -0.2 to 1.6 V at a scan rate of 0.5 $V \cdot s^{-1}$. Finally, the electrodes were rinsed with Milli-Q water and dried with nitrogen. Modification of the cleaned electrode arrays was carried out via co-immobilisation of the specific thiolated probe (1 μM) and DT1 (100 μM) in 1 M KH_2PO_4 aqueous solution (pH 3.5) by deposition of 1 μL of the mixture over the working electrodes for 3 h at room temperature in a humid (>90%) environment. Dithiol DT1 was co-immobilised with the thiolated probe in order to eliminate non-specific binding of the labeled reporter probe, whilst also spacing out and orientating the probe to facilitate efficient hybridisation of the target. In order to remove the non-attached molecules, the electrode arrays were washed in a stirring solution of 0.1 M PBS-Tween for 20 min, rinsed with water and dried with nitrogen.

4.3.4 Electrochemical DNA detection

DNA detection of both synthetic oligonucleotides and PCR product from clinical samples (see section 4.3.6) was performed in a sandwich hybridisation format (Figure 4.1).

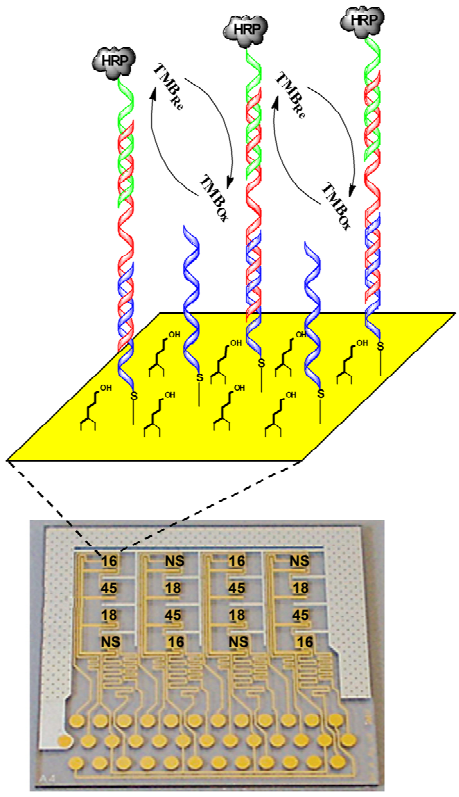

Figure 4.1. Schematic view of the sensor array used and the developed assay based on co-immobilisation of thiolated probe with bipodal alkanethiol, hybridisation process and electrochemical detection.

To construct the calibration curves of HPV16, 18 and 45, 0.5 µL of each HPV target of various concentrations ranging from 0 to 50 nM (in triplicate) in 0.1 M PBS-Tween were deposited on each of the oligonucleotide modified gold electrodes and incubated for 20 minutes at room temperature. The sensors were subsequently washed for 15 min, under stirring conditions, in 0.1 M PBS-Tween and then dried with nitrogen. A second hybridisation was performed by spotting 0.5 µL of 10 nM labelled reporter in 0.1 M PBS-Tween and incubating for another 20 minutes at room temperature with both hybridisations carried out in a humid environment. The hybridised microarray was subsequently washed with 0.1 M PBS-Tween for 15 min and dried in nitrogen. For real sample analysis, 0.5 µL of an unknown concentration of the ssDNA generated from PCR product, in 0.1 M PBS-Tween, was applied to the

array and incubated for 20 minutes. The rest of the steps were performed as explained above. The modified electrode arrays were assembled on a microfluidic cell similar to that described previously[17] to perform the electrochemical detection. The detection process was carried out in the created microfluidic channels in the presence of TMB substrate where the HRP-catalysed reduction of TMB[18-19] was detected by steps and sweeps technique by applying two consecutive potential steps of 0 V for 1 ms and -0.2 V for 0.5 s.

4.3.5 Multiplexed detection

Clean electrode arrays were modified by spotting 1 μL of a mixture of 1 μM thiolated probes (HPV16E7p, HPV18E6, HPV45E6 and a non-specific probe, HPV45E7) and 100 μM DT1 on alternating working electrodes for 3 h at room temperature. A mixture of the three targets at a concentration of 5 nM for HPV16E7p and HPV18E6 and 0.5 nM for HPV45E6 in 0.1 M PBS-Tween, pH 7.4 was then added and incubated for 20 min. The sandwich complex was formed by subsequent hybridisation with a 10 nM mixture of the three HRP-labelled probes, in 0.1 M PBS-Tween pH 7.4, for 20 min. Washing steps and electrochemical detection were carried out as explained in Section 4.3.4.

4.3.6 Hospital laboratory analysis of cervical scrapes

In order to test the performance of the developed electrochemical genosensor array for the detection of high-risk HPV DNA in clinical samples, a number of cervical scrapes obtained from patients attending the Dysplasia Unit of the Department for Gynecology at the Jena University Hospital were evaluated. These samples had been HPV-genotyped at the Jena University Hospital using the GP5+/GP6+ protocol of Jacobs *et al.*[20] and were provided for this study as anonymous samples thus not requiring ethical permission for use. The PCR assay routinely conducted at the Jena University Hospital comprises 10 μl DNA (up to 50 ng), 1X reaction buffer, 3.5 mM $MgCl_2$, 200 μM of each dNTP, 1U of thermostable DNA polymerase (AmpliTaq,

Roche) and 50 pmol each of the GP5+/GP6+ primers (which allow the amplification of all genital HPV types) to a final volume of 50 µl. DNA was extracted from cervical scrapes using the QIAmp DNA Mini Kit from Qiagen according to the manufacturer's recommendations. The DNA was dissolved in 80 µl of H_2O, with typical DNA concentrations ranging from 0.5 to 5 ng μL^{-1}.

The PCR products were detected by an enzyme immunoassay (EIA) which can differentiate high risk from low risk HPV groups, using a cocktail of digoxygenin labelled probes. For HPV genotyping, individual digoxygenin labelled probes were used. The GP5+/GP6+ assay has a semi-qualitative read-out and a sensitivity of about 100 HPV genome copies per reaction. Based on this assay the genomic DNA from 3 HPV16- , 3 HPV18- , 3 HPV45- positive patients and 3 HPV-negative patients were provided for evaluation of the developed sensors. A biotinylated forward primer was used for generation of single stranded DNA (ssDNA) and 5 µL of the provided aliquots were used.

HPV16E7p PCR protocol. The 100 µL reaction mixture contained 1 U of Taq polymerase (Invitrogen), 1X PCR reaction buffer, 3 mM $MgCl_2$, 200 µM dNTP and 400 nM of each primer. Thermal conditions were optimised to be 2 min at 95°C followed by 30 cycles of 20 s at 95°C, 20 s at 60°C, and 20 s at 72°C.

HPV18E6 and HPV45E8 PCR protocols. The 100 µL reaction mixture contained 1U of Taq polymerase, 1X PCR reaction buffer, 2 mM $MgCl_2$, 200 µM dNTP and 200 nM of each primer. Thermal conditions for HPV18E6 were optimised to 2 min at 95°C followed by 30 cycles of 20 s at 95°C, 20 s at 55°C, and 20 s at 72°C. Thermal protocol for HPV45E6 is: 2 min at 95°C followed by 25 cycles of 20 s at 95°C, 20 s at 60°C, and 20 s at 72°C.

A final extension step of 72°C for 7 min was included in all protocols. Thermal cycling was performed in an ICycler Thermal Cycler (Bio-Rad Laboratories, S.A, Barcelona).

4.3.7 Generation of ssDNA from amplified products

Following amplification, strand separation was performed with streptavidin-coated magnetic beads (Dynabeads MyOne Streptavidin C1, Invitrogen, Barcelona), which were prepared according to the manufacturer's recommendations. Briefly, 200 μL of PCR product was mixed with the same volume of 2X B&W buffer (10 mM Tris-HCl pH 7.5, 1 mM EDTA and 2 M NaCl) and 0.1 mg of pre-washed beads and incubated for 30 min at RT under gentle shaking conditions. The tubes were then placed in proximity to a magnet for 2-3 min, and the beads were held in place, the supernatant was discarded and the isolated beads were washed twice with 1X B&W buffer. Denaturation of the immobilised double stranded (dsDNA) was performed by the addition of 60 μL of 100 mM NaOH for 3 min. The supernatant containing ssDNA was recovered, precipitated and rehydrated in PBS-Tween (0.1 M, pH 7.4) and stored at -20ºC.

4.4 Results and discussion

4.4.1 Individual detection of HPV16, HPV18 and HPV45

Calibration curves were constructed for each sequence studied to evaluate the analytical performance of the genosensor using synthetic oligonucleotides (Figure 4.2). The current responses showed a linear relationship with target concentration in the range of 0.1-10 nM with a sensitivity of 0.15 $\mu A \cdot nM^{-1}$ ($r^2 = 0.997$) and LOD of 220 pM for HPV16E7p, from 0.1 to 12 nM with a sensitivity of 0.119 $\mu A \cdot nM^{-1}$ ($r^2 = 0.987$) and LOD of 170 pM for HPV18E6 and in the range of 0.1-1 nM with a sensitivity of 1.02 $\mu A \cdot nM^{-1}$ ($r^2 = 0.999$) for HPV45E6 with LOD of 110 pM. These differences in sensor parameters may be due to the fact that HPV16E7p and HPV18E6 targets are considerably longer (159-mer and 139-mer) than the HPV45E6 (78-mer) target. The low background signal obtained in the absence of target, as evidenced with the intercept in the calibration curve, demonstrates that there is no-specific adsorption of the reporter probe on the electrode surface.

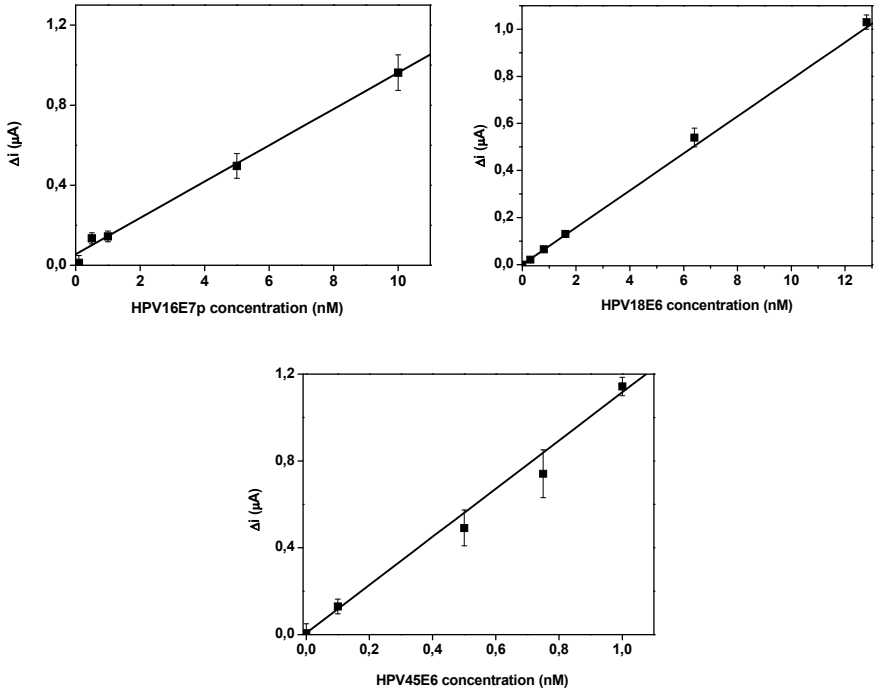

Figure 4.2. Dynamic linear ranges in the calibration curves obtained for HPV16E7p, HPV18E6 and HPV45E6.

4.4.2 Cross-hybridisation studies

Selectivity and specificity are fundamental in the performance of multiplexed detection using an electrode array. Hence, discrimination between the three high-risk sequences studied is essential for a reliable response. Furthermore, co-storage of a mixture of HRP-labeled reporter probes would simplify the assay for the end-user. To evaluate possible cross-reactions between the selected HPV types, a series of experiments were performed using mixtures of targets and reporter HRP-labeled probes and the responses were compared with measurements using the single specific target and probe (Figure 4.3).

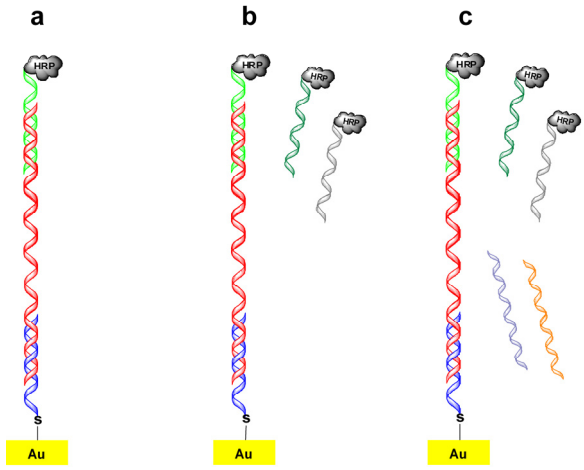

Figure 4.3. Schematic representation of the cross-hybridisation studies based on the comparison of (a) detection of a given sequence with its specific reporter probe, (b) detection of a given probe with a mixture of reporter probes and (c) detection of a mixture of the three sequences with a mixture of reporter probes.

The electrode array was modified with thiolated HPV16E7p, HPV18E6 and HPV45E6 capture probes on different working electrodes and target hybridisation was performed using aliquots of the single specific target or a mixture of the three targets at concentrations of 1 or 10 nM on the electrode surface. Similarly, hybridisation of single specific or a mixture of 10 nM HRP-labelled reporter probes was carried out. Responses were plotted by comparing the signal of the specific hybridisations with the responses obtained when the hybridisations were carried out in the presence of the mixture of targets and/or HRP labeled probes (Figure 4.4), and no significant interference was observed (RSD < 7%, n = 3), and it can thus be concluded that there is negligible cross-hybridisation for HPV16E7, HPV18E6 and HPV45E6.

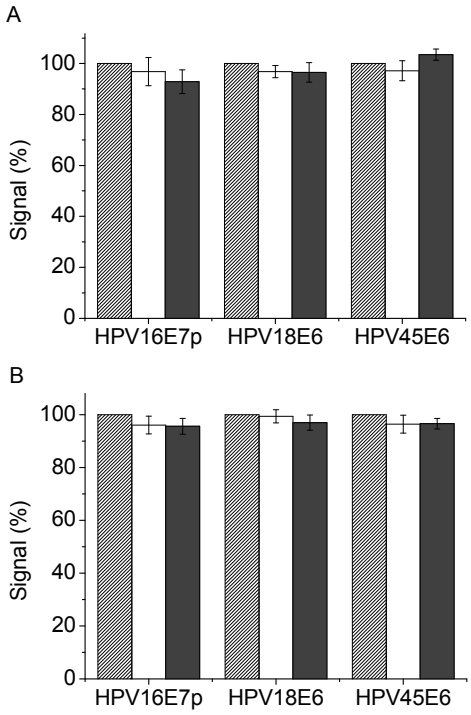

Figure 4.4. Cross-hybridisation studies results for (A) 1 nM target and (B) 10 nM target. grey column: specific target and specific HRP-labelled probe; white column: specific target and mixture of HRP-labelled probes; black column: mixture of targets and mixture of HRP-labelled probes.

4.4.3 Multiplex measurements

For the simultaneous detection of three high-risk HPV sequences, the electrode array was modified with HPV16E7p, HPV18E6 and HPV45E6 probes on alternating electrodes as well as with HPV45E7 as a non-specific probe (Figure 4.5).

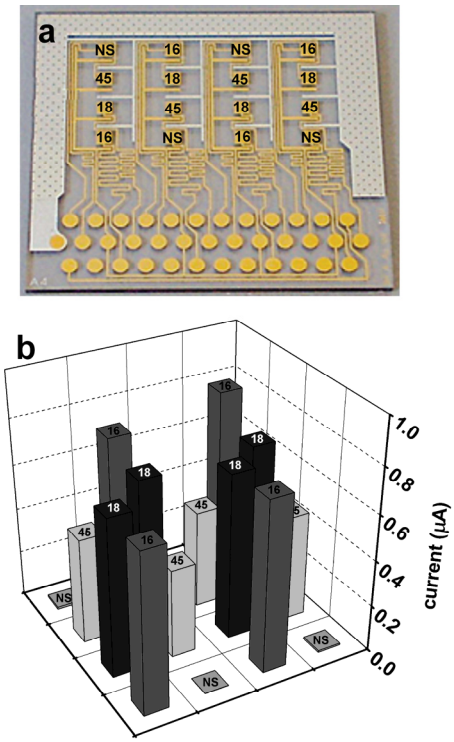

Figure 4.5. (A) Map of positions of the immobilised probes on the electrode array for multiplexed studies (NS: non-specific). (B) Signal obtained for the simultaneous detection of HPV16E7p, HPV18E6 and HPV45E6.

The average current values were (0.73 ± 0.04) μA for HPV16E7p, (0.68 ± 0.03) μA for HPV18E6, (0.43± 0.03) μA for HPV45E6 and (0.007± 0.005) μA for the non-specific probe. As can be seen, the signal obtained for the detection of HPV16E7, HPV18E6 and HPV45E6 as well as for the non-specific is very reproducible and the ability to differentiate the four signals and detect the three HPV targets simultaneously is clearly demonstrated.

4.4.4 Reusability and stability

Whilst it would never be envisaged that gensosensors applied to clinical analysis would be recycled, for developmental work, it is useful to be able to re-use the

genosensors. Reusability of the genosensor was thus tested in the HPV18E6 platform. The sensor array was modified as described above, and a complete sandwich was built for the detection of 10 nM synthetic target. Electrochemical signal was recorded and used as total signal to compare for subsequent runs. Regeneration of the surface was performed by de-hybridising the HRP-labelled probe and target from thiolated probe using 100 μL of 50 mM of NaOH. Detection was then performed another four times following the same procedure, in the next four consecutive days, storing the sensor array in the fridge. After five cycles of regeneration, the hybridisation capacity of the genosensor was maintained, with a relative standard deviation of 1.77%, n = 3.

To study the stability of the genosensor platform, chips were modified with thiolated probes as described above, stored in dry conditions at 4ºC and the response in the detection of 10 nM of target was measured weekly. No significant decrease in amperometric response (<5%) was observed after one month of storage, indicating that the immobilised probes do not lose their recognition ability upon storage in these conditions.

4.4.5 Analysis of clinical samples

The genosensor array was evaluated with clinical samples obtained from Jena University Hospital. DNA extracted from cervical scrapes that were positive for HPV16, HPV18 and HPV45 (three cases for each HPV type) and 3 HPV negative cases were provided. These samples had been HPV-genotyped using the GP5+/GP6+ assay at the Jena University Hospital. Five μL of these DNA samples were amplified and ssDNA was generated using streptavidin-coated magnetic beads. Following precipitation of the ssDNA, it was rehydrated in 20 μL of 0.1 M PBS-Tween pH 7.4. To check the quality of the generated ssDNA, an agarose gel (4 %, certified low range ultra agarose, Bio-rad) was performed comparing the sample obtained with an aliquot of a synthetic DNA sequence equivalent in length and sequence to the amplicon. In all cases, a band of expected size was obtained, indicating that the correct sequence had been amplified. One μL of each of the samples was added to HPV genosensor array, in

order to identify which strain of HPV was present and to further highlight the flexibility of the developed platform to also quantify the amount of DNA present in the samples. Samples were previously diluted in a 1/10 factor in the case of HPV16 and HPV18 and in a 1/30 dilution factor for HPV45 (due to its lower linear range). Analytical responses obtained in three measurements were quantified, and as summarised in Table 4.1, the HPV electrochemical genosensor had an excellent correlation with the HPV genotyping carried out within a hospital laboratory. The reported genosensor multiplexed approach could thus be extended and applied to the detection of other high-risk, and low-risk HPV sequences for HPV genotyping.

Table 4.1. Results obtained for electrochemical detection of ssDNA generated from amplified DNA extracted from clinical samples of cervical scrapes.

Sample	**HPV genotyping**	**Genosensor array (nM)**		
		HPV16	HPV18	HPV45
1A	HPV16	3.60	0.19	0.12
1B		4.28	0.17	0.15
1C		4.06	0.21	0.14
2A	HPV18	0.23	3.90	0.11
2B		0.25	2.74	0.12
2C		0.29	2.55	0.13
3A	HPV45	0.29	0.17	0.67
3B		0.27	0.18	0.78
3C		0.24	0.23	0.73
10	Negative	0.27	0.29	0.12
11		0.37	0.21	0.13
12		0.41	0.20	0.12

4.5 Conclusions

An electrochemical genosensor array for the multiplexed detection of three of the most representative high-risk HPV types (16, 18 and 45) was performed and applied to the analysis of real clinical samples. A co-immobilisation strategy of a thiolated probe and a bipodal alkanethiol was used for the modification of the gold working electrodes and a sandwich assay was carried with a HRP-labelled probe out for the detection of the three HPV types. The surface chemistry facilitated a highly sensitive genosensor, with limits of detection of 220 pM, 170 pM and 110 pM, for HPV16E7p, 18E6 and 45E6 respectively with negligible non-specific binding. Cross-reactivity between targets and HRP-labelled probes was tested, and insignificant cross-hybridisation was obtained. Multiplexed studies further demonstrated the specificity of the genosensor. Finally, the genosensor was applied to the quantitative detection of DNA in clinical samples from cervical scrapes positive for the three HPV types studied, showing an excellent degree of correlation with HPV genotyping carried out in a hospital laboratory. The developed platform, capable of multiplexed, quantitative detection of nucleic acids could find widespread application, particularly in the detection of RNA expression profiles for use in theranostics.

4.6 Acknowledgements

HPV sequences used in this work were identified by TATAA Biocenter, www.tataa.com (Gothenburg, Sweden). Electrodes arrays were fabricated by the Institut für Mikrotechnik Mainz, Germany, www.imm-mainz.de. This research has been carried out with financial support from the Commission of the European Communities, RTD programme "Smart Integrated Biodiagnostic Systems for Healthcare, SmartHEALTH, FP6-2004-IST-NMP-2-016817". A. F. thanks Ministerio de Ciencia y Tecnología, Spain, for a "Ramón y Cajal" Research Professorship. L.C. acknowledges the Departament d'Enginyeria Química of the Universitat Rovira i Virgili for a pre-doctoral scholarship.

4.7 References

1. H. z. Hausen, *Biochimica et Biophysica Acta (BBA) - Reviews on Cancer*, 1996, **1288**, F55-F78.
2. N. Muñoz, F. X. Bosch, S. de Sanjose, R. Herrero, X. Castellsague, K. V. Shah, P. J. F. Snijders, C. Meijer and C. Int Agcy Res Canc Multicenter, *New England Journal of Medicine*, 2003, **348**, 518-527.
3. J. Thomison Iii, L. K. Thomas and K. R. Shroyer, *Human Pathology*, 2008, **39**, 154-166.
4. M. H. Stoler, *International Journal of Gynecological Pathology*, 2000, **19**, 16-28.
5. Y. Nomine, M. Masson, S. Charbonnier, K. Zanier, T. Ristriani, F. Deryckere, A. P. Sibler, D. Desplancq, R. A. Atkinson, E. Weiss, G. Orfanoudakis, B. Kieffer and G. Trave, *Molecular Cell*, 2006, **21**, 665-678.
6. X. Liu, A. Clements, K. H. Zhao and R. Marmorstein, *Journal of Biological Chemistry*, 2006, **281**, 578-586.
7. M. Arbyn, P. Sasieni, C. J. L. M. Meijer, C. Clavel, G. Koliopoulos and J. Dillner, *Vaccine*, 2006, **24**, S78-S89.
8. J. Cuzick, M. Arbyn, R. Sankaranarayanan, V. Tsu, G. Ronco, M.-H. Mayrand, J. Dillner and C. J. L. M. Meijer, *Vaccine*, 2008, **26**, K29-K41.
9. D. Dell'Atti, M. Zavaglia, S. Tombelli, G. Bertacca, A. O. Cavazzana, G. Bevilacqua, M. Minunni and M. Mascini, *Clinica Chimica Acta*, 2007, **383**, 140-146.
10. Y. Wang, M. Chen, L. Zhang, Y. Ding, Y. Luo, Q. Xu, J. Shi, L. Cao and W. Fu, *Biosensors and Bioelectronics*, 2009, **24**, 3455-3460.
11. L. Xu, H. Yu, M. S. Akhras, S.-J. Han, S. Osterfeld, R. L. White, N. Pourmand and S. X. Wang, *Biosensors and Bioelectronics*, 2008, **24**, 99-103.
12. R. E. Sabzi, B. Sehatnia, M. H. Pournaghi-Azar and M. S. Hejazi, *Journal of the Iranian Chemical Society*, 2008, **5**, 476-483.
13. S. D. Vernon, D. H. Farkas, E. R. Unger, V. Chan, D. L. Miller, Y. P. Chen, G. F. Blackburn and W. C. Reeves, *Bmc Infectious Diseases*, 2003, **3**:12.
14. N. Zari, A. Amine and M. M. Ennaji, *Analytical Letters*, 2009, **42**, 519-535.
15. C.-y. Zhang and J. Hu, *Analytical Chemistry*, 2010, **82**, 1921-1927.
16. L. Civit, A. Fragoso and C. K. O'Sullivan, *Biosensors and Bioelectronics*, 2010, **26**, 1684-1687.

17. O. Y. Henry, A. Fragoso, V. Beni, N. Laboria, J. L. A. Sanchez, D. Latta, F. Von Germar, K. Drese, I. Katakis and C. K. O'Sullivan, *Electrophoresis*, 2009, **30**, 3398-3405.
18. Z. Wang, L. Liu, Y. Xu, L. Sun and G. Li, *Biosensors and Bioelectronics*, 2011, **26**, 4610-4613.
19. J. Wang, Y. Cao, Y. Li, Z. Liang and G. Li, *Journal of Electroanalytical Chemistry*, 2011, **656**, 274-278.
20. M. V. Jacobs, P. J. F. Snijders, A. J. C. vandenBrule, T. J. M. Helmerhorst, C. Meijer and J. M. M. Walboomers, *Journal of Clinical Microbiology*, 1997, **35**, 791-795.

Chapter 5

Thermal stability of diazonium derived and thiol derived layers on gold for application in genosensors

Electrochemistry Communications 12 (2010) 1045-1048

Laia Civit[a], Alex Fragoso[a*], Ciara K. O'Sullivan[a,b *]

[a] *Departament d'Enginyeria Química, Universitat Rovira i Virgili, Tarragona, Spain.*

[b] *ICREA, Passeig Lluís Companys 23, 08010 Barcelona, Spain*

Keywords: Thermal stability, diazonium salts, self assembled monolayers, gold electrode

5.1 Abstract

DNA analysis using variable temperature technologies such as melting curve analysis, high temperature mutant discrimination or immobilised PCR relies upon the use of immobilised probes that need to be stable over a wide temperature range. In this work a comparison of the thermal stability of gold surfaces modified with alkanethiol and diazonium salt derived layers is presented. Electrochemical impedance spectroscopy and cyclic voltammetry were used to characterise the electrode arrays. The applicability of the surfaces for DNA sensing was demonstrated following the thermal treatment, with the diazonium-modified surface being markedly more stable.

5.2 Introduction

The formation of self-assembled monolayers (SAMs) of thiol, sulphide or disulphide containing molecules is one of the most widely used methods for the modification of metal surfaces.[1-2] It is well known that gold-thiol chemistry produces well ordered monolayers with a reasonably strong bond.[3-4] However, the tendency of gold to oxidise in air media,[5] the narrow potential window[6] and low thermal stability of SAMs on gold[7-8] have limited their usefulness for certain applications. Attempts to increase the stability of SAMs on gold have been made using multi-thiol anchored molecules[9-10] or via the incorporation of cross-linking groups within the alkyl chains.[11-14]

An attractive alternative is the grafting of aryl group via the reduction of diazonium salts, as the carbon-gold bond is more stable than the thiol-gold bond due to a lower bond strength and higher bond order, which translates into a higher stability of the modified surfaces.[15] Gooding and McDermott have compared the stability in terms of resistance to sonication, exposure to refluxing solvents, displacement using thiolated molecules[16] and under laboratory atmosphere conditions[17] reporting that the aryl diazonium derived films are, under certain conditions, more strongly bound to gold as compared to alkanethiol layers. Applications of diazonium chemistry for the

immobilisation of a variety of biomolecules, including DNA and proteins, have been reported.[18-19]

In the present work we studied the thermal stability of a series of modified gold surfaces with mono- and di-thiol molecules compared with diazonium salts with one and two diazo- groups for the grafting on the gold electrode (Figure 5.1). Electrochemical techniques were used to control the influence of the thermal treatment on the formed layers. The functionality of the grafted surfaces was tested by application to genosensing using human papillomavirus oncogene sequences.

5.3 Experimental

5.3.1 Chemicals

6-mercaptohexanoic acid (**1**) and 4-aminophenylacetic acid (**3**) were obtained by Sigma-Aldrich; 3,5-bis(4-aminophenoxy)benzoic acid (**4**), from TCI Europe and (22-(3,5-bis((6-mercaptohexyl)oxy)phenyl)-3,6,9,12,15,18,21-heptaoxadocosanoic acid) **(2)**, from Sensopath Technologies. 3,3',5,5'-Tetramethylbenzidine (TMB) liquid substrate was purchased from Sigma.

Amino terminated HPV16E7p probe:

(5'-NH2-C_6-GAGGAGGAGGATGAAATAGATGGT-3'),

HPV16E7p target:

(5'-GCCCATTAACAGGTCTTCCAAAGTACGAATGTCTACGTG TGTGCTTTGTACGCACAACCGAAGCGTAGAGTCACACTTGCAACAAAAG GTTACAATATTGTAATGGGCTCTGTCCGGTTCTGCTTGTCCAGCTGGACC ATCTATTTCATCCTCCTCCTC-3') and

HRP labelled HPV16E7p secondary probe

(5'-TTGGAAGACCTGTTAATGGGC-HRP-3') were purchased from Biomers.

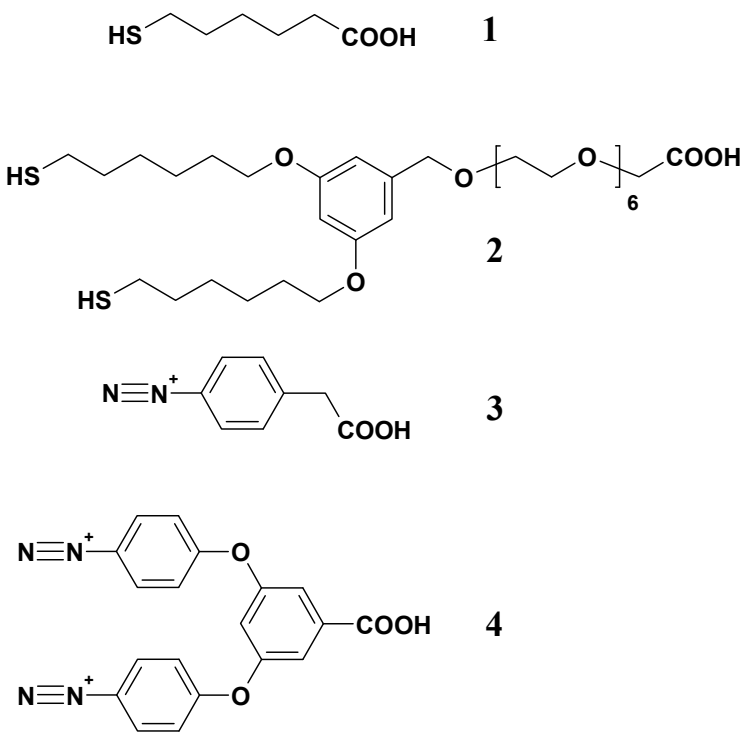

Figure 5.1. Structures of thiols and diazonium salts used

5.3.2 Electrode preparation and procedures

Arrays consisting of 5 rectangular sputtered gold electrodes (area 5 mm^2) were used. The arrays were sequentially sonicated with acetone, 2-propanol, acetone for 5 minutes and rinsed with Milli-Q water. The electrodes were placed in warm Piranha's solution (1:3 v/v 30% H_2O_2 in concentrated H_2SO_4) for 5 min. Finally electrochemical cleaning of the arrays was performed in 0.5M H_2SO_4 solution by cycling the potential between –0.2V and 1.6V at 100 mVs^{-1} for 25 cycles. Bare electrodes were characterised by CV and EIS using a PGSTAT12 potentiostat. All potentials were measured with respect to Ag/AgCl (sat) reference electrode and a platinum wire used as counter electrode.

5.3.2.1 Diazonium salt derived layers preparation

Diazonium salts were prepared *in situ* by adding 1 mL sodium nitrite solution (2 M) to an ice-cold stirred solution of 3 mL of the amine (0.1 M) and 1mL of HCl (1 M) and the mixture was stirred for 25 min at 4ºC. For surface modification, electrode arrays were immersed in the diazonium salt solution and potential cycling was carried out between 0.2 V and -0.6 V at 100mVs^{-1} for 2 cycles. After modification, the arrays were rinsed with Milli-Q water and dried with nitrogen gas.

5.3.2.2. Thiol-derived layers preparation

Clean gold arrays were immersed in 1 mM of the corresponding thiol in ethanol overnight to facilitate the formation of the self-assembled monolayers. Following modification, the arrays were rinsed with ethanol in order to remove physically adsorbed molecules.

5.3.3. Thermal stability studies

Modified electrode arrays were immersed in approximately 15 mL of phosphate buffer solution (0.1 M pH7.4) containing 500 mM NaCl that was maintained at a constant temperature ranging from 25 to 95ºC. Electrode arrays were removed at specific times, rinsed with water and left to reach room temperature. CVs and EIS were measured and the electrode arrays were re-immersed in the heated bath. A single electrode array (n=5) was used for the exploration of the entire temperature range from 25 to 95ºC.

5.3.3 DNA detection

Electrodes were modified with compounds **2** and **4** as described above. The carboxyl groups of the layers were activated by stirring the electrode with 0.2 M EDC and 50 mM NHS for 30 min followed by 5 μM of amino terminated probe HPV16E7p (24-bp) in 10 mM HEPES pH6 overnight. A washing step consisting of 15 min stirring

in 10 mM PBS-Tween (0.05% Tween 20) and 10 min stirring in MilliQ water was performed. Any remaining carboxylic groups were blocked with 0.1 M ethanolamine hydrochloride (pH8.5) for 30 min. HPV target (159-bp, 100 nM) in PBS-Tween was applied to each of the electrodes and incubated for 1 h at room temperature. Subsequently, the arrays were washed for 15 min with PBS-Tween and dried with nitrogen. The reporter probe (21-bp, 10 nM) in PBS-Tween was then incubated for 1 h at RT. The hybridisations of the target and detection probe were performed under a humid environment to avoid drying. After final washing, the detection step was carried in the presence of TMB substrate. The reduction of TMB was detected by steps and sweeps technique by applying two consecutive pulses of 0 V for 1 ms and -0.2 V for 0.5 s.

5.4 Results and discussion

5.4.1 Thermal stability studies

The modification of gold electrode arrays by electrodeposition of *in situ* prepared diazonium salts or *via* the formation of alkanethiol SAMs was confirmed by CV (Figure 5.2). Following modification of the electrodes the redox peaks of ferricyanide observed at bare electrodes were almost completely suppressed due to the formed layer.

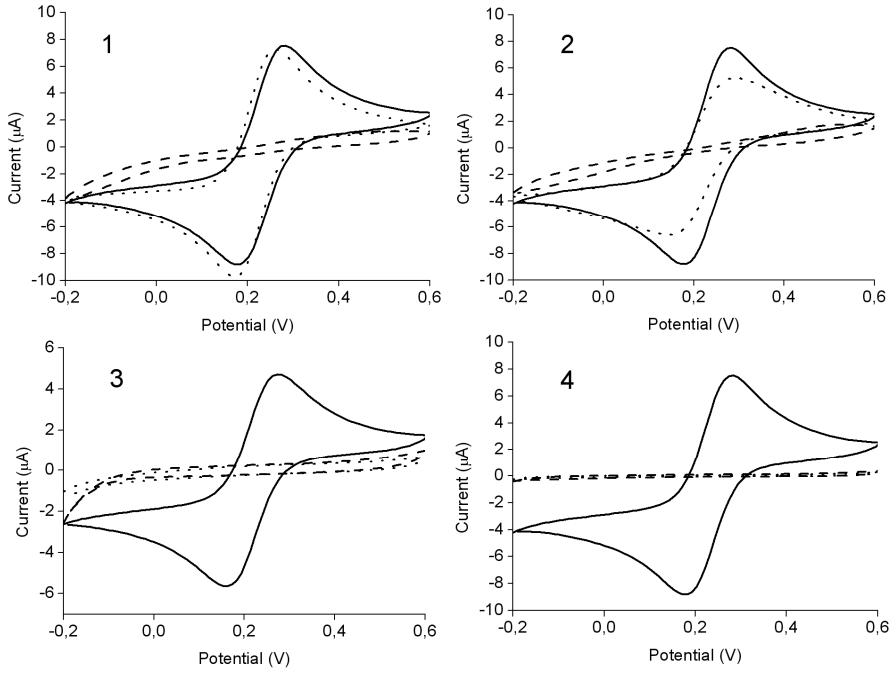

Figure 5.2. Cyclic voltammograms of 1 mM ferricyanide (in 0.1 M phosphate buffer, pH 7.4) at a scan rate of 100 mVs^{-1} before (——), after the modification of gold electrode arrays with compounds 1-4 (----) and after thermal treatment (·····)

The thermal stability of diazonium films on gold was compared by subjecting the modified electrodes to a treatment consisting of the immersion of the electrodes in phosphate buffer solution (0.1 M pH7.4) containing 500 mM NaCl (typically used for optimal DNA hybridisation), and increasing the temperature in the range 25 - 95ºC at intervals of 10ºC with changes in the array surface being monitored by CV and EIS. Figure 5.3 A shows the variation of the charge transfer resistance (R_{ct}) at each stage of the thermal treatment. In the 25 - 50ºC temperature range no significant changes can be appreciated in the R_{ct}, indicating the stability of the films within this temperature range. At about 65ºC the R_{ct} started to decrease for thiol SAMs films (10% for **1** and 38% for **2**), due to the temperature induced loss in density of such films, allowing more accessibility for the redox species. The desorption of **2** at a lower temperature

can be explained by the lower packing density of those films as compared to MHA, as well as its structure as its distribution generates some intermolecular empty space, facilitating access of the redox species to the electrode surface, in contrast to the insulating behaviour of the aliphatic monothiol.[20] Therefore, desorption of at least one of the thiol-gold bonds of the dithiol molecule results in an easier diffusion of the redox species to the gold surface decreasing the R_{ct}. At temperatures above 80ºC the R_{ct} dramatically drops for **1** (92%) indicating the desorption of a significant part of the film, being practically removed after exposure at 95ºC, while for the film of **2** 26% of the initial R_{ct} value can be observed. This indicates that monothiols generate more stable SAMs that dithiols at low temperature, while the stability trend is reversed at high temperature (>70ºC) where the dithiols have a higher stability.

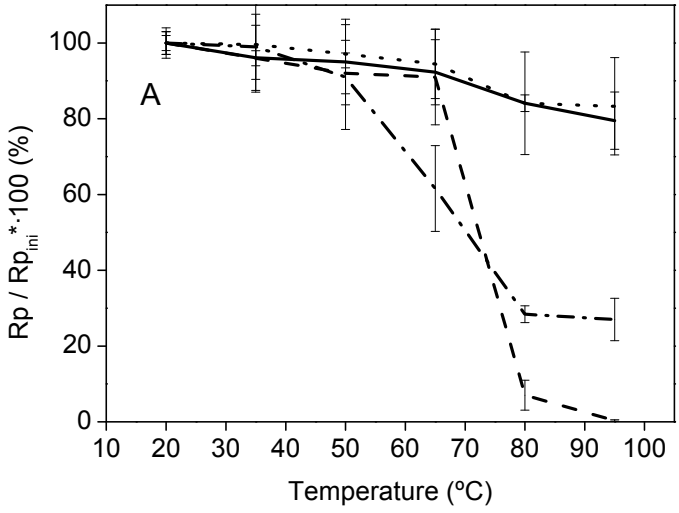

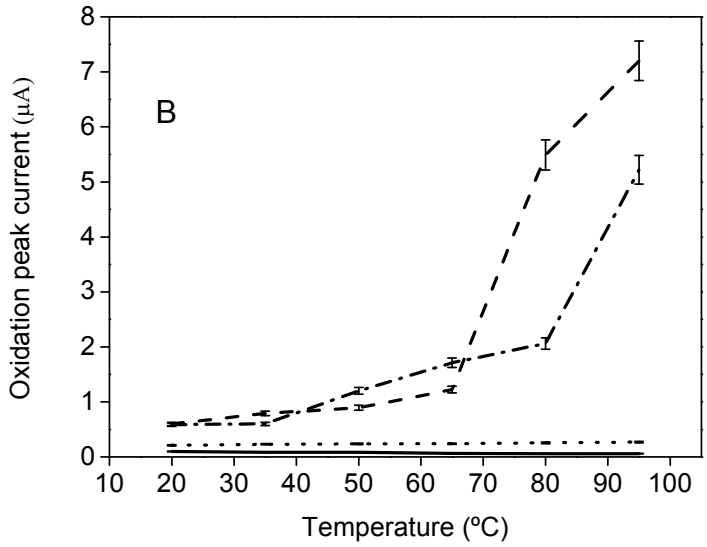

*Figure 5.3. Temperature dependence of R_{ct} (A) and peak current (B) for surfaces modified with **1** (-------), **2** (- - - - -), **3** (——) and **4** (·····).*

In contrast, there was a small decrease in the R_{ct} of around 20% for both diazonium salt derived films during the whole thermal treatment. This can be attributed to desorption of some possible unbound species that could be produced by recombination of two phenyl radicals and a diazonium and a phenyl radical. This decrease in response could also be due to the breakage of Au-N bonds from Au-N N-C, which has been proposed as an alternative mechanism to the rupture of Au-C bonds.[21]

CVs were also performed at each stage of the thermal treatment (Figure 5.3 B). At temperatures below 50ºC no ferricyanide redox peaks were observed, as expected for completely blocked surfaces. The electrochemical response of ferricyanide then started to be significant for the alkanethiol films, reaching nearly the same intensity as observed on the bare gold electrodes above 80ºC in the case of **1**. In the case of the

dithiol films a sufficient amount of **2** is maintained on the electrode even at high temperature with a moderate degree of blocking of electron transfer. In contrast the diazonium films demonstrate resistance to the thermal treatment, with blocking of electron transfer for ferricyanide even at very high temperatures again highlighting the thermal stability of these films (Figure 5.2).

5.4.2 Functionality of modified surfaces

DNA analysis using variable temperature technologies such as melting curve analysis, high temperature mutant discrimination or immobilised PCR relies upon the use of immobilised probes that need to be stable over a wide temperature range.

In order to test the functionality of the prepared surfaces, a complete sandwich assay with the corresponding DNA probes was built as described in the experimental part and used for the detection of human papillomavirus sequences on electrodes modified with **2** and **4**. A control consisting of no target hybridisation showed a non-significant signal, indicating no non-specific adsorption of the HRP-labelled secondary probe.

The modified electrodes were then subjected to the thermal treatment described above, ramping the temperature to 95ºC, followed by a re-immersion of the dithiol modified electrode in a 1 mM solution of **2** in ethanol to cover the free gold after desorption in order to avoid non-specific adsorption of the target or reporter probe on golf free surface during the hybridisation processes. This is not possible for the diazonium salt derived layer as the diazo group could interact with the aromatic rings of certain DNA bases (adenine, cytosine or guanine) resulting in loss of specificity for the target.[22] The last step was to re-construct the complete "sandwich" following the same procedure as above and proceed to detection. As expected, a significant decrease in the signal due to TMB reduction of about 45% after thermal treatment was observed due to the desorption of the dithiol SAM (**2**), while only a 7% of the initial signal decreases in the diazonium derived layer (**4**) (Figure 5.4). This demonstrates that

an electrode prepared with diazonium salts derived layers is highly suitable for temperature-modulated electrochemical DNA sensing applications mentioned above.

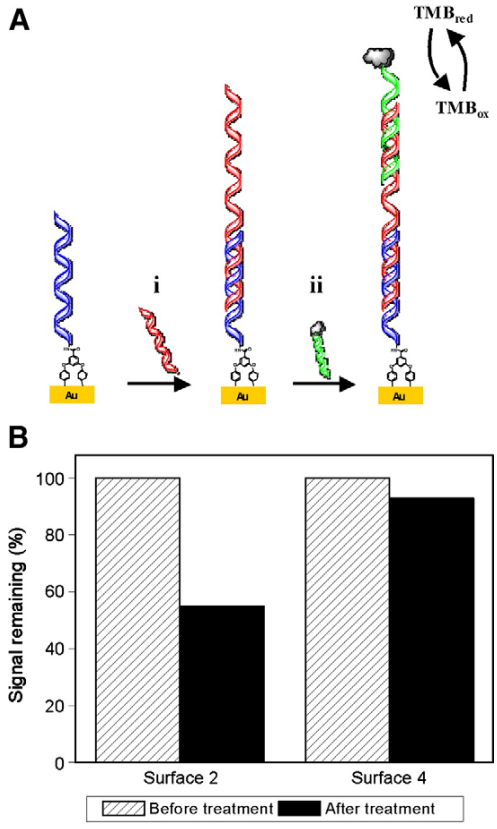

Figure 5.4. (A) Schematic of DNA detection. (B) Variations in amperometric signal (TMB reduction) for the detection of 100 nM of HPV16E7p target before and after exposure of the electrodes to thermal treatment for surfaces modified with 2 and 4.

5.5 Conclusions

Diazonium salt derived layers were found to be thermally stable to significantly higher temperatures than alkanethiol SAMs on gold surfaces. Of the alkanethiol SAMs surfaces tested, monothiol were less stable starting to desorb at temperatures around 65ºC, and at temperatures higher than 95ºC the layer was completely removed. Dithiol SAMs are more resistant to the thermal treatment, remaining around 26% after

exposure to 95ºC of the layer on the surface. On the other hand, both the diazonium salt derived layers respond equally to the thermal treatment, with minor losses that can be attributed to the removal of non-specifically attached molecules. This surface has been proved to be an excellent alternative for the application in temperature modulated electrochemical DNA sensing.

5.6 Acknowledgements

HPV16E7p sequences were identified by TATAA Biocenter. This research has been carried out with financial support from the RTD programme SmartHEALTH, FP6-2004-IST-NMP-2-016817. L. C. thanks URV for a doctoral scholarship. A. F. thanks the MCYT, Spain, for a "Ramón y Cajal" Research Professorship.

5.7 References

1. J. C. Love, L. A. Estroff, J. K. Kriebel, R. G. Nuzzo and G. M. Whitesides, *Chemical Reviews*, 2005, **105**, 1103-1169.
2. C. D. Bain, E. B. Troughton, Y. T. Tao, J. Evall, G. M. Whitesides and R. G. Nuzzo, *Journal of the American Chemical Society*, 1989, **111**, 321-335.
3. R. G. Nuzzo and D. L. Allara, *Journal of the American Chemical Society*, 1983, **105**, 4481-4483.
4. M. D. Porter, T. B. Bright, D. L. Allara and C. E. D. Chidsey, *Journal of the American Chemical Society*, 1987, **109**, 3559-3568.
5. T. M. Willey, A. L. Vance, T. van Buuren, C. Bostedt, L. J. Terminello and C. S. Fadley, *Surface Science*, 2005, **576**, 188-196.
6. H. O. Finklea, S. Avery, M. Lynch and T. Furtsch, *Langmuir*, 1987, **3**, 409-413.
7. F. Bensebaa, T. H. Ellis, A. Badia and R. B. Lennox, *Langmuir*, 1998, **14**, 2361-2367.
8. E. Delamarche, B. Michel, H. Kang and C. Gerber, *Langmuir*, 1994, **10**, 4103-4108.
9. Z. Li, R. C. Jin, C. A. Mirkin and R. L. Letsinger, *Nucleic Acids Research*, 2002, **30**, 1558-1562.
10. T. T. Wooster, P. R. Gamm, W. E. Geiger, A. M. Oliver, A. J. Black, D. C. Craig and M. N. PaddonRow, *Langmuir*, 1996, **12**, 6616-6626.

11. N. Garg, E. Carrasquillo-Molina and T. R. Lee, *Langmuir*, 2002, **18**, 2717-2726.
12. R. Valiokas, M. Ostblom, S. Svedhem, S. C. T. Svensson and B. Liedberg, *Journal of Physical Chemistry B*, 2002, **106**, 10401-10409.
13. R. S. Clegg, S. M. Reed and J. E. Hutchison, *Journal of the American Chemical Society*, 1998, **120**, 2486-2487.
14. T. Kim, K. C. Chan and R. M. Crooks, *Journal of the American Chemical Society*, 1997, **119**, 189-193.
15. R. G. Nuzzo, L. H. Dubois and D. L. Allara, *Journal of the American Chemical Society*, 1990, **112**, 558-569.
16. D. M. Shewchuk and M. T. McDermott, *Langmuir*, 2009, **25**, 4556-4563.
17. G. Z. Liu, T. Bocking and J. J. Gooding, *Journal of Electroanalytical Chemistry*, 2007, **600**, 335-344.
18. J. C. Harper, R. Polsky, D. R. Wheeler, S. M. Dirk and S. M. Brozik, *Langmuir*, 2007, **23**, 8285-8287.
19. B. P. Corgier, A. Laurent, P. Perriat, L. J. Blum and C. A. Marquette, *Angewandte Chemie-International Edition*, 2007, **46**, 4108-4110.
20. A. Fragoso, N. Laboria, D. Latta and C. K. O'Sullivan, *Analytical Chemistry*, 2008, **80**, 2556-2563.
21. A. Laforgue, T. Addou and D. Belanger, *Langmuir*, 2005, **21**, 6855-6865.
22. P. L. Dolan, Y. Wu, L. K. Ista, R. L. Metzenberg, M. A. Nelson and G. P. Lopez, *Nucleic Acids Research*, 2001, **29**, e107.

Chapter 6

Spectroscopic and atomic force microscopy characterisation of the electrografting of 3,5-bis(4-diazophenoxy)benzoic acid on gold surfaces

Manuscript submitted

Laia Civit,[a] Osama El-Zubir,[b] Alex Fragoso,[a] Ciara K. O'Sullivan*[a,c]

[a] Nanobiotechnology and Bioanalysis Group, Department of Chemical Engineering, Universitat Rovira i Virgili, Avd. Països Catalans, 26, 43007 Tarragona, Spain.
[b] Department of Chemistry, University of Sheffield, Sheffield S3 7HF, U.K.
[c] Institució Catalana de Recerca i Estudis Avançats, Passeig Lluís Companys 23, 08010 Barcelona, Spain.

Keywords: diazonium salts, electrochemical deposition, atomic force microscopy, X-ray photoelectron spectroscopy

6.1 Abstract

The synthesis of a bipodal diazonium salt, 3,5-bis(4-diazophenoxy)benzoic acid, and the study of its electrochemical deposition on gold surfaces is presented. The presence of the organic layer on the gold surface was characterised using atomic force microscopy and X-ray photoelectron spectroscopy, demonstrating the presence of phenyl groups, indicative of the grafted layer as well as the formation of multilayers, dependent on the electrografting conditions.

6.2 Introduction

In 1992 Pinson and co-workers demonstrated that the electrochemical reduction of diazonium salts on carbon surfaces leads to strong chemisorption rather than mere physisorption.[1] Although modification of carbon surfaces was initially the most studied,[2-5] interest has also focused on substrates such as metals[6-8] and semi-conductors.[9] In addition, the variety of substituents with aryl rings for surface functionalisation permits their application to an extensive range of areas such as biosensors,[10] catalysis,[11] nanotubes[12] and anti-corrosive agents[8] among other applications. The modification of substrates with diazonium salts has been carried out in aqueous[13] or organic[14] media and by electrochemical[4] or, spontaneous grafting.[15] Reduction of the diazonium cation close to the electrode surface causes elimination of N_2, yielding an aryl radical which attacks the substrate to form a covalent bond.[16] Multilayer film structures may form as a result of radical attack on surface-grafted aryl groups[6] and the thickness of the resulting layers prepared by electrografting depends on time and applied potential as well as the nature of the starting material.[6] Anariba *et al.*, reported the layer thickness obtained for four different diazonium salts deposited, obtaining different film thicknesses and multilayers were formed for increased electrolysis or diazonium ion concentrations.[3] The introduction of substituents to the diazonium ion may yield a slower growth rate, depending on the position of the substitutent.[17] Reports have detailed that grafting efficiency depends on the nature of

the amine, the chain length of the alkyl substituent and the substitution position on the aromatic ring.[18]

In this communication we report on the synthesis and characterisation of the electrografting of a diazonium salt with two diazo- groups 3,5-(4-diazophenoxy)benzoic acid (3,5-BDBA). Characterisation of the synthesised 3,5-BDBA was performed using NMR and IR, and of the electrografted gold surfaces using AFM and XPS.

6.3 Experimental

3,5-bis(4-aminophenoxy)benzoic acid was obtained from TCI Europe and octadecanethiol was purchased from Sigma Chemical Company. 1H NMR spectra were recorded on a Bruker Avance 400 Ultrashield NMR spectrometer operating at 400 MHz. FTIR spectra were recorded with a Jasco FT/IR-600 Plus ATR Specac Golden Gate. Spectra were collected with a spectral resolution of 4 cm^{-1} accumulating 32 scans. All FTIR spectra were recorded in transmission mode.

6.3.1 Synthesis of 3,5-bis(4-diazophenoxy)benzoic acid tetrafluoborate

A solution of 1 mmol of 3,5-bis(4-aminophenoxy)benzoic acid in MilliQ water was added to a flask placed in an ice bath and 8 mmol of fluoroboric acid 50% was added dropwise and mixed for 10 min. Subsequently, 2.5 mmol of sodium nitrite in water was added to the reaction mixture and the final solution was cooled and the precipitated white solid collected, washed with cold water, centrifuged and finally dried under vacuum.

^{1}H-NMR (400 MHz, CD_3CN) δ 8.50-8.45 (m, 4H, H_{Ar}), 7.87 (d, J = 2.45 Hz, 2H, H_{Ar}), 7.46-7.41 (m, 5H, H_{Ar}). ^{13}C-NMR (100 MHz, CD_3CN) δ 167.8 (COOH), 164.5, 154.4 ($C_{Ar}O$), 136.0 ($CH_{Ar}C_{Ar}N$), 135.2 ($C_{Ar}COOH$), 120.6, 119.8, 119.1 (C_{Ar}), 105.3 ($C_{Ar}N$).

The IR spectrum of the free diazonium salt was characterised by four strong bands in the 3500−1000 cm^{-1} region: ν^{O-H} at 3100 cm^{-1}, $\nu^{N\equiv N}$ at 2300 cm^{-1}, $\nu^{C=O}$ at 1700 cm^{-1} and ν^{C-O} at 1040 cm^{-1}.

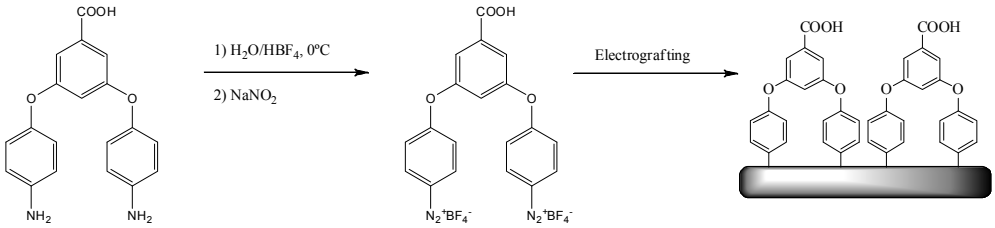

Scheme 6.1 Synthesis and electrodeposition of 3,5-bis(4-diazophenoxy)benzoic acid tetrafluoborate (BDBA).

6.3.2 Modification of gold surfaces

1-octadecanethiol (ODT) SAM was prepared by immersing freshly deposited gold-coated chromium-primed glass substrates (100 Deckglaser 22x64 mm # 1.5, Menzel-Gläser) in 1 mM solution of the thiol in ethanol for a minimum of 18 h. The thickness of the gold film was 150 nm, and the chromium layer was 20 nm thick.

Photopatterning of the surfaces was performed by the exposure of the SAM modified gold surfaces to light from a frequency doubled argon ion laser emitting at 244 nm (55 mW) for 70 min. The patterned structure was obtained through a 2000 square Cr mask. Photopatterned surfaces were rinsed with ethanol and electrochemically modified using either cyclic voltammetry (CV) or chronoamperometry (CA) in 1 mM 3,5-bis(4-diazophenoxy)benzoic acid tetrafluoborate prepared in 0.1 M Bu_4NBF_4 in acetonitrile, deaerated with nitrogen for 5 min prior to each experiment. 1, 5, 10, 20 or 30 potential cycles were performed from 0.2 to -0.6 V at a scan rate of 100 $mV \cdot s^{-1}$. CA was carried out at a constant potential of -0.45 V for 15, 60, 300 and 600 seconds. A silver wire reference and platinum wire counter electrode were used.

6.3.3 Surface analysis

AFM measurements were carried out on a Digital Instruments Multimode Nanoscope IIIa. Silicon nitride cantilevers (Veeco) with a nominal force constant of 0.12 Nm^{-1} were used in contact mode to image the patterned surfaces. All images were obtained in ambient conditions. Samples were rinsed in acetone, sonicated for 1 minute in ethanol, and finally thoroughly rinsed in ethanol and dried by a stream of nitrogen gas prior to imaging. Random areas (n = 5) of the samples were imaged and averaged to obtain the final result.

XPS was performed using a Kratos Axis Ultra spectrometer equipped with a monochromatised Al Kα X-ray source (hν = 1486.6 eV) operating with a base pressure in the range of 10^{-8} to 10^{-10} mbar. Survey scans were acquired at a pass energy of 160 eV, and the high-resolution spectra were acquired at a pass energy of 20 eV. XPS spectra were analysed by CasaXPS software. The spectra were calibrated against the C1s peak at 285 eV.

6.4 Results and discussion

6.4.1 X-ray Photoelectron Spectroscopy of diazonium layers

Survey spectra of the gold surface after modification exhibited a high background, due to the inelastic scattering of the photoelectrons by the grafted layer.[19] B1s (187eV) and F1s (687 eV) were not observed, indicating that the BF_4^- counterion was eliminated from the diazonium complexes during the electrochemical modification of the gold substrates.[20] The N1s signal, attributable to the diazonium moiety (at about 400 eV), is small in the spectra obtained for all tested surfaces, corroborating the hypothesis that the reduction of the diazonium cation close to the surface leads to elimination of N_2 forming an aryl radical that attacks the substrate[16] and suggests that the 3,5-BDBA molecule is doubly bonded to the surface conferring the layer a high stability.[21] The small signal observed can be attributed to nitrogen atoms retained during the formation of multilayers, for example by forming –N=N- bridges.[19]

The C1s core level spectrum (Figure 6.1a) exhibited three principal components at 284.6, 286.2 and 288.9 eV. The component at 284.6 eV was attributed to the aromatic carbons, the component at 286.2 eV to ring carbon atoms bound to oxygen (joined by ether linkages). The component at 288.9 eV was ascribed to the substituent carboxylic acid (288.9 eV). The C-O-C and CH peaks were in a 1:3.05 ratio, consistent with the molecular formula of a doubly-linked 3,5-BDBA molecule, which contains 4 C-O-C and 11 CH groups.

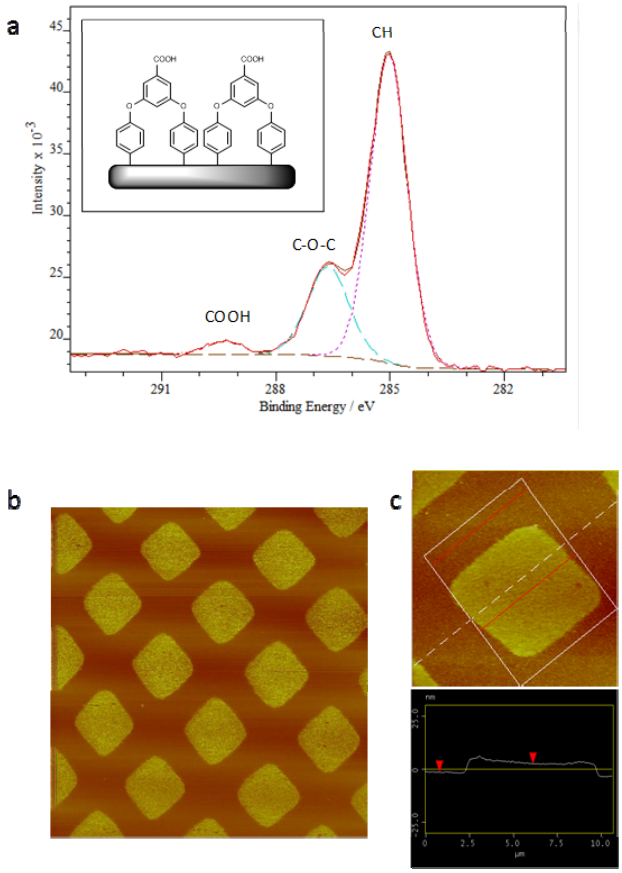

Figure 6.1 a) C1s spectra for 3,5-BDBA modified gold substrates by cyclic voltammetry, b) Contact mode AFM image showing micrometer scale patterns produced by ODT SAMs to UV light through a mask, followed by modification with 3,5-BDBA by 20 potential cycles (general friction image of 50 x 50 μm), c) detailed height image of 14 x 14 μm.

6.4.2 Atomic Force Microscopy

A photo-patterned template was formed on an ODT SAM, defining regions of bare gold to grow films of diazonium salt. Taking advantage of the ability of alkylthiolates to be photo-oxidised on exposure to UV light (λ = 244 nm) to yield weakly bound sulfonates,[22] SAMs of ODT on gold were exposed through a mask to form the desired pattern. In exposed regions, thiols were converted to sulfonate species.[23] Once the optimal exposure time was determined (90 min), patterning was performed by electrochemically modifying the exposed free areas with the diazonium salt, yielding a surface that consisted of square regions, where the carboxylic terminated organic film (3,5-BDBA) was deposited, whilst in the masked regions the original chemistry remained (methyl group).

Samples were imaged by AFM in contact mode. The thickness of the deposited layer was determined from line sections through height images corrected for the thickness of the intact SAM in the masked regions. The thickness of the intact ODT SAM was assumed to be 2.6 nm[24] and the height of a monolayer of 3,5-BDBA ca. 0.8 nm. Representative AFM images of patterned surfaces obtained are shown in Figure 6.1b-c. The 3,5-BDBA layer deposited in the UV exposed areas formed homogeneous structures and show high friction (bright contrast) in contrast to the masked areas that exhibit darker contrast, indicative of lower friction. As the outer surface of the silicon nitride probes used consists of a thin layer of polar silicon dioxide they strongly interact with the COOH terminated regions, leading to a larger friction force and an increased deflection of the cantilever.

The thickness of the resulting diazonium layer for both of the electrochemical techniques increased as the grafting time/number of cycles increased, reaching a value that was substantially greater than the expected height of a 3,5-BDBA molecule, indicating that multilayer formation was occurring (Figure 6.2). The 3,5-BDBA film reached thicknesses of 7.3 nm (equal to around 9 molecular layers) for CV treatment with 30 potential cycles, and 11.0 nm in the case of CA modification after 600 s (equal to 14 molecular layers). In the case of 1 potential cycle (CV), the height measured of the 3,5-BDBA layer was 2.8 nm, so it can be assumed that the thickness corresponds

to the deposition of between 3 and 4 molecular layers. For 5, 10 and 20 potential cycles, measured thickness was 4.1, 5 and 5.8 nm respectively, equivalent to around 5, 6 and 7 molecular layers.

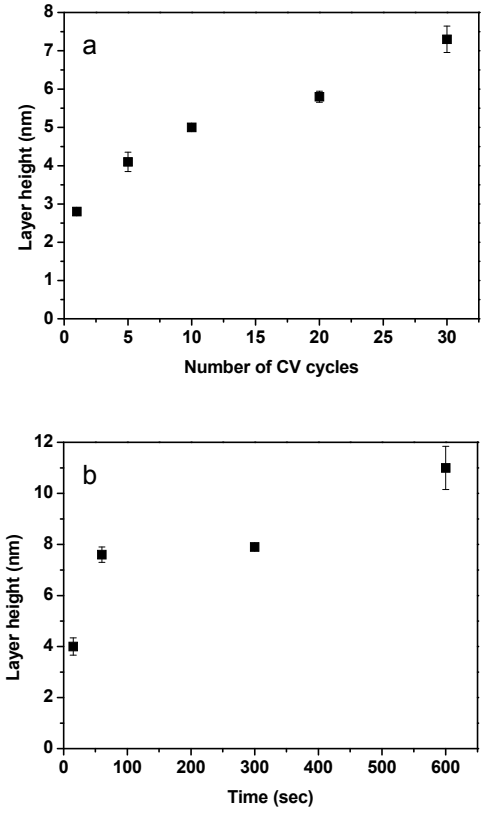

Figure 6.2. Height of the deposited 3,5-BDBA film by the two electrochemical techniques; a) CV and b) CA.

For CA deposition, a layer of 4 nm was obtained after 15 s and after 60 s the layer grew to 7.6 nm, around 10 molecular layers. Then the thickness was maintained constant with 7.9 nm obtained until 300 s. From these results, it can be concluded that CA deposition formed thicker films of 3,5-BDBA than CV deposition.

6.5 Conclusions

A bipodal diazonium salt, 3,5-bis(4-diazophenoxy)benzoic acid, was synthesised and characterised using NMR and IR, whilst its electrochemical deposition on gold substrates was characterised using two different techniques, XPS and AFM. Cyclic voltammetry and chronoamperometry were used for the electrografting of the aryl moieties. XPS studies confirmed the deposition of the bipodal diazonium. The small peak of nitrogen at about 400 eV can be explained due to its involvement in the formation of multilayers. Patterning of the surfaces is a good approach to determine the thickness of the organic layers deposited. The photo-oxidation of the thiols by its exposure to UV light for the formation of the patterns was exploited, and the thickness was calculated by adding the difference in height measured by contact mode to the thickness of the SAM. It was observed that one potential cycle forms more than a tri-layer, while for the other deposition conditions, multilayers were formed, reaching a height of 7.3 nm for CV treatment with 30 potential cycles, and 11 nm in the case of CA modification after 600 s.

6.6 Acknowledgements

This research has been carried out with financial support from the Commission of the European Communities, RTD programme FP7-2008-ICT-216031 CD-MEDICS. A. F. thanks Ministerio de Ciencia y Tecnología, Spain, for a "Ramón y Cajal" Research Professorship. L. C. acknowledges Universitat Rovira i Virgili for a predoctoral scholarship and Ministerio de Educación for a mobility grant.

6.7 References

1. M. Delamar, R. Hitmi, J. Pinson and J. M. Saveant, *Journal of the American Chemical Society*, 1992, **114**, 5883-5884.
2. C. Saby, B. Ortiz, G. Y. Champagne and D. Belanger, *Langmuir*, 1997, **13**, 6805-6813.
3. F. Anariba, S. H. DuVall and R. L. McCreery, *Analytical Chemistry*, 2003, **75**, 3837-3844.

4. S. Baranton and D. Belanger, *Journal of Physical Chemistry B*, 2005, **109**, 24401-24410.
5. P. Allongue, M. Delamar, B. Desbat, O. Fagebaume, R. Hitmi, J. Pinson and J. M. Saveant, *Journal of the American Chemical Society*, 1997, **119**, 201-207.
6. A. Ricci, C. Bonazzola and E. J. Calvo, *Physical Chemistry Chemical Physics*, 2006, **8**, 4297-4299.
7. A. Adenier, C. Combellas, F. Kanoufi, J. Pinson and F. I. Podvorica, *Chemistry of Materials*, 2006, **18**, 2021-2029.
8. A. Chausse, M. M. Chehimi, N. Karsi, J. Pinson, F. Podvorica and C. Vautrin-Ul, *Chemistry of Materials*, 2002, **14**, 392-400.
9. J. Pinson and F. Podvorica, *Chemical Society Reviews*, 2005, **34**, 429-439.
10. H. M. Nassef, L. Civit, A. Fragoso and C. K. O'Sullivan, *Analyst*, 2008, **133**, 1736-1741.
11. S. Liu, Z. Tang, Z. Shi, L. Niu, E. Wang and S. Dong, *Langmuir*, 1999, **15**, 7268-7275.
12. C. S. Lee, S. E. Baker, M. S. Marcus, W. S. Yang, M. A. Eriksson and R. J. Hamers, *Nano Letters*, 2004, **4**, 1713-1716.
13. C. Combellas, M. Delamar, F. Kanoufi, J. Pinson and F. I. Podvorica, *Chemistry of Materials*, 2005, **17**, 3968-3975.
14. S. Baranton and D. Bélanger, *Electrochimica Acta*, 2008, **53**, 6961-6967.
15. A. Adenier, N. Barré, E. Cabet-Deliry, A. Chaussé, S. Griveau, F. Mercier, J. Pinson and C. Vautrin-Ul, *Surface Science*, 2006, **600**, 4801-4812.
16. K. Boukerma, M. M. Chehimi, J. Pinson and C. Blomfield, *Langmuir*, 2003, **19**, 6333-6335.
17. C. Combellas, F. Kanoufi, J. Pinson and F. I. Podvorica, *Journal of the American Chemical Society*, 2008, **130**, 8576-8577.
18. C. Combellas, D.-e. Jiang, F. d. r. Kanoufi, J. Pinson and F. I. Podvorica, *Langmuir*, 2008, **25**, 286-293.
19. J. Lyskawa and D. Belanger, *Chemistry of Materials*, 2006, **18**, 4755-4763.
20. M. P. Stewart, F. Maya, D. V. Kosynkin, S. M. Dirk, J. J. Stapleton, C. L. McGuiness, D. L. Allara and J. M. Tour, *Journal of the American Chemical Society*, 2003, **126**, 370-378.
21. L. Civit, A. Fragoso and C. K. O'Sullivan, *Electrochemistry Communications*, 2010, **12**, 1045-1048.
22. S. Q. Sun, D. Thompson, U. Schmidt, D. Graham and G. J. Leggett, *Chemical Communications*, 2010, **46**, 5292-5294.

23. G. J. Leggett, *Chemical Society Reviews*, 2006, **35**, 1150-1161.
24. C. D. Bain, E. B. Troughton, Y. T. Tao, J. Evall, G. M. Whitesides and R. G. Nuzzo, *Journal of the American Chemical Society*, 1989, **111**, 321-335.

Chapter 7

Real-time electrochemical monitoring of solid-phase isothermal helicase-dependent amplification of nucleic acids

Laia Civit,[a] Alex Fragoso,[a] Ciara K. O'Sullivan*[a,b]

[a] Nanobiotechnology and Bioanalysis Group, Department of Chemical Engineering, Universitat Rovira i Virgili, Avd. Països Catalans, 26, 43007 Tarragona, Spain.
[b] Institució Catalana de Recerca i Estudis Avançats, Passeig Lluís Companys 23, 08010 Barcelona, Spain.

Keywords: helicase dependent amplification, solid-phase amplification, electrochemical detection.

7.1 Abstract

A proof-of-concept of a real-time electrochemical monitoring of solid-phase isothermal helicase-dependent amplification (HDA) of nucleic acids is reported. The optimum conditions for surface chemistry preparation were investigated. Electrostatic interaction of ruthenium with the negatively charged DNA was used to monitor the progress of HDA.

7.2 Introduction

In recent years, there has been an increased interest in the generation of point-of-care (POC) molecular diagnostic devices. Miniaturisation of nucleic acid amplification methods offers several advantages such as the possibility to decrease required time, the use of lower sample volumes, reduction of instrumentation costs and the ability to perform the complete analysis on a single chip.

Whilst the use of polymerase chain reaction (PCR)-based amplification is extensive, the need for temperature cycling to separate the two strands is a drawback, limiting its use in point-of-care applications, particularly in low resource settings. To overcome this, different isothermal amplification methods which do not require extreme heating or thermal cycling of the dsDNA for the separation of the two strands have been developed.

The most common isothermal methods include nucleic acid sequence-based amplification (NASBA),[1-2] loop-mediated isothermal amplification (LAMP),[3] rolling circle amplification (RCA),[4] strand displacement amplification (SDA)[5-6] and helicase-dependent amplification (HDA).[7]

Isothermal helicase-dependent amplification was introduced by Vincent *et al.* in 2004 and is based on the natural mechanism of the DNA replication fork.[7] The advantage of HDA is its PCR like reaction scheme (denaturation, primer annealing and primer extension steps).[8] The key difference relies on the use of helicase to unwind the dsDNA subsequently allowing annealing of the two specific primers.

HDA has the potential to be integrated in miniaturised, automated point-of-care devices and in microarray technology due to its simplicity, multiplexing capability and isothermal characteristics, thus avoiding thermocycling and Peltier integration.[8] Andersen *et al.* reported the adaptation of HDA on a microarray for the detection of two pathogens. One primer was immobilised on the microarray surface (glass slide) and the second labelled primer was added to the reaction solution. Amplified products remained attached and were detected by laser scanning or total internal reflection fluorescence (TIRF) technologies.[9]

The first electrochemical detection of isothermal HDA was reported by Kivlehan *et al.,* who used a DNA intercalating redox probe that becomes less electrochemically detectable upon binding with the amplified dsDNA, in comparison with the signal obtained when it is free in solution.[10]

In the present work, the proof-of-concept of electrochemical detection in real-time of immobilised isothermal HDA is presented. Forward primer was immobilised on a gold surface, whilst the Rv primer was added to the HDA reaction mixture. Human papillomavirus (HPV) associated high-risk type 45 exon was used as a model target sequence. Monitoring of the amount of DNA present in the gold surface was performed by the electrostatic interaction of Ru (III) complexes that are 3^+ positively charged, and the DNA phosphate sugar backbone, that is negatively charged. Differential pulse voltammetry was used for the detection of Ru. Preliminary studies for the application of the developed proof-of-concept in a microfluidic system were performed.

7.3 Experimental

7.3.1 Materials

Dithiol 2 (DT2, 22-(3,5-bis((6-mercaptohexyl)oxy)phenyl)-3,6,9,12,15,18,21-heptaoxadocosanoic acid) was purchased from SensoPath Technologies (Bozeman, NT). Phosphate buffered saline with Tween 20 (pH 7.4) and 3,3',5,5'-Tetramethylbenzidine (TMB) liquid substrate system were from Sigma-Aldrich

(Barcelona, Spain). All solutions were prepared with MilliQ water (18 MΩ) produced with a Milli-Q RG system (Millipore Ibérica, Madrid, Spain). Maleimide activated plates were purchased from Thermo Scientific (Barcelona, Spain.

IsoAmp® II Universal tHDA kit (New England Biolabs Inc.) was obtained from Servicios Hospitalarios (Barcelona, Spain).

Synthetic target sequence (HPV45E6 of 78-mer), modified and non-modified forward (HPV45E6 of 23-mer), and reverse primers (HPV45E6 of 18-mer) were purchased from Biomers.net (Ulm, Germany). TATAA Biocentre (www.tataa.com) can be contacted for further details on the specific sequences of the probes, primers and target amplicons.

7.3.2 Electrochemical measurements

All electrochemical measurements were performed with a PGSTAT 12 potentiostat (Autolab, The Netherlands) controlled with the General Purpose Electrochemical System (GPES) software and equipped with a MUX module (Eco Chemie B.V., The Netherlands).

A three-configuration system was used for the demonstration of the proof-of-concept of real-time electrochemical solid-phase HDA, with gold electrode (CHI 101 gold disk working electrode, from CH Instruments) as working electrode, a platinum wire (BAS model MW-1032) as counter electrode and a silver wire as a pseudo reference electrode. All potentials were reported with respect to this reference electrode.

7.3.2.1 Electrochemical real-time HDA on microfluidics

A first design was performed by the integration of an electrochemical array within a microfluidic cell, where the microfluidic channels were realised by mounting the array onto a polycarbonate fluidic chip using double-sided medical grade adhesive foil of 50 μm thickness, which had been previously laser machined to generate microchannel structures of 1 mm width. The electrode array consists of 16 gold working electrodes

arranged in a four by four distribution on a glass chip measuring 21 mm × 23 mm, fabricated at the Institut für Mikrotechnik Mainz (www.imm-mainz.de). Each working electrode (1mm × 1 mm) was placed between a silver pseudo reference (0.2 mm × 1 mm) and a gold counter electrode of the same size in order to create 16 planar electrochemical cells. Connection of the assembled chip was realised via pogopin connectors to each of the 18 electrodes (16 working electrodes and 1 plus 1 reference and counter electrodes).

The idea of the design is to carry out the HDA reaction in the meandering channel in the upper half of the chip. This chip is then assembled in the platform depicted in figure 7.1. The heater is an aluminium block located above the electrode array controlled by a PT100 temperature sensor, which is cooled with a cooling fan placed on top. The software developed for thermal control is based on LabView and is able to set up a variable number temperatures and times controlled via a proportional-integral-derivative controller (PID gain).

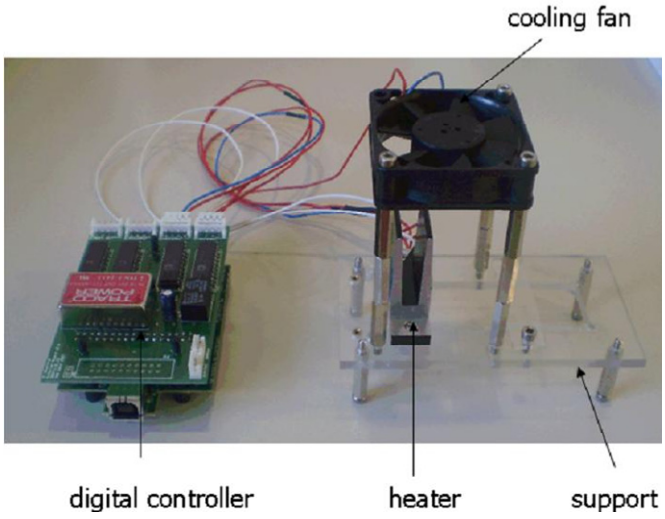

Figure 7.1. Electrochemical real-time HDA setup assembly.

7.3.3 Primer immobilisation on array surface

Prior to modification of the electrode arrays, a two-step cleaning protocol was applied. Initially in order to remove the protective resist used during storage, the arrays were sonicated for 5 min in acetone, 5 min in iso-propanol (3 times) and rinsed with water. In a second step, electrochemical cleaning was performed in 0.5 M H_2SO_4 by application of a constant potential of 1.6 V for 10 sec followed by 30 voltammetric cycles in the potential range -0.2 to 1.6 V at a scan rate of 0.5 $V \cdot s^{-1}$. Finally, the electrodes were rinsed with Milli-Q water and dried with nitrogen. Modification of the cleaned electrode arrays was carried out via immobilisation of DT2 (200 μM) in 1 M KH_2PO_4 for 3 hours at room temperature in a humid environment to prevent evaporation. The carboxyl groups of the SAM were activated with an aqueous mixture of EDC (0.2 M) and NHS (50 mM) for 30 min followed by spotting of 1 μL of 7 μM amino modified HPV45E6 forward primer (with a 10T spacer) in acetate buffer pH 5 for 1 h. The non-specific control was performed by immobilising amino modified HPV16 primer. The remaining carboxyl groups were then blocked with 0.1 M ethanolamine hydrochloride (pH 8.5) for 30 min, and the electrode array was then washed in a stirring solution of 0.1 M PBS for 20 min, rinsed with water and dried with nitrogen.

7.3.4 Helicase-dependent amplification protocol.

The reaction mix for solid-phase HDA contained 2x Annealing buffer II, 4 mM $MgSO_4$, 40 mM NaCl, 2.1 μL of dNTPs, 50 nM of Rv primer and and 2 μL of Enzyme mix for a final volume of 30 μL. For control HDA, 50 nM of Fw primer was incorporated to the master mix.

Sample analysis was performed by electrophoresis on a 4% agarose gel (Certified Low Range Ultra Agarose, Bio-rad, Barcelona).

7.3.5 Electrochemical monitoring of nucleic acid amplification

To detect the DNA present in the surface after HDA reaction at regular time intervals by means of electrostatic interaction of $Ru(NH_3)_6Cl_3$ with the negatively charged DNA backbone, electrodes were first washed with 0.1 M PBS pH 7.4 and rinsed with 10 mM Tris buffer pH 7.4 and incubated for 5 min with 660 μM of $Ru(NH_3)_6Cl_3$ in 10 mM Tris pH 7.4. After this, electrodes were rinsed with Tris buffer and DPV was performed. Differential pulse voltammograms were collected at 50 mV/s from -0.6 V to -0.1 V, after a conditioning potential at -0.6 V for 10 s.

The detection of hybridised HRP-labelled Rv primer carried out in the created microfluidic channels was performed in the presence of TMB substrate where the HRP-catalysed reduction of TMB[11-12] was detected by steps and sweeps technique by applying two consecutive potential steps of 0 V for 1 ms and -0.2 V for 0.5 s.

7.3.6 Enzyme-linked oligonucleotide assay (ELONA)

Thirty μL of 50 μM of DT2 in binding buffer (0.1 M NaH_2PO_4, 0.15 M NaCl, 10 mM EDTA, pH 7.2) were prepared for the modification of maleimide activated wells of a microtitre plate and incubated for 2 h and 30 min. Then, 3 consecutive washing steps of 200 μL 10 mM PBS-tween (pH 7.4) were performed performed using a HydroFlex microplate washer (TECAN, Barcelona). Inactivation of excess maleimide groups was carried out by incubating 150 μL of 128 μM of mercaptoethanol for 1 hour. A second washing step was carried out in an identical way as above. For the immobilization of the HPV45 forward primer, activation of carboxyl groups of the DT2 SAM were activated with an aqueous mixture of EDC (0.2 M) and NHS (50 mM) for 30 min followed by a washing step with milliQ water. Then, 30 μL of 200 nM of amino modified HPV45E6 forward primer (with a 10T spacer) in acetate buffer pH 5 was added and incubated for 1 h. A second washing step with milliQ water was performed. Finally, the remaining carboxyl groups were blocked with 30 μL of 0.1 M ethanolamine hydrochloride (pH 8.5) for 30 min. A final washing step with PBS-Tween was carried out. All steps were carried out at room temperature.

To perform immobilised HDA, 30 µl of HDA reaction mixture were added to each well and incubated at 55ºC for a total of 2 h. Every 10 min, solution from one well was recovered, stopping the amplification. After incubation, a denaturation step was performed with 100 mM NaOH for 3 min, followed by a washing step with 0.1 M PBS-Tween pH 7.4. In order to determine the amplification of the immobilised primer, 30 µl of 4 nM HRP labelled Rv primer in 0.1 M PBS (pH 7.4) was incubated for 1 h at RT. A final washing step was performed.

For the detection step, 30 µl of TMB substrate was added to each well and allowed to react for a minimum of 15 min. Then, 30 µl of 1 M H_2SO_4 was added to stop reaction, turning to blue colored solution to yellow, and the absorbance was read at 450 nm.

7.4 Results and discussion

7.4.1 Proof-of-concept of immobilised HDA on ELONA

The HDA reaction is able to amplify short DNA sequences, from 70 – 120 bp, at a constant temperature, so HPV45 target (79-bp) was chosen for this study. Prior to electrochemical detection, ELONA platform was used in order to evaluate the amplification of DNA by HDA with one primer immobilised on the surface. The same surface chemistry was used in order to mimic the electrochemical immobilised HDA assay (Figure 7.2).

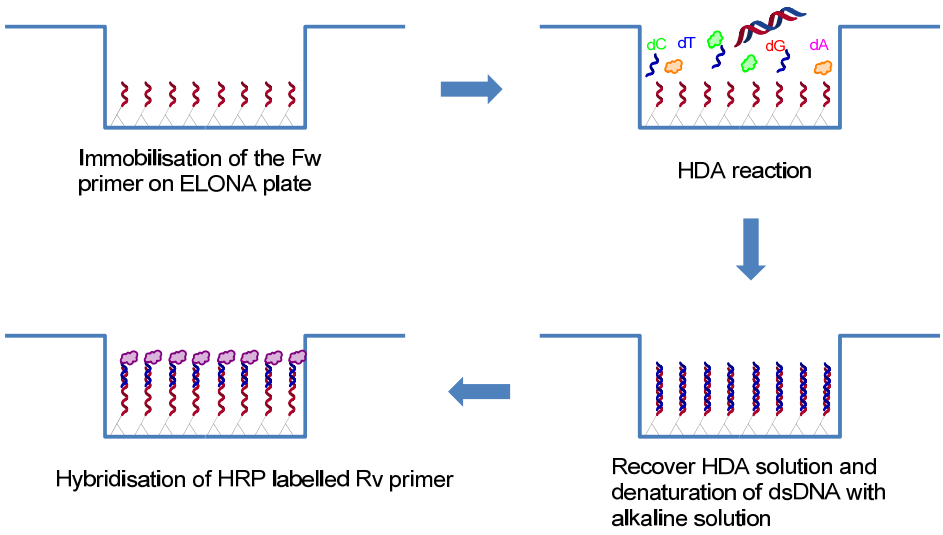

Figure 7.2. Schematic representation of HDA reaction on microtitre plates.

Figure 7.3 shows the amplification curve generated at a constant temperature of 55ºC for an initial dsDNA template concentration of 400 pM. An exponential increase of the signal as a function of amplification time can be observed, which is proportional to the extension of the primer immobilised on the surface of the wells. It can be observed that at a reaction time of 100 min a plateau was reached.

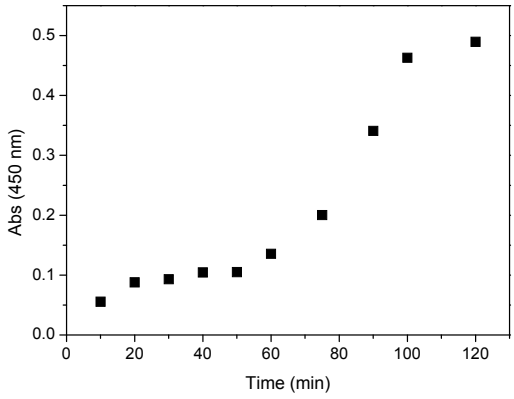

Figure 7.3. Isothermal amplification curve (T = 55ºC) obtained for immobilised HDA ELONA of HPV45 sequence (79-bp).

In figure 7.4, three different template (0.4, 1 and 5 nM) and Rv primer (50 and 100 nM) concentrations were tested. As expected, after 90 min of reaction at 55ºC, the response obtained was dependent on the starting concentration of DNA template.

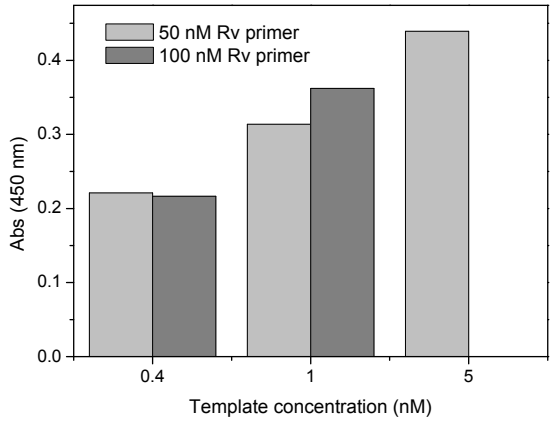

Figure 7.4. Absorbance obtained after 90 min amplification at 55ºC for different initial concentration of DNA template and Rv primer.

7.4.2 Proof-of-concept of the real-time electrochemical-based solid phase HDA

Six modified gold electrodes were used to demonstrate the proof-of-concept of an electrochemical real-time monitoring of an immobilised helicase-dependent amplification system. In this case, the electrostatic interaction of ruthenium with the negatively charged DNA was used to monitor the progress of HDA with time (Figure 7.5). Forward primer was immobilised on the surface, whilst reverse primer was added to the reaction mixture.

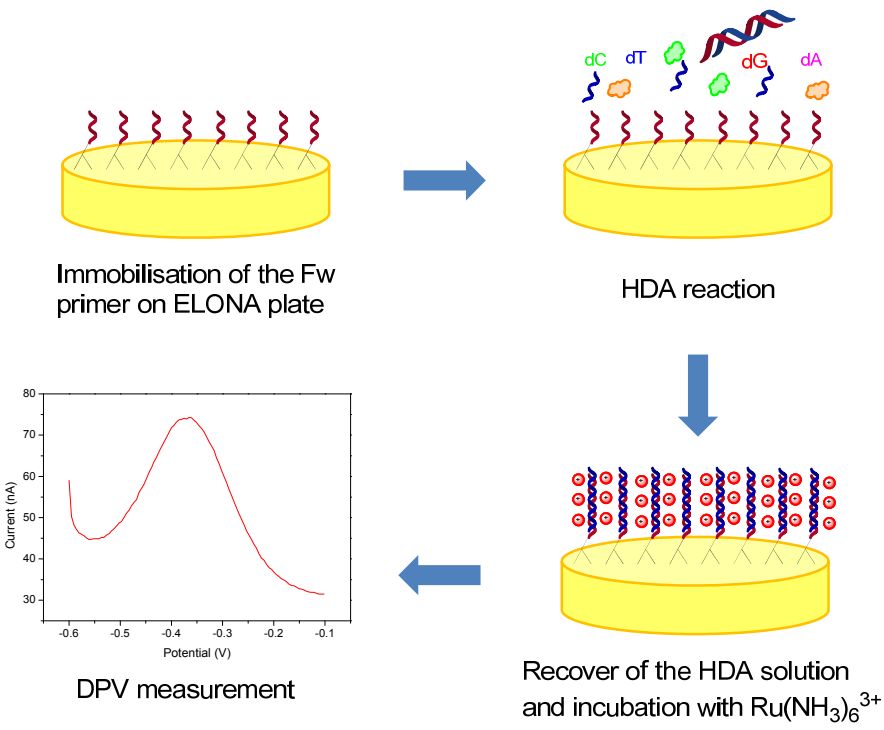

Figure 7.5. Schematic representation of HDA reaction on gold electrodes with electrochemical detection.

Thirty microlitres of HDA reaction mixture were added in each gold electrode and incubated at 55ºC for 20, 40, 60, 80, 100 and 120 minutes. After incubation, electrodes were washed with 0.1 M PBS pH 7.4 and rinsed with 10 mM Tris buffer pH 7.4 and incubated for 5 min with 660 μM of $Ru(NH_3)_6Cl_3$ in 10 mM Tris pH 7.4. After this, electrodes were rinsed with Tris buffer and DPV was performed. Differential pulse voltammograms were collected at 50 mV/s from -0.6 V to -0.1 V, after a conditioning potential at -0.6 V for 10 s. Signal obtained was substracted with the initial measured related to the electrostatic interaction of ruthenium with the immobilised primer. Electrodes were incubated 10 min more in Ru, to check if the incubation time of 5 min was not enough, but no increase in the signal was observed. Results are depicted in Figure 7.6. An increase of the signal due to the accumulation of $[Ru(NH_3)_6]^{3+}$ on the negatively charged ss/dsDNA with time can be observed. This increase is related to the extension of the immobilised primer and the formation of the duplex, due to the

annealing of the Rv primer to the extended primer, and its posterior amplification. After 60 min, slight decrease in the current at 80 min, that could be explained by the saturation of the signal, and the possibility that all immobilised primers have been extended.

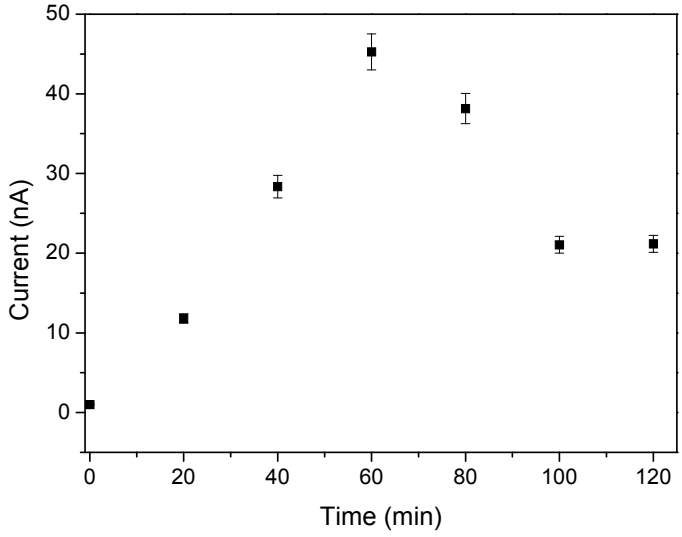

Figure 7.6. Peak current signal in differential pulse voltammetric scans vs HDA reaction time.

HDA solution was recovered and gel electrophoresis was performed to check amplification of the HPV45 target (Figure 7.7). We can observe that the gel electrophoresis analysis is consistent with the electrochemical measurements for 20 – 80 min of HDA reaction. For 100 and 120 min, we can observe in the gel that amplification takes place, whilst a decrease in the electrochemical current was observed.

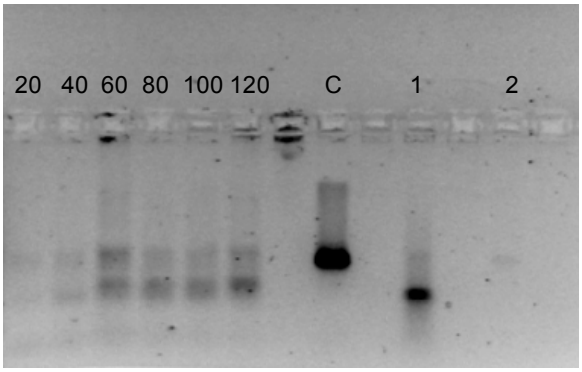

Figure 7.7. Gel electrophoresis (4%) of the immobilised HDA reaction with time (20 – 120 min). C: is the control of HDA reaction on solution, 1: is 100 nM synthetic ssDNA and 2: is 10 nM synthetic dsDNA.

Also, in the gel it can be seen that both dsDNA and ssDNA were generated, which could be explained by a competition between the Rv primer (in solution) and the immobilised Fw primer for the target amplicon. Moreover, once all immobilised primers were amplified, only one of the strands could be generated (Rv primer is in excess), potentially explaining the presence of ssDNA.

7.4.3 Amplification in microfluidics

7.4.3.1 Test of the biocompatibility of the microfluidics

In the miniaturisation of nucleic acid amplification methods, the study of the biocompatibility of the microfabricated material is a key factor. On the other hand, the high surface area-to-volume ratio of the microchannels can lead to possible interactions between the biomolecules and the surface, causing a decrease in the efficiency of the reaction, and totally inhibiting the reaction in some cases, where primer and enzyme concentration is crucial.[2]

HDA master mixes were prepared, including both primers in solution, and injected in the created channels in a treated and untreated microfluidic chip. Treatment of the surface was performed by coating it with polyethylene glycol (PEG) under UV light (350 W) for 1 hour. A control was performed by carrying out the HDA reaction on a

bench thermocycler. As it can be observed in Figure 7.8, no amplification was observed in the untreated chip (7.8A), while amplification occurred when the microfluidic was treated with PEG (7.8B), highlighting the importance of the proposed surface treatment to avoid interaction with the nucleic acids or the enzymes.

Another important aspect to take into consideration is evaporation. The low volumes used (20 μL) could be susceptible to partial evaporation at the reaction temperature, and therefore, can lead to changes in the initial HDA component concentrations. The performance of HDA is extremely sensitive to changes in magnesium and salt concentrations of the reaction, so evaporation should be avoided. Mineral oil is usually used as a vapour barrier to prevent evaporation, and it was injected in the inlet and outlet of the microfluidics.

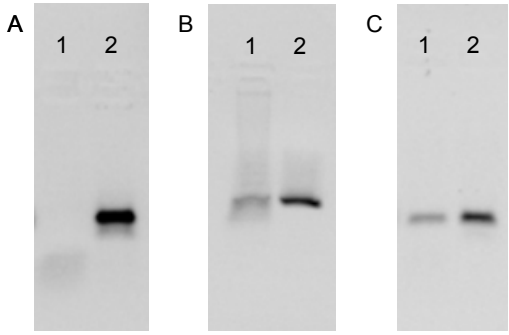

Figure 7.8. On chip (1) and in tube (2) HDA amplification for A) no treated microfluidics double-sided medical grade adhesive foil, B) treated microfluidics with double-sided medical grade adhesive foil and C) treated microfluidics with UV glue.

In the first design of the set-up, a double-sided medical grade adhesive foil of 50 μm thickness was used in order to create the microchannel structures of 1 mm width. It was observed that during the thermal amplification, the adhesive changed its initial conformation, becoming more porous, affecting the reaction mixture and making its recovery more difficult. An alternative way to assemble the microarray to the microfluidics was the use of an adhesive (PERMABOND UV360) that cures upon exposure to UV light, forming excellent bonds between an injected moulded

microfluidic chip and the electrode array (Figure 7.9). This bond was tested to be stable after exposure at 55ºC for a period time of 2 hours. The HDA reaction inside the microfluidics was slightly improved by using this set-up (7.8C), but still there is evidence that efficiency of HDA reaction in microfluidics is still not as good as in eppendorf tubes.

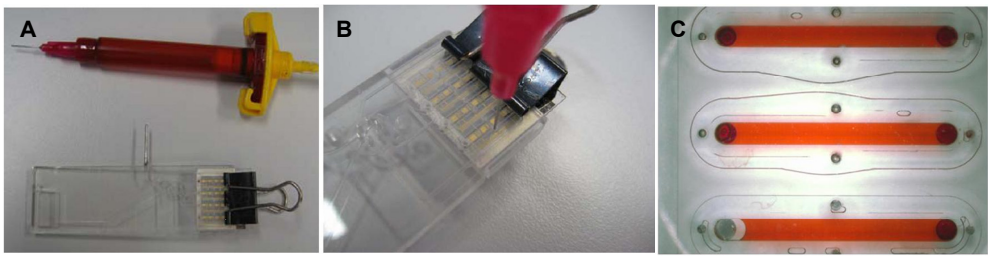

Figure 7.9. Experimental procedure for channel distributed gluing. A) Dosage needle and the chip with the sensor clamped to it, B) Insertion of the dosage needle into the glue port and C) detection chambers being filled with red food colour.

7.4.3.2 Solid-phase amplification in microfluidics

A first attempt to perform the HDA reaction within microfluidic chips was carried out employing the same strategy used in ELONA and gold electrodes. Twenty microliters of reaction mixture were added to the microfluidic chips to cover all the surface of the channels contacting the electrode array. The temperature was then increased to 55ºC and the reaction was carried out for a total of 90 min. After the HDA amplification reaction, the sensor array was washed with 0.1 M PBS pH 7.4 and incubated with 10 nM of HRP-labeled Rv primer in 0.1 M PBS for 30 min. Following this, a second washing step was performed and amperometric detection of HRP was performed by steps and sweeps (SAS) technique as explained above. The duplex on the electrodes were then de-hybridised with 100 mM NaOH for 3 min, in order to separate the dsDNA, and hybridisation of HRP-labelled Rv primer was performed again. The results are depicted in Figure 7.10. We can clearly see that the signal obtained before de-hybridisation is lower than the one performed after. This is due to

the presence of dsDNA on the surface generated during the HDA reaction, that did not permit the hybridisation of the labelled Rv primer. On the other hand, after de-hybridisation, only the DNA extended from the Fw primer is present on the surface, so the Rv primer can hybridise, obtaining a higher amperometric signal, demonstrating successful solid-phase HDA in the electrochemical HDA microfluidics setup.

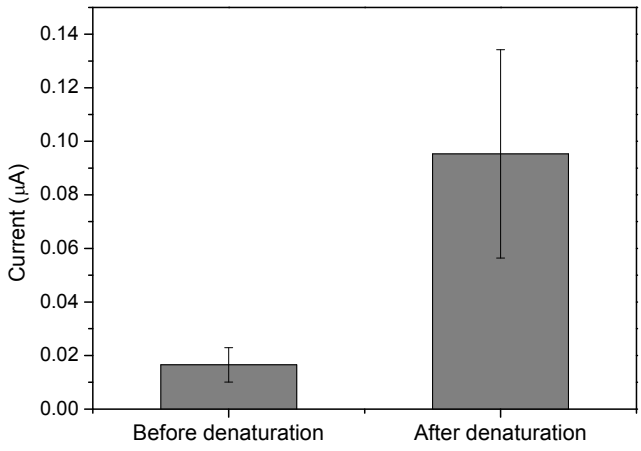

Figure 7.10. Signal obtained for the detection of the amplification of the immobilised Fw primer.

7.5 Conclusions

The proof-of-concept of an electrochemical monitoring of solid-phase helicase-dependent amplification was demonstrated. First, the extension of the immobilised Fw primer was evaluated using ELONA, an exponential amplification of the immobilised primer was observed. For electrochemical detection, the electrostatic interaction of ruthenium with the negatively charged DNA was used to monitor the progress of HDA, and an increase in the $[Ru(NH_3)_6]^{3+}$ signal from 0 – 60 min of HDA reaction at 55ºC, was observed followed by saturation of the signal. Electrophoresis gel analysis of the HDA reaction solution was in agreement with the electrochemical results, and

dsDNA and ssDNA were in the final reaction mixture following amplification. First studies for the application of the developed proof-of-concept to a microfluidic chip system for multiplexed HDA were performed.

7.6 References

1. J. Compton, *Nature*, 1991, **350**, 91-92.
2. P. J. Asiello and A. J. Baeumner, *Lab on a Chip*, 2011, **11**, 1420-1430.
3. T. Notomi, H. Okayama, H. Masubuchi, T. Yonekawa, K. Watanabe, N. Amino and T. Hase, *Nucleic Acids Research*, 2000, **28**, e63.
4. D. Liu, S. L. Daubendiek, M. A. Zillman, K. Ryan and E. T. Kool, *Journal of the American Chemical Society*, 1996, **118**, 1587-1594.
5. G. T. Walker, M. S. Fraiser, J. L. Schram, M. C. Little, J. G. Nadeau and D. P. Malinowski, *Nucleic Acids Research*, 1992, **20**, 1691-1696.
6. G. T. Walker, M. C. Little, J. G. Nadeau and D. D. Shank, *Proceedings of the National Academy of Sciences*, 1992, **89**, 392-396.
7. M. Vincent, Y. Xu and H. Kong, *EMBO Rep*, 2004, **5**, 795-800.
8. D. Andresen, M. Von Nickisch-Rosenegk and F. F. Bier, *Expert Review of Molecular Diagnostics*, 2009, **9**, 645-650.
9. D. Andresen, M. von Nickisch-Rosenegk and F. F. Bier, *Clinica Chimica Acta*, 2009, **403**, 244-248.
10. F. Kivlehan, F. Mavré, L. Talini, B. Limoges and D. Marchal, *Analyst*, 2011, **136**, 3635-3642.
11. Z. Wang, L. Liu, Y. Xu, L. Sun and G. Li, *Biosensors and Bioelectronics*, 2011, **26**, 4610-4613.
12. J. Wang, Y. Cao, Y. Li, Z. Liang and G. Li, *Journal of Electroanalytical Chemistry*, 2011, **656**, 274-278.

General conclusions

This thesis overviews the development of electrochemical DNA biosensors for the multiple detection of high-risk human papillomavirus sequences, and the proof-of-concept for the development of solid-phase amplification methods with electrochemical monitoring. Fundamental aspects such as the surface chemistry for both electrochemical platforms, the preparation of ssDNA target for its quantification and the analytical performance of the electrochemical DNA biosensor were evaluated. Finally, a proof-of-concept electrochemical detection of solid-phase DNA amplification using helicase-dependent amplification (HDA) is described.

A comparative study of different methods for the preparation of single-stranded DNA (ssDNA) is presented in Chapter 2. To truly quantify clinical samples it is crucial to generate high quality ssDNA. To date, thermal denaturation (also called *heat and cool*) is the most widely used technique for the generation of ssDNA for DNA biosensors, although it has important drawbacks in terms of recovery and reproducibility. Other techniques have also been used to generate ssDNA, such as the use of magnetic separation and exonuclease digestion. To determine the best technique for the preparation of ssDNA from amplified clinical HPV samples, a comparison of various techniques was performed, and the generated ssDNA was evaluated in terms of quality and quantity by gel electrophoresis and Enzyme Linked OligoNucleotide assay (ELONA), respectively. Two different length amplicons, of 79 bp (HPV45) and 159 bp (HPV16) were used as a model. As expected, the widely used *heat and cool* methodology was found to be the least reliable, showing very low efficiency and reproducibility, even though it is still extensively used in the biosensors field.[1-3] The alternative methods studied were found to be rapid and highly efficient methods for ssDNA generation, providing recoveries between 50-70% of the theoretical maximum with excellent reproducibility, RSD% < 8 (n=5). For the detection of the HPV sequences studied, the use of biotinylated primers with streptavidin coated magnetic beads was observed to be optimal and was used in later studies with real samples.

To our knowledge, this is the first comparative study of the recovery obtained for different methodologies widely used for the preparation of ssDNA for subsequent biosensoric detection that has been carried out to date.

The development of an electrochemical DNA genosensor array for the detection of two high-risk HPV sequences (HPV16 and HPV45) is described. Primarily, the proof-of-concept was demonstrated using an electrode array consisting of 16 gold working electrodes arranged in a four by four distribution on a borosilicate glass chip. Each working electrode has its own silver pseudo reference and a gold counter electrode. The electrode array was integrated within a microfluidic cell. Co-immobilisation of the HPV target with a dithiolated alkanethiol (DT1) in a ratio of 1/100 was found to be optimal in terms of probe density, spacing and orientation. Individual detection of HPV sequences exhibited high sensitivity and selectivity, obtaining LOD in the pM range (220 pM and 110 pM for HPV16 and HPV45, respectively). In a multiplexed detection format, high selectivity was observed for the target sequence over the non-specific one.

With these promising results in hand, a more detailed study was then performed including a new high-risk HPV sequence (HPV18). Different parameters such as cross-reactivity, reusability and stability were assessed. First, individual detection of HPV18 was performed, obtaining a LOD of 170 pM. In order to evaluate possible cross-reactions between the selected HPV types, a series of experiments were performed with mixtures of targets and reporter HRP-labeled probes and the responses were compared using the single specific target and probe. Results showed no significant interference and multiplexed studies further demonstrated the specificity of the genosensor. To assess stability issues, electrodes were prepared and no significant decrease in amperometric response (<5%) was observed after a month, indicating that the immobilised probes do not lose their recognition ability upon storage in these conditions. Finally, the genosensor array was evaluated with clinical samples obtained from Jena University Hospital. DNA extracted from cervical scrapes that were positive for HPV16, HPV18 and HPV45 and 3 HPV negative cases were provided. These

samples were firstly amplified by PCR using biotinylated HPV primers, and ssDNA was generated using streptavidin coated magnetic beads. Results showed an excellent correlation between the HPV genotyping carried out in a hospital laboratory and the quantification performed with our genosensor array.

Overall, the presented electrochemical genosensor array for the multiple detection of high-risk HPV sequences showed a reliable performance and discrimination between the three studied sequences.

In Table C1, the analytical performance of the developed genosensor array is compared with those previously reported for the electrochemical detection of HPV sequences.

Table C1. Comparison of the analytical parameters of different electrochemical biosensors for HPV determination.

Reference	HPV region	Linear range	LOD	Electrochemical method	Electrode
[4]	L1	12.5 – 350.0 nM	3.8 nM	DPV	Gold
[5]	L1	0 – 1.7 μM	200 nM	SW	Graphite
	HPV16	0.1 – 10.0 nM	0.22 nM		
This work	HPV18	0.1 – 12.0 nM	0.17 nM	Steps and sweeps	Gold array
	HPV45	0.1 – 1.0 nM	0.11 nM		

As depicted, the limit of detection of the proposed sensor improved previous reports.[4-5] One of the advantages of our approach is the facile integration of the biosensor in an electrochemical portable instrument which makes it very attractive for point-of-care applications.

For the development of solid-phase amplification methods, the choice of surface chemistry is essential in order to meet important requirements such as robustness, thermal stability and reproducibility.

In Chapter 5, the thermal stability of four surface chemistries was studied. Two alkanethiols (mono and dithiol) and two diazonium salts (with one and two diazo groups) were compared and the thermal stability was evaluated in the temperature range of 25-95ºC, monitoring changes in the array surface using CV and EIS. A comparison between the different alkanethiol SAMs clearly indicated that the monothiol ones were less stable, starting to desorb at temperatures around 65ºC, and at temperatures higher than 95ºC the layer was completely removed, whereas dithiol SAMs were more resistant to the thermal treatment, with 26% remaining after exposure to 95ºC of the layer on the surface. On the other hand, both diazonium salt derived layers responded similarly the thermal treatment, with minor desorption that could in fact be attributed to the loss of non-specifically attached molecules, indicative of the excellent stability of this surface.

Prior reports on the stability of these surface chemistries in terms of resistance to sonication, exposure to refluxing solvents, displacement using thiolated molecules[6] and under laboratory atmosphere conditions[7] concluded that the aryl diazonium derived films are more strongly bound to gold as compared to alkanethiol layers. The work presented in the thesis was the first study on the thermal stability of diazonium modified gold surfaces.

An electrochemically grafted film of 3,5-(4-diazophenoxy)benzoic acid on gold surfaces was then characterised. For the deposition of the organic films, the use of cyclic voltammetry (CV) and chronoamperometry (CA) was compared, using XPS and AFM. Immobilisation of the bipodal diazonium on the gold surface was confirmed using XPS and AFM was used for the determination of the film thickness. For this, a gold substrate was first modified with an alkanethiol SAM, and then photo-oxidation of the thiols with UV light through a mask was performed, resulting in exposed areas for the grafting of the organic films and the thickness was calculated. As expected, it was observed that even one potential cycle generated a bi- or maximum tri-layer, while for the other deposition conditions, multilayers were formed.

In this chapter, the grafting of a compound with two diazonium groups to obtain a bipodal group attached to the gold surface is described. An approach for measuring average film height by AFM was proposed using a surface patterned with an alkanethiol SAM film of known height and comparing to the grafted film of interest. This methodology offers an easy and direct way of determining film height in comparison with other methodologies such as AFM "scratching",[8] ellipsometry,[9] or FT-IRRAS.[10]

Finally, in Chapter 7, the proof-of-concept of an electrochemical monitoring of solid-phase helicase-dependent amplification (HDA) was demonstrated. First, the extension of the immobilised Fw primer was evaluated using ELONA technique and a real-time exponential amplification of the immobilised primer was demonstrated. For electrochemical detection, the electrostatic interaction of a ruthenium probe with the negatively charged DNA was used to monitor the progress of HDA with time. An increase in the $[Ru(NH_3)_6]^{3+}$ signal over 60 minutes of HDA reaction at 55ºC was observed, followed by, saturation of the signal at longer reaction times. Electrophoresis gel analysis of the HDA reaction solution was in agreement with the electrochemical results. Preliminary studies for the application of the developed proof-of-concept in a microfluidic system were performed.

Using HDA, the reaction could be performed at a single temperature (55ºC) in which a Au-SH surface preparation could be implemented as thiolated molecules on gold are stable up to 60ºC.

An electrochemical real-time solid-phase PCR assay has been developed by Hsing and co-workers,[11-12] and a recent report detailed the electrochemically monitoring of HDA,[13] but to date, no solid-phase HDA amplification by using gold electrodes has been described yet.

References

1. W. Sun, X. Qi, Y. Chen, S. Liu and H. Gao, *Talanta*, 2011, **87**, 106-112.
2. S. Aydinlik, D. Ozkan-Ariksoysal, P. Kara, A. A. Sayiner and M. Ozsoz, *Analytical Methods*, 2011, **3**, 1607-1614.
3. P. Geng, X. Zhang, Y. Teng, Y. Fu, L. Xu, M. Xu, L. Jin and W. Zhang, *Biosensors and Bioelectronics*, 2011, **26**, 3325-3330.
4. N. Nasirizadeh, H. R. Zare, M. H. Pournaghi-Azar and M. S. Hejazi, *Biosensors and Bioelectronics*, 2011, **26**, 2638-2644.
5. R. E. Sabzi, B. Sehatnia, M. H. Pournaghi-Azar and M. S. Hejazi, *Journal of the Iranian Chemical Society*, 2008, **5**, 476-483.
6. D. M. Shewchuk and M. T. McDermott, *Langmuir*, 2009, **25**, 4556-4563.
7. G. Z. Liu, T. Bocking and J. J. Gooding, *Journal of Electroanalytical Chemistry*, 2007, **600**, 335-344.
8. F. Anariba, S. H. DuVall and R. L. McCreery, *Analytical Chemistry*, 2003, **75**, 3837-3844.
9. J. C. Harper, R. Polsky, D. R. Wheeler and S. M. Brozik, *Langmuir*, 2008, **24**, 2206-2211.
10. A. Ricci, C. Bonazzola and E. J. Calvo, *Physical Chemistry Chemical Physics*, 2006, **8**, 4297-4299.
11. S. S. W. Yeung, T. M. H. Lee and I. M. Hsing, *Journal of the American Chemical Society*, 2006, **128**, 13374-13375.
12. S. S. W. Yeung, T. M. H. Lee and I. M. Hsing, *Analytical Chemistry*, 2008, **80**, 363-368.
13. F. Kivlehan, F. Mavré, L. Talini, B. Limoges and D. Marchal, *Analyst*, 2011, **136**, 3635-3642.

Outlook

The results and the conclusions derived from this thesis can serve to guide future research that would improve the knowledge gained in the field of electrochemical detection of DNA.

An electrochemical genosensor array for the multiple detection of high-risk HPV sequences has been developed and an excellent performance of this sensor was accomplished. Due to the design of this sensor array that comprises 16 independent gold working electrodes, the introduction of new high-risk or low-risk HPV sequences could definitely improve and expand the usability of these new biosensors. Moreover, it could be implemented for the detection and monitoring of other diseases.

The proof-of-concept of an electrochemical monitoring of helicase-dependent amplification in solid-phase has been accomplished. However, there are still some parameters and issues to improve apart from the obvious technological development required to achieve a final prototype of portable device.

Once it has been demonstrated that immobilised primer could be amplified and this extension could be electrochemically detected, a novel strategy for the electrochemical real-time monitoring has to be implemented. One possibility would be the use of redox-labeled nucleotides with, i.e. methylene blue.

A second goal to be achieved would be the implementation in a microfluidic system with a sensor array. With this technology in hand, multiplex amplification of different HPV sequences could be possible, making the system more robust and increasing its usability and applications.

Finally, and taking advantage of the high thermal stability obtained with diazonium-derived aryl films on gold substrates, a solid-phase PCR assay can be

proposed once the optimum conditions for the preparation of the surface chemistry will be assessed.